Contents lists available at ScienceDirect

Arabian Journal of Chemistry

journal homepage: www.ksu.edu.sa

Review article

MXenes the future of solid-state supercapacitors: Status, challenges, prospects, and applications

Nujud Badawi [a,*], Mrutunjaya Bhuyan [b], Mohammad Luqman [c], Rayed S. Alshareef [c], Mohammad Rafe Hatshan [d], Abdulrahman Al-Warthan [d], Syed Farooq Adil [d,*]

[a] University of Hafr Al–Batin College of Science, Hafer Al-Batin 39921, Saudi Arabia
[b] Center for Theoretical and Computational Physics, Department of Physics, Faculty of Science University of Malaya, Kuala Lumpur, Malaysia
[c] Department of Chemical Engineering, College of Engineering at Yanbu, Taibah University, Yanbu Al-Bahr 41911, Saudi Arabia
[d] Department of Chemistry, College of Science, King Saud University, Riyadh, Saudi Arabia

ARTICLE INFO

Keywords:
MXene
Supercapacitors
Microelectronic device
Micro-supercapacitors
Energy storage

ABSTRACT

Due to the rapid technological advancements of various sectors in recent decades, there has been a growing need for energy, necessitating the development of large-capacity, robust, adaptable, and economical energy storage systems. The most current energy-storage material known as "MXene" is a two-dimensional layered transition metal nitride or carbonitride and carbide. A covalently bonded layer is exfoliated from its parent MAX ($M_{n+1}AX_n$) phase by selective chemical etching. MXene commands the highest demand of all the two-dimensional families of materials due to its extraordinary characteristics, which include high conductivity, flexible surface functional groups, excellent mechanical properties, superior hydrophilicity, electrochemical nature, and the thickness of its atomic layers. MXene is used in solid-state supercapacitors, batteries, antimicrobial films, gas and biosensors, water splitting, electromagnetic interference shielding, and photo- and electrocatalysis. Because of MXene's special qualities, researchers are concentrating on developing the material further, both theoretically and experimentally. Utilizing a variety of microfabrication processes, MXene microelectrodes of micro-sized energy storage devices (MESDs) have been previously created. Distinct methodologies influence not only the apparatus's arrangement but also the composition of MXene microelectrodes and the electrochemical efficacy of MESDs. ,This review study addresses relevant topics and provides a topical summary of the state-of-the-art regarding MXene-based energy storage devices. The field's challenges and prospects for the future are discussed in the final part.

1. Introduction

Given the imminent depletion of fossil resources and the enormous growth in human population, energy storage technologies are being discussed extensively in the present scenario. Sodium and lithium-ion batteries, among other battery and capacitor types, are highly regarded among the many electrochemical energy storage technologies (Lin et al., 2024; Naguib et al., 2013; Wang, S. et al., 2024). Regrettably, the short lifespans, low power densities, and short cycle lives (Kewate and Punniyakoti, 2023; Panda et al., 2022) of current energy storage systems present a challenge for the future. Research is being done on the next generation of energy storage devices, called electrochemical capacitors or supercapacitors (SCs), to avoid these problems. Electrochemical reactions are the foundation of these devices (Kewate and Punniyakoti, 2023). Research has been conducted on SCs that employ a variety of novel materials in an attempt to get around the drawbacks of battery-type electrode materials. However, one of the primary issues that cannot be disregarded is the low energy density of electrochemical capacitors. Because carbon-based SCs produce electrochemical double layers at the electrode-electrolyte interface; they are also known as electrostatic double-layer charge storage mechanisms or EDLCs. They are primarily responsible for the low energy density (Maqsood et al., 2023). As a result, studies are being done on several types of SCs based on pseudocapacitive mechanisms, i.e., faradic charge storage mechanisms, and have a greater energy density than EDLC SCs. However, to create high-performing energy storage devices, certain shortcomings with each type of electrode material must be addressed (Kumar et al., 2023; Okubo et al., 2018). Recently, there has been a surge in research

* Corresponding authors.
E-mail addresses: nujuds@uhb.edu.sa (N. Badawi), sfadil@ksu.edu.sa (S. Farooq Adil).

https://doi.org/10.1016/j.arabjc.2024.105866
Received 28 March 2024; Accepted 6 June 2024
Available online 13 June 2024

on improving the performance of SCs by using different novel and advanced materials as electrodes (Kewate and Punniyakoti, 2023; Kumar et al., 2023; Okubo et al., 2018; Panda et al., 2022; Wang, H. et al., 2018).

As mentioned (Kewate and Punniyakoti, 2023; Naguib et al., 2013; Panda et al., 2022), after graphene was discovered in 2004, interest in the remarkable properties of various two-dimensional materials increased. A new class of two-dimensional transition metal (TM) nitrides, carbonitrides, and carbides was discovered in 2011 by Drexel University researchers. They named this class MXenes (pronounced "maxines") (Kumar et al., 2023; Lei et al., 2015; Okubo et al., 2018; Wang, H. et al., 2018).

Since they were founded, Scientists have been interested in MXenes because of their diverse and intriguing chemical, mechanical, electronic, and magnetic properties (Kewate and Punniyakoti, 2023; Sheikh et al., 2023). $M_{n+1}X_nT_x$ (n = 1–3) is the general formula for MXene, where M is an early TM (e.g., Mo, Cr, Nb, V, W, Ta, Ti, Sc, Hf, or Y), X could be either nitrogen or carbon, and T could be any of the following: zinc (−Z), hydroxyl (–OH), chlorine (−Cl), oxygen (−O), and fluorine (−F) (An et al.; Dall'Agnese et al., 2014; Hart et al., 2019; Khazaei et al., 2017; Raghavendra et al., 2020; Thomas et al., 2022). The thickness of MXenes, usually in the range of 1 nm, is determined by the value of n in MXenes ($M_{n+1}X_nT_x$) (Maleski et al., 2017). Selective wet chemical etching techniques exfoliate MXenes from their parent MAX phases (Maleski et al., 2017). Their name is derived from graphene due to their similarities (Cai et al., 2018; Ma et al., 2017; Wang, Y. et al., 2019; Zhan et al., 2018). MXenes are potential 2D materials for a variety of applications because of their graphene-like structure, metallic conductivity, redox capability, and flexible surface chemistry. MXenes have potential uses in the environment because they are typically composed of innocuous elements like Ti, C, and N (Wang, Z. et al., 2024). Hydrofluoric acid (HF) was used to carefully etch the Al atoms out of layered hexagonal ternary carbide, or Ti_3AlC_2, at room temperature to produce the first-ever MXene from two-dimensional titanium carbide (Ti_3C_2) (Kumar et al., 2023). Since its discovery in 2011, MXene has been called the "next wonder material" (Kumar et al., 2023; Panda et al., 2022). Notable features include a high surface (specific) area, good surface chemistry due to functionalization (An et al.; Lei et al., 2015), good dispersion in a variety of solvents, including water (Dall'Agnese et al., 2014), and excellent electrical conductivity, e.g., 2×10^5 Sm^{-1} comparable to multi-layered graphene. It is appropriate for energy storage applications due to its exceptional electrochemical qualities. The electrical double-layer mode of charge storage is enhanced by MXene's pseudocapacitive component, which can undergo redox reactions (Fatima et al., 2024). Additionally, its two-dimensional structure facilitates rapid ion transport in two- and three-dimensional channels (Hart et al., 2019; Raghavendra et al., 2020; Thomas et al., 2022). Because of its balanced mechanical flexibility at the nanosheet level, lithium-ion batteries can also hold large ions (Khazaei et al., 2017).

Invan Technology advancements have led to the development of energy-consuming devices, ranging in size from microchips to much larger ones. This calls for affordable, long-lasting energy storage devices with minimal production and processing expenses. Batteries such as SCs, Li-ion batteries (Maleski et al., 2017), sodium-ion batteries, and sodium-sulfur batteries (Wang Y. et al., 2019) are very beneficial for energy storage applications. Batteries have a greater energy density than capacitors, but capacitors have a higher power density (Zhan et al., 2018). However, SCs are far more advantageous as energy storage devices than batteries and capacitors due to their enormous cycle life, high energy storage capacity, and incredible power density (Zhan et al., 2018).

Nevertheless, the applicability of these energy storage devices is limited because they are often rigid and non-flexible. The last several decades have witnessed the advancement of wearable electronics, including health monitors, intelligent clothes, displays, and other incredibly comfortable and adaptable items (Bhimanapati et al., 2015; Cai et al., 2018; Liu et al., 2016; Ma et al., 2017). This led scientists to create flexible, durable gadgets with a large energy storage capacity (Li et al., 2018; Peng et al., 2018). MXene materials exhibit great potential for flexible electrochemical energy storage applications due to their multiple surface terminations, distinct layered structure, enhanced electrical conductivity, larger specific surface area, and high hydrophilicity (Wang et al., 2016). This article examines the composition, synthesis, electrochemical performance-influencing variables, and other aspects of MXene, keeping in mind its immense potential for use in electrochemical energy storage devices in the future. It also contains details on MXene-based SCs, how they store charge, the most recent cutting-edge advancements in SCs based on MXene composites, and their prospects for the future.

The electrode materials, which are the main component of MESDs, are essential in determining the device's overall performance. Therefore, developing novel, high-performing electrode materials with substantial charge storage capacities and high conductivities is imperative. Since its discovery in 2011, MXenes has been recognized as a promising electrode material for MESDs (Li et al., 2018; Liu et al., 2016; Peng et al., 2018; Radovic and Barsoum, 2013; Wang et al., 2016). Its high conductivity, which enables rapid ionic diffusion and electronic transport, good hydrophilicity, adjustable interlayer spacing, high thermal stability, and controllable morphology and thickness are just a few unique advantages (Barsoum and Radovic, 2011; Ingason et al., 2016; Ronchi et al., 2019; Sokol et al., 2019). The term "next magical material" has been applied to MXene relatively easily (Kajiyama et al., 2017; Khazaei et al., 2013; Kumar et al., 2022).

In smart electronics, flexible fiber-shaped supercapacitors, which are the basis of this promising energy-storage device, hold great promise. However, solid-state supercapacitors (SCs) still face difficulties in balancing processing technologies, mechanical stability, and electrochemical performance for flexible and wearable electronics (Wang, M. et al., 2018). The perfect material for supercapacitor electrodes must have high energy and power density, a large surface area, great cyclic and chemical stability, and significant ion/electron conductivity. It's also important to take into account aspects like price, toxicity, durability, safety, and dependability (Wei et al., 2020). Interestingly, a variety of extremely durable materials, including carbon nanotubes (CNT), graphene oxide, reduced graphene oxide, porous carbon, one-dimensional wires, nanorods, nanofibers, and other polymers, are included in the category of flexible energy storage materials. Flexible energy storage is based on these materials as well as supporting components such as dichalcogenides (TMC and TMD), transition metal carbides, and other organic and inorganic compounds. MXene exhibits remarkable mechanical characteristics, hydrophilicity, metallic conductivity, and a rich surface chemistry, making it a promising electrode material for supercapacitors. Using MXene ink painting, a high-performance, customizable, and foldable solid-state asymmetric supercapacitor is created (Wang et al., 2021). $Ti_3C_2T_x$ MXenes' outstanding flexibility, metallic conductivity, and good hydrophilicity make them a promising material for flexible supercapacitors. A good way to modify the layer spacing and mitigate a number of drawbacks is to dope the MXenes' surfaces with heteroatoms. The all-solid-state supercapacitor (SSS)-based device provides a framework for logical flexible electronics designs that make use of a wide range of MXenes and their heterostructures (Hu et al., 2017). When combined or altered with other compounds, MXene demonstrates remarkable material properties. These qualities include increased flexibility, exceptional mechanical durability, and resistance to a range of deformative circumstances. Integrating MXene with other bonding materials, such as different types of graphene (graphene allotropes), carbon nanotubes, carbon fibers, wires, rods, and porous materials, is crucial to maximizing these properties. Research could result in the creation of novel electrode materials that greatly increase energy storage capacity. Wang et al. (2019a,b) described a novel, simple technique that combines plasma exfoliation and graphene wrapping to create graphene-wrapped MXene. This material, known as MXene@rGO, has a layered structure with reduced

graphene on the MXene surfaces, and it has been used to create solid-state, flexible supercapacitors. The MXene@rGO supercapacitors demonstrated superior mechanical stability, excellent charge/discharge, and a specific capacitance that was twice as high (Wang K. et al., 2019). The layer spacing of $Ti_3C_2T_x$ MXene can be effectively increased by nitrogen doping, and the N-$Ti_3C_2T_x$ supercapacitor can produce an energy density of 12.78 Wh kg^{-1} (Cai et al., 2023). P-doped $Ti_3C_2T_x$ exhibits a greater capacitance of 476.9F/g as the flexible electrode of a solid state flexible supercapacitor compared to $Ti_3C_2T_X$ (344.4F/g). Phosphorus doping can produce P-O and P-C bonds in $Ti_3C_2T_x$ and widen its layer spacing, which will speed up the migration of electrolyte ions into the electrode and increase the number of active sites for pseudocapacitance effects (Wei et al., 2022). Karmur et al., (2024) developed a flexible SSS device by assembling spherical $NiCo_2S_4$ as a cathode, and a MXene-reduced graphene oxide sponge (rGO_{sp}) nanocomposite as an anode, with polyvinyl alcohol (PVA) hydrogel comprising a mixture of 3 M KOH and 0.1 M $K_4[Fe(CN)_6]$ as a membrane for electrolyte/cum separation. This device ($NiCo_2S_4$//MXene-rGO_{sp}) has a specific capacitance (C_S) of 98F/g (at 4.5 A/g), coulombic efficiency of ~99 % at 15 A/g, and C_S of ~95 % after 4000 cycles (Karmur et al., 2024). The significant surface area and abundant hydrophilic groups on MXene promote nucleation and uniform growth of three-dimensional interconnected structures with composites, leading to surface porosity and stable chemically bonded heterostructures.

This work aims to give a thorough overview of the various synthesis methods, structures, characteristics, ion intercalation and uses of MXenes for energy storage. The most recent developments in the design and microfabrication techniques of MXene-based microelectrodes for MESDs are presented in this work in a thorough and critical analysis. The pros and cons of these microfabrication techniques are first provided in detail. The most popular ones are the spray printing and mask-assisted vacuum filtration processes, the recently invented fiber-spinning technique, highly scalable printing techniques, and automated processes, e.g., etching based on ion or laser beam patterns. The creation of an MXene precursor that is appropriate for various methods, particular device integration scenarios, and associated applications, and meticulous analysis of the performance metrics acquired by using multiple approaches. Related technical problems are identified, and a brief discussion of future perspectives is presented to support the ongoing development of MXene-based MESDs. Our goal is to raise awareness regarding the environmental effects of MXene synthesis and to implement a multidisciplinary strategy to customize MXene derivatives that are efficient, scalable, and safe for use in commercial energy applications. It is anticipated that this review's direction will help in the logical construction of highly efficient, multifunctional MXene-based MESDs.

2. $M_{n+1}AX_n$ (MAX) phases

The discovery of the powder form of the MAX phases is attributed to Dr. Radovic, Dr. Nowotny, and their colleagues (Kewate and Punniyakoti, 2023; Panda et al., 2022), which rekindled interest in phase-pure bulk Ti_3SiC_2 samples that was sparked by Barsoum and El-Raghy's 1996 report on their synthesis and unique set of properties. The precursor phases in the MAX ($M_{n+1}AX_n$) have an intercalated layer "A" and layer "M" with a hexagonal structure (space group $P6_3/mmc$). Subsequently, the focus of MAX phase research has shifted. The octahedral sites that the "M" elements form is home to the "X" atoms (Wang et al., 2016).

The Barsoum group has identified a novel class of layered materials comprising over 60 different ternary nitrides and carbides (Barsoum and Radovic, 2011). More attention is being paid to the layered structure, with the fact that, at room temperature, basal dislocations multiply and are mobile, as well as other unusual and sometimes unique properties of the $M_{n+1}AX_n$ phases. Because of their structural and chemical similarities, the MAX and the corresponding MX phases share many chemical and physical properties. The mechanical and elastic properties of bulk MAX phases—very different from their MX counterparts—have been covered here. Generally speaking, the MAX phases have isotropic elastic properties that are relatively stiff.

These phases are easily machined, damage-resistant, and relatively soft (2–8 GPa). Furthermore, some are fatigue, oxidation, heat shock, and creep resistance, as well as being lightweight. Moreover, under compressive cycling loading of up to 1 GPa, they exhibit nonlinear elastic solid behavior at room temperature, losing 25 % of mechanical energy.

They go through a brittle-to-plastic transformation at higher temperatures, and their mechanical behavior is highly dependent on the deformation rate—Sokol, among other locations. The structure of the majority, if not all, of the known MAX phases—also referred to as $M_{n+1}AX_n$ or MAX phases—has been reviewed in the current study. [Aside from Sokol, naturally] in these phases are currently 16 A and 14 M elements. Since quaternary in- and out-of-plane ordered MAX phases have been discovered, there might be more. The MAX phases' chemical diversity will eventually allow for optimizing specific properties for possible uses. The study of MAX phases, a recently identified family of unusual magnetic nanolaminates with a distinctive combination of ceramic and metallic properties, is presented by Ingason et al. (Ingason et al., 2016). Density functional theory was used to evaluate phase stability before the generated magnetic MAX phases were synthesized as heteroepitaxial thin films. Thus far, reports have been made of the following bulk and thin-film magnetic MAX phases (in Cr and/or Mn form): $(V,Mn)_3GaC_2$, Mn_2GaC, Cr_2GeC and Cr_2AlC. Moreover, reports of $(Mo,Mn)_2GaC$, $(Cr,Mn)_2GaC$ and $(Cr,Mn)_2GeC$ have been made. Their structural alterations are associated with magnetic anisotropy. Numerous magnetic characteristics have been discovered, including ferromagnetic responses well above room temperature.

2.1. Structure of MXenes

To better understand the synthesis methods selected, a thorough examination of the structural appearance of MXene has been conducted (Kumar et al., 2022). MXenes represent a novel class of two-dimensional nanomaterials that exhibit exceptional mechanical, thermal, and biological characteristics. They are widely used in many vital research areas, from environmental applications and energy to cancer treatment. MXenes have great potential as advanced composite structures because of their unique properties, including their mechanoceramic nature with superior mechanical performance, rich surface properties, and thermal stability. This is especially true for composite structures made of polymers since macromolecules have a strong affinity for the terminating groups of two-dimensional MXenes. MXenes are widely used in solid or liquid-based lubrication systems and metal matrix nanocomposites due to their antifriction properties and two-dimensional structure.

The $P6_3/mmc$ space group and hexagonal symmetry of MXenes are inherited from their parent MAX precursor. The (X) element atoms in this example are located in the octahedral interstitial sites, whereas the TM (M) atoms are arranged in an almost closely packed structure. In the MAX phases containing A1, the M−Al bond exhibits metallic properties, while the in-plane MAX bond shows a combination of covalent, metallic, and ionic properties. This makes it easier to selectively etch the Al layer out of the MAX phases, making the synthesis of MXenes easier (Jiang, Q. et al., 2020). After etching, surface terminations such as F, O, or OH are bonded to the outer TM layers and replace the A layers. A recent study reports that Cl atoms on Ti_2CT_x and Ti_3C_2Tx can also functionalize surfaces that are etched in a Cl^-containing environment. Additionally, a strong bond between the surface terminations and the TMs is indicated by a high negative formation energy, which implies that MXenes will likely remain fully terminated (Kajiyama et al., 2017). Furthermore, all fully terminated MXenes have positive phonon frequencies contributing to local stabilization. The two places on the surface of MXenes where these terminations can occur are hollow site I, situated between three nearby X atoms below the TMs, and hollow site II, which is directly on

top of the TM atoms. Density functional theory (DFT) calculations indicate that surface terminations at site I on both sides of MXenes sheets are the most stable configuration for most MXenes due to their low steric hindrance (Khazaei et al., 2013). However, when the TMs cannot provide sufficient electrons to help both surface and X terminations, site II becomes energetically more favorable for MXenes (Khazaei et al., 2015).

To put it another way, F- and OH– OH-terminations only need one electron from the surface of TM to stabilize their adsorption position, whereas O-terminations require two. In MXenes that contain low valency TMs, the O-terminations typically exhibit a site II configuration or a combination of sites I and II (Enyashin and Ivanovskii, 2013; Khazaei et al., 2017).

The synthesis and delamination of $Ti_3C_2T_x$ can be done in a variety of ways, leading to differences in flake size, interlayer spacing, surface chemistry, and other defects (Sarycheva and Gogotsi, 2020). As detailed in the Experimental section and schematically shown in Fig. 1a, $Ti_3C_2T_x$ was synthesized by a LiF/HCl method, in which HF is formed in situ by mixing LiF and HCl, via a mixed-acid method, in which HF and HCl were mixed, and by etching in aqueous HF solutions of various concentrations: 5, 10, 20, and 30 %. The material was extracted in various forms and concentrations according to the requirements of the study, thanks to the chemical top-down approach: a multilayer powder without intercalants, a claylike material with intercalants (like Li^+ and water), single flakes on a Si/SiO_2 substrate, a colloidal suspension of delaminated flakes, and a vacuum-filtered film of delaminated material. As seen in (Fig. 1b), the MXene Raman spectrum can be divided into multiple regions. The plasmonic peak is coupled with the resonant peak, which is first seen when the 785 nm laser is used. The flake region follows, which is made up of the in-plane and out-of-plane vibrations of titanium atoms in the outer layer as well as carbon and surface groups, respectively, represented by the E_g(Ti, C, O) and A_{1g}(Ti, C, O) modes.

Peak assignment for $Ti_3C_2T_x$ based on our experimental data and theoretical studies. $Ti_3C_2T_x$ has a Raman spectrum with several features in the range of 100–800 cm^{-1}. The spectrum that is being presented

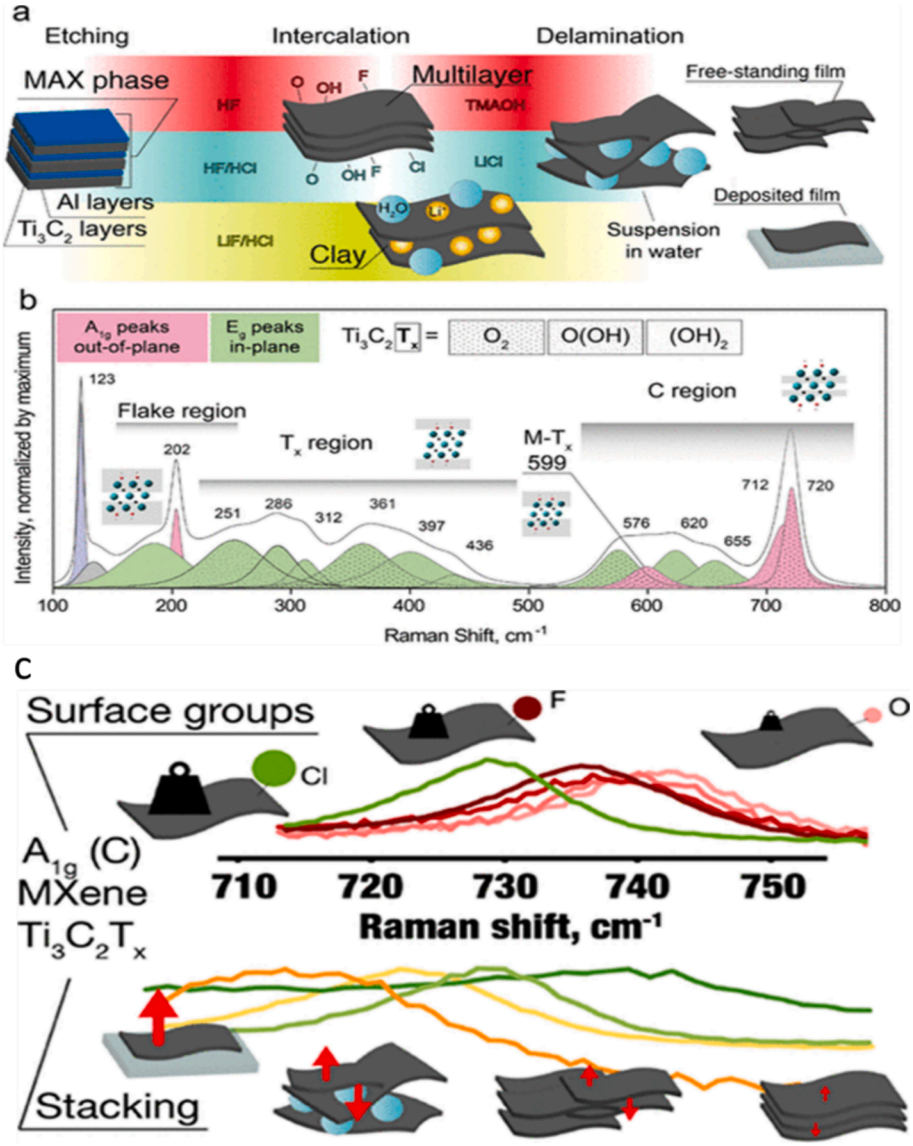

Fig. 1. Synthesis of $Ti_3C_2T_x$ and Raman peak assignment. (a) Schematics showing the $Ti_3C_2T_x$ at various processing stages, such as etching, intercalation, and delamination, as well as the synthesis and delamination techniques used in this investigation. (b) A deconvoluted Raman spectrum derived from a $Ti_3C_2T_x$ film excited by a 785 nm laser and synthesized via HF–HCl etching. The spectrum is separated into three regions: the flake region, which is associated with surface groups, two titanium layers, and a group vibration of carbon; the Tx region, which is associated with surface group vibrations; and the carbon region, which is associated with both in-plane and out-of-plane vibrations of carbon atoms. (c) Raman Spectroscopy Study of $Ti_3C_2T_x$ MXene's Structure and Surface Chemistry (Sarycheva and Gogotsi, 2020).

differs significantly from the Ti_3AlC_2 precursor MAX phase (Fig. 1c). At lower wavenumbers, the A_{1g}(Ti, Al), also called the ω4 vibration of the MAX phase, is shifted. This vibration now involves C and surface groups instead of just Al. The MAX phase's full width at half-maximum (FWHM) is 16 cm^{-1}, whereas the MXene phase's FWHM is 9 cm^{-1}. A different out-of-plane vibration, denoted as ω6, moves from 660 to 720 cm^{-1} at higher wavenumbers. Peak broadening in the case of MXene happens between 15 and 22 cm^{-1}.

AFM (Nanoman) technology was used to study X-ray diffraction's friction and adhesion behaviors, and MXene was employed to determine the material's chemical structure. AFM tests revealed that at higher temperatures MXene showed friction and decreased adhesion but increased friction and adhesion at higher pressures (Guo et al., 2019). It was discovered that the AFM probe's sliding speed and delay time had minimal impact on the friction. X-ray photoelectron spectroscopy determines how MXene's chemical structure changes at different temperatures. Guo et al. (Guo et al., 2019) found that MXene experienced increased substitution and oxidation of O atoms for C atoms at higher temperatures. This significantly impacts the friction and adhesion between the probe tip and MXene (Fig. 2). By providing a foundation for comprehending MXene's dynamic adhesion mechanism and behavior in friction, this discovery broadens the range of possible applications.

MXenes also have maximum higher conductivity, chemical stability, hydrogen storage ability, and environmental friendliness. MXene, particularly on its surface, can absorb various ionic and molecular species due to its hydrophobicity and active functional groups. This property makes it useful for environmental sensing and stopping ecological contamination.

In 2011, the general formula $M_{n+1}X_nT_x$, where M stands for early TM, A for groups IIIA or IVA element, and (X) for carbon or nitrogen, represents a new class of non-standard two-dimensional materials called MXene that was discovered (Chen et al., 2021; Thomas et al., 2022). Put differently, the most widely used research material currently is MXene. Remember that to create MXene ($Ti_3C_2T_x$), the (Al) atom layer must be removed from the MAX phase (Ti_3AlC_2) due to the (M – A) bond's relatively weaker bond strength than the (M – X) bond (Hart et al., 2019). MXene's exceptional mechanical qualities, chemical resistance, and superior metallic conductivity make it a promising platform for energy storage electrodes that have sparked interest in various beneficial application areas (Khazaei et al., 2017; Li et al., 2021). However, Van der Waals (vdW) force between neighboring layers causes MXene nanosheets to re-stack, which can worsen ion transport and reduce specific surface area (Chen et al., 2021). For EDLCs, carbon materials might be the best choice for electrode material. 1D carbon nanotubes, or CNTs, have high conductivity and surface area and are cheap and environmentally friendly. These qualities make them a popular choice for electrochemical materials (Li et al., 2021). Significantly, a three-dimensional cross-linking composite structure that prevents layer restacking and increases interlayer spacing can enhance surface charge capacity, speed up ion intercalation and deintercalation, and increase interlayer spacing when moderate amounts of CNT are added to MXene (Li et al., 2021).

The primary goal of Liu L et al.'s work was to synthesize nanosheets of Ni_3S_2 along with nanoparticles based on Co_9S_8, which were anchored on a three-dimensional crosslinked composite structure five mLCNT@MXene matrix (Ni/Co@C_5M) (Liu et al., 2023). Following a two-step hydrothermal process, the material was successfully annealed and demonstrated superior reversible capacity, excellent electrochemical performance, high-rate capability, and remarkable durability. Because CNT cross-linking conductive bridges and sulfides are added, the electrode materials' unique three-dimensional X-linking composite structure properties greatly enhance capacitive storage performance. Additionally, CNT can increase electrical conductivity and stop MXene layers from stacking again. Regarding cycling stability, the Ni/Co@C_5M electrode maintains 88.57 % of its value after 10,000 cycles at a high current density of 30 A/g. As expected, its specific capacitance at 1 A/g is 1827.5 Fg^{-1}. An asymmetric supercapacitor, Ni/Co@C_5M // AC, has an enormous energy density of up to 78.4 Wh kg^{-1} at a power density of 699.3 W kg^{-1}, and a remarkable capacitance retention of 86.67 % at 20 A/g for 10,000 cycles. Fig. 3(a) presents the schematic diagrams for the Ni/Co@C_5M and intermediate products, while Fig. 3(b) displays the etching process diagram for MXene. From the SEM image, it is evident that MXene has well-stacked layers in an accordion-like layered structure. The distinct 3D cross-linking composite structure formed by the

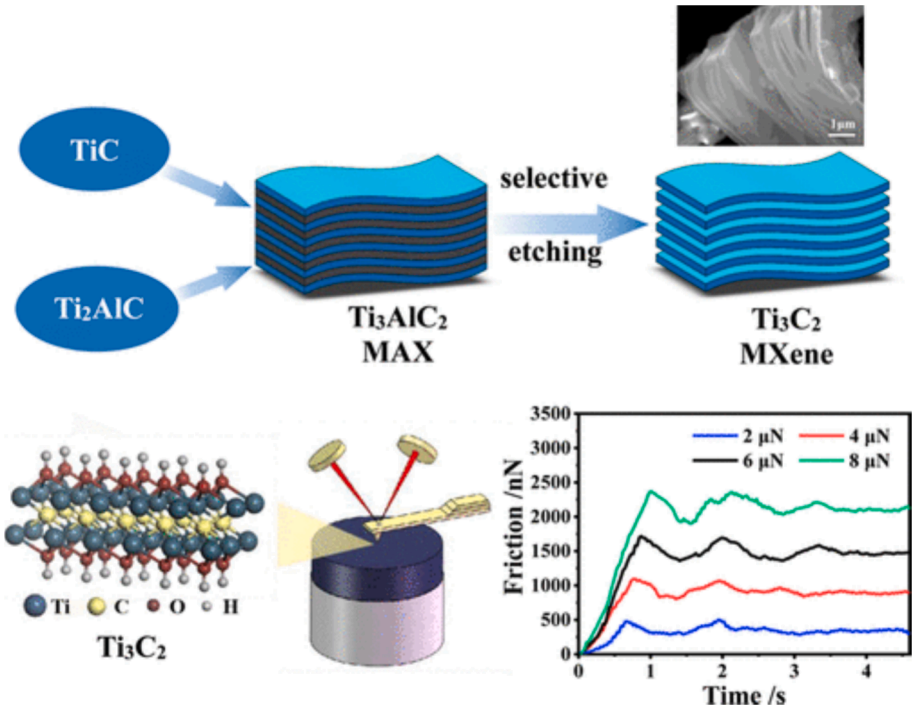

Fig. 2. Ti_3C_2 MXene's Nanomechanical Properties (Guo et al., 2019).

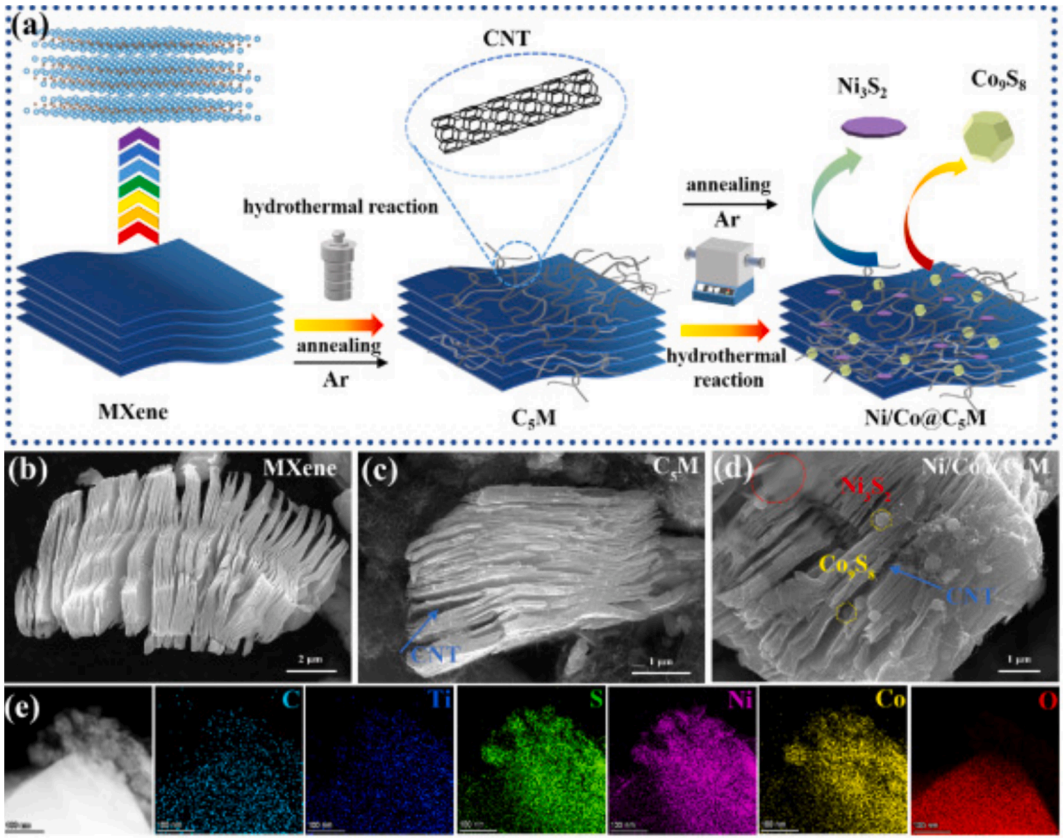

Fig. 3. (a) The schematic diagrams of MXene, C_5M, Ni/Co@C_5M, the low-magnification SEM images for (b) MXene, (c) C_5M, (d) Ni/Co@C_5M, (e) the elemental mapping images of Ni/Co@C_5M (Liu et al., 2023).

moderate CNT on MXene nanosheets is exhibited in Fig. 3(c). However, the SEM image of C_7M shows that there is a significant increase in re-stacking and encapsulation due to the excessive and dense CNT coating on the entire surface of MXene. This is causing an obstruction to electron mobility as well as ion transport because of the dispersed Ni_3S_2 thin-layer nanosheets and Co_9S_8 nanoparticles anchored on the C_5M matrix, the morphology shown in (Fig. 3(d)) is different. These features can shorten the ion's transport distance, increase interlayer spacing, and enhance electrochemical performance. Additionally, as can be seen in (Fig. 3(e)), the matching EDS mapping images of Ni/Co@C_5M demonstrate a uniform distribution of C, Ti, S, Ni, Co, and O elements, indicating the presence of Co_9S_8 nanoparticles and Ni_3S_2 thin-layer nanosheets on the C_5M matrix.

A 3D-printed structural supercapacitor made of thermoset polyester resin and woven carbon fiber is described by Deka, B. et al. (Deka et al., 2023). By N-doped Zn-Co selenide nanowires, the surface area and specific capacitance of the electrodes were hydrothermally increased. The N@$ZnCoSe_2$-MXene supercapacitor showed Coulombic efficiency of 88.8 %, energy of 2.69 Wh kg^{-1}, and power density at 1000 mA g^{-1} is 43.20 W kg^{-1} of current density (Fig. 4). After 6000 consecutive charge–discharge cycles the capacitance retention at the same current density was 83.7 %, indicating that cyclic stability was satisfactory and the device's multi-functionality. The device's high modulus (36.92 GPa) and tensile strength (637.679 MPa) combined with its impact energy absorption capacity (2.22 J g^{-1}) proved its mechanical robustness. The gadget performs similarly in a range of climates. At 70 degrees Celsius, it maintains its power density at 39.11F/g, 4.62 Wh kg^{-1}, and 67.29 W kg^{-1}, and it keeps its power density[1] at −5 degrees Celsius at 7.87F/g, 1.78 Wh kg^{-1}, and 20.98 W kg^{-1}, respectively.

Various etching techniques are presented for the production of MXene. A class of two-dimensional (2D) materials known as transition metal nitrides and/or carbides (MXenes) has exceptional mechanical strength, carrier mobility, and other desirable properties. An extensive summary of the most recent developments in the morphological design of 2D MXene materials is given in this section.

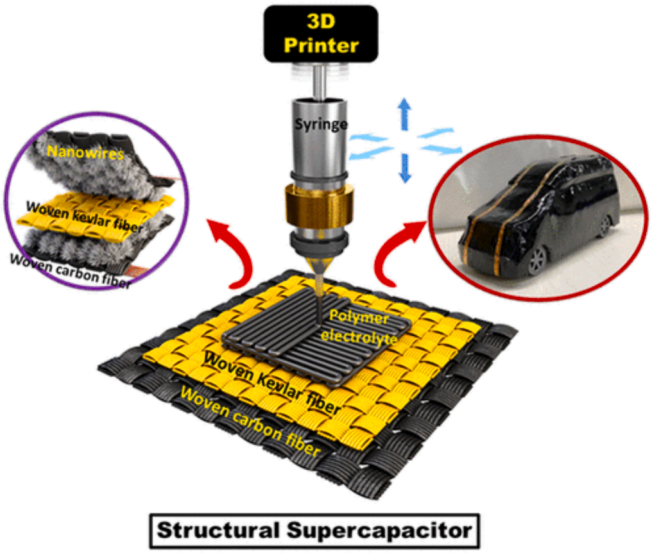

Fig. 4. Based on 3D-Printed Structural Supercapacitor with Woven Carbon Fiber Electrodes and MXene-N@Zn-Co Selenide Nanowire Deka, B et al. (Deka et al., 2023).

2.2. Synthesis methods of MXenes

The most common way to make MXenes is to carefully etch element 'A' from the parent MAX phases. The HF-based etchant's high selectivity allowed for the selective etching of SiC polytypes, making this process possible. In contrast to mixed metallic/ionic/covalent bonds, metallic MAX bonds exhibit higher reactivity in an etchant containing fluoride. At first, the only technique available for producing MXenes was etching in an HF aqueous solution at various concentrations and conditions depending on the MAX phases (Kajiyama et al., 2017). Subsequent research revealed that $Ti_3(C,N)_2T_x$, $Ti_3C_2T_x$, and Ti_2CT_x could be successfully produced using a combination of HCl and LiF solution. Moreover, reports have indicated that hydrothermally etching MAX phases can yield MXenes. Moreover, bifluoride salt (NH_4HF_2) can also be used to create Ti_3C_2Tx (Shao et al., 2010). For $Ti_3C_2T_x$, a comprehensive synthesis protocol was recently published. Because each MAX phase has a distinct reactivity and stability to various etchants, the conditions used for synthesis for one MXene should not be used for another. M_4AX_3 (413 phase) usually needs more aggressive etching conditions (312 phase) compared to M_2AX (211 phase) and M_3AX_2. However, only two of the over ten elements found in MAX phases have been effectively etched to create MXenes thus far: Si and Al. It has only recently been found that an oxidant is needed to form $Ti_3C_2T_x$ MXene by etching Si from Ti_3SiC_2, just like SiC is. High HF concentrations, high temperatures, extended etching times, and the use of C_{l2} etchant are examples of aggressive etching conditions that can lead to over-etching and leave carbon derived from carbide or cause defects in the M sites. When using the etching process, bear this in mind as well. Therefore, to create two-dimensional MXenes with the proper properties, etching and MAX stability must be balanced.

According to Shao et al., 2010, as research has progressed, MXene synthesis techniques have changed from single transition MXene to double transition based MXenes. Finding non-toxic alternatives to hydrofluoric acid-based fast etching is the primary objective (Shao et al., 2010). Wet etching and chemical vapor deposition techniques have been widely reported for the synthesis of MXenes. Table 1 depicts the commonly used method for MXenes synthesis and summarizes their advantages and disadvantages.

The shortcomings of conventional methods are compensated for by printing and stamping processes, which provide homogeneity in mass fabrication. Thus, in order to thoroughly explore the breadth and implications of MXene's discovery, despite the difficulties associated with material/electrode synthesis, researchers are working to develop ideal architectures for storage batteries and super-capacitor materials. Two-dimensional MXene-based nanomaterials have piqued the interest of researchers due to their distinct physical and chemical properties, as well as their numerous uses in photonics, catalysis, electronics, optoelectronics, and energy storage (Nan et al., 2021; Shao et al., 2010). MXenes and their derivatives are constrained in their energy storage applications by several inherent factors. To further enhance these two-dimensional materials' functionality for real-world uses, extensive research is being done on their nanoengineering. In 2021, Nan et al. provided an overview and a presentation of the most recent research on two-dimensional MXene-based nanostructures, with a focus on the properties, methods of preparation, and applications of these materials in energy storage devices including SCs and lithium/sodium-ion batteries (Nan et al., 2021).

The development of a novel material called MXene is currently underway in an effort to address the limitations of conventional components. It can be expanded to include dichalcogenides based on metal oxides, TMs, and polymers (two-dimensional) and materials (two-dimensional) based on graphene (Zhan et al., 2020). The notation $M_{n+1}X_nT_x$ is commonly used to represent the family of TM-based two-dimensional carbide and nitride components. In this notation, T stands for the functional group (e.g., hydroxyl, oxygen, fluorine), X for carbon or nitrogen, and M for the TM. According to Bhimanapati et al., these components have an unequal distribution of different functional groups

Table 1
MXenes synthesis and their pros and cons of each synthesis procedure.

Method	Advantages	Disadvantages	Reference
Using various etchants and delamination techniques, titanium carbide (Ti_3C_2Tx), the most studied MXene, was synthesized through experimental methods and best practices. (HF etching)	It is suitable for a variety of MXene compounds and permits intercalation to occur simultaneously with etching.	It is dangerous because it produces MXenes that are terminated with −F, which negatively affects applications and further cleaning procedures are necessary.	(Alhabeb et al., 2017)
A number of synthesis techniques (such as top-down and bottom-up methods) along with a synopsis of the structural characteristics, encompassing surface chemistries, structural defects, and crystal lattice. (Alkali etching)	It is safe and feasible to remove the F terminals from MXenes.	Conditions for harsh reactions might be necessary and the organic base reaction's mechanism is unknown.	(Yu et al., 2021)
Electrochemical Synthesis of MXenes without Acid/Alkali (Electrochemical etching)	Control over the surface terminations and safety because the synthesis is free of fluorine.	Expensive set up is required.	(Li et al., 2020)
Creating a range of Zn-based MAX phases and Cl-terminated MXenes, which come from the MAX phase's replacement reaction with late transition-metal halides. (Molten salt etching)	The etching action of Lewis acid in molten salts offers a sustainable and green way to prepare MXenes using a chemical method free of HF. Lewis acidic salts are effective in preparing MXenes from MAX phase, including Zn, Ga, and Si.	Requires harsh experimental conditions- And Produce –F terminated MXenes.	(Li et al., 2019)
Improved pulsed laser deposition with plasma. Using a plasma-enhanced pulsed laser deposition technique, continuous Mo_2C ultrathin single-crystalline films were successfully fabricated at 700°C. The Mo_2C films were identified as single crystals with an uncommonly reported face-centered cubic structure through advanced structural analyses. Additional electrical transport measurements show that the Mo_2C films' superconductivity exhibits a characteristic two-dimensional feature that is in line with Berezinskii-Kosterlitz-Thouless transitions.	It is possible to control the crystal structure and cultivate vast areas of superior TMCs at comparatively low temperatures.	Energy-intensive process and an unclear mode of operation.	(Zhang et al., 2017)

concealed on the surface of metal (Bhimanapati et al., 2015). The separation of graphene from graphite in 2004 marked the beginning of the field of two-dimensional materials. Transition-metal dichalcogenides (TMDs) are one class of non-graphene layered material, and their unique properties and applications have led to a sharp increase in the number of papers published in this field in recent years. Bhimanapati et al. (Bhimanapati et al., 2015) provided clarification on the excitonic properties and growth morphologies of the two-dimensional layers in bulk solids and the theoretical modeling and comprehension of the vdW forces holding them together. Furthermore, the most recent two-dimensional material families were discussed, and monoelement two-dimensional materials (e.g., silicon, and phosphorene) demonstrated recent developments in TMD synthesis and characterization Fig. 5 (Bhimanapati et al., 2015). MXenes based on carbon nitride and TM carbides were among the material families studied.

Lim et al. (Lim et al., 2022) provide a summary of the variables influencing effective (and ineffective) delamination and etching protocols. The objective is to pinpoint the motivating factors at every phase to guide the creation of MXenes with enhanced quality, yield, and adjustable characteristics in the future. In 2011 from the first report on $Ti_3C_2T_x$, the two-dimensional TM nitride family, carbonitrides and carbides (MXenes) has expanded considerably. The class MXenes currently includes both single- and multi-element compounds; many more are anticipated to have advantageous properties but have not yet been synthesized. Further, deep mechanistic understanding of the precursors, etching–exfoliation, and final intercalation–delamination steps of the known MXene synthesis processes is required in order to synthesize these elusive compounds and to enhance and increase the production of known MXenes. Fig. 6 illustrates how the dominant precursor, MAX phases, and extra non-MAX layered materials influence the synthesis of MXene and its ensuing properties.

It is now more common to search for MXenes based on double TMs rather than single TMs (Das and Wu, 2020). To make the whole process non-toxic, research was being done on substitutes for HF-based selective etching (Fig. 7(left)). The conventional methods of preparing electrodes for devices destined for homogenized mass production are being taken over by stamping and printing techniques (Peng et al., 2016; Tao et al., 2017) (Fig. 7 (middle). With the gradual lifting of limitations on the electrode and material fabrication, scientists are finding complex battery and supercapacitor architectures to expand the number of applications for MXene Fig. 7 (Ling et al., 2014).Fig. 8..

The M−A and M−X bond strengths are the main distinctions between MAX phases, as was previously mentioned by Orangi et al. However, in comparison to M−X bonds, M−A bonds are weaker and more brittle (Orangi et al., 2020). The fundamental goal of the synthesis is to remove weakly bonded layers of A atoms in order to obtain nitrides, carbides, or both (Nan et al., 2021), which is an essential step in the synthesis of MXenes (Zhan et al., 2020). X, T_x, and M stand for TM, nitrogen or carbon, and surface terminals like −O, –OH, −F, and −Cl species, respectively, in the structural formula of MXenes, which is $M_{n+1}X_nT_x$ (n = 1–4). The process of making MXene the A layer, an element of group IIIA, or IVA, is usually selectively etched away from its precursor MAX phase using a wet chemical technique. The well-known MAX phases, with their hexagonal crystal structure, closely packed X layers, and M atoms occupying octahedral interstitial sites, satisfy the $P6_3/mmc$ space group symmetry (Wang et al., 2016). Much work has recently been done on the synthesis of MXenes to improve their electrochemical performance. The two main synthesis techniques, top-down and bottom-up, have been the focus of most of these initiatives (Sokol et al., 2019). The bottom-up method combines elements to create MXene, while the top-down method uses a selective etching technique to remove the A-layer from the precursor MAX phase or non-MAX phase. The properties, morphology, and structure of MXenes are determined by the elements' composition and the processes that were used to create them (Dai et al., 2023).

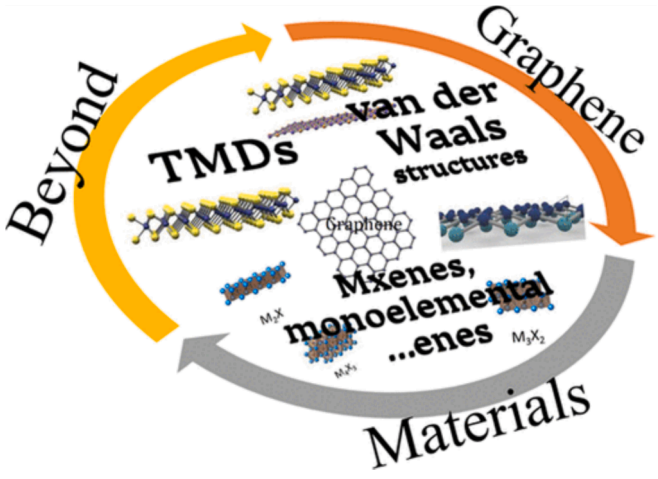

Fig. 5. Beyond Graphene: Recent Developments in Two-Dimensional Materials (Bhimanapati et al., 2015).

λ-MnO_2 nanoplates were created by Thanigai Vetrikarasan et al. (Thanigai Vetrikarasan et al., 2023) using a one-step co-precipitation method, and they were applied in flexible asymmetric SCs (SCs). The morphological, structural, and electrochemical properties of the synthesized λ-MnO_2 were thoroughly examined. Density functional theory (DFT) calculations and UV–vis spectroscopy were used to investigate the optical and electronic properties of −MnO_2. Their findings showed that an electrode resembling pseudocapacitive λ −MnO_2 nanoplates had a maximum specific capacitance of 288.5F/g when scanned at a rate of 5 mV s^{-1}. The feasibility was investigated by constructing symmetric (λ −MnO_2//- λ MnO_2) and asymmetric (λ-MnO_2//AC and λ-MnO_2//$Ti_3C_2T_x$ MXene) SCs and evaluating their performances. According to extensive comparative studies, the asymmetric λ-MnO_2//$Ti_3C_2T_x$ MXene SC at a power density of 1100 W kg^{-1} demonstrated a maximum energy density of 15.5 Wh kg^{-1} and 86.3 % capacitive retention after 5000 cycles. Additionally, a flexible λ-MnO_2//$Ti_3C_2T_x$ asymmetric SC was constructed using a PVA: Na_2SO_4 gel polymer electrolyte that operated in the potential window of 2 V and provided a high areal energy density of 39.9 μWh cm^{-2} at a power density of 8586 μW cm^{-2} in order to confirm that these electrodes are suitable for flexible energy storage. Consequently, the λ-MnO_2 generated through a simple, large-scale co-precipitation process may be helpful for flexible energy storage (Thanigai Vetrikarasan et al., 2023).

The Pros and cons of each synthesis procedure for MXenes are summarized in Table 1.

The fact that the number of papers on MXenes has increased exponentially indicates that these materials' intrinsic electronic conductivity, superior hydrophilicity, rich surface chemistry, and layered structure have opened up an exciting new field in 2D inorganic functional materials.

2.3. Properties of MXenes

There are currently over 40 MXene compositions in the MXene family (Naguib et al., 2021). They might become the largest known family of two-dimensional materials because their much larger total MXenes are used in a variety of industries, including biomedicine, energy storage, communications, optoelectronics, and the environment, because of these unique properties. Their roughly 20,000 S cm^{-1} metal-like electrical conductivity is one of these features. Publications and patents pertaining to MXene are easily accessible. The first generation of MXene is made by layering TM carbides and carbonitrides and selectively etching the metal layers from the MAX phases with hydrofluoric acid. Since then, a number of synthesis methods have been created that enable the production of novel MXenes with increased control over their surface chemistries (Shahzad et al., 2016).

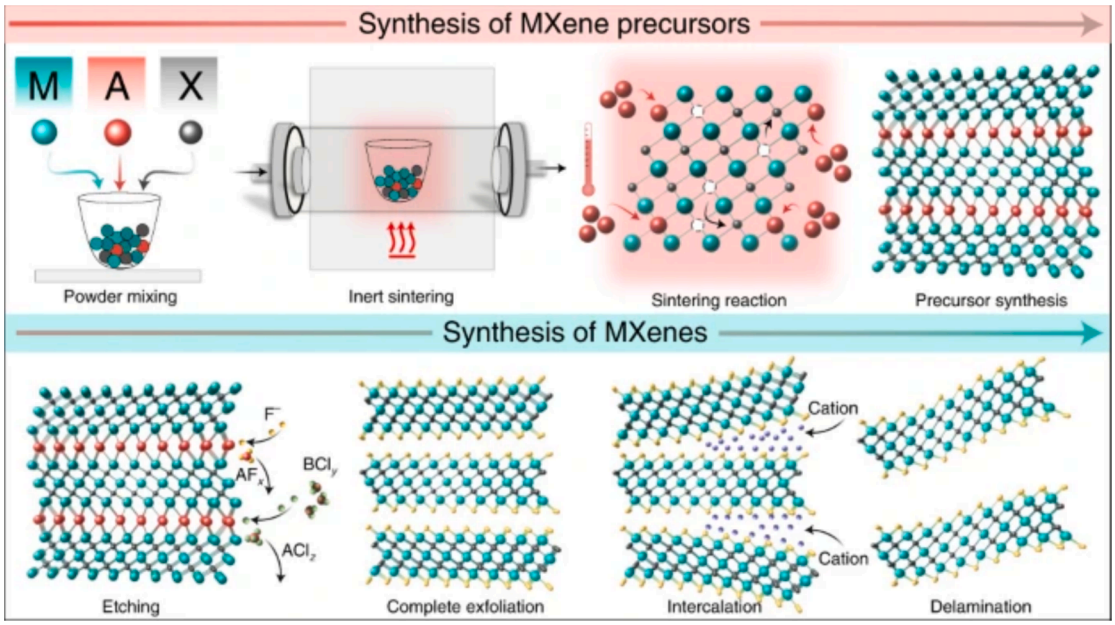

Fig. 6. Fundamentals of MXene Synthesis (Lim et al., 2022).

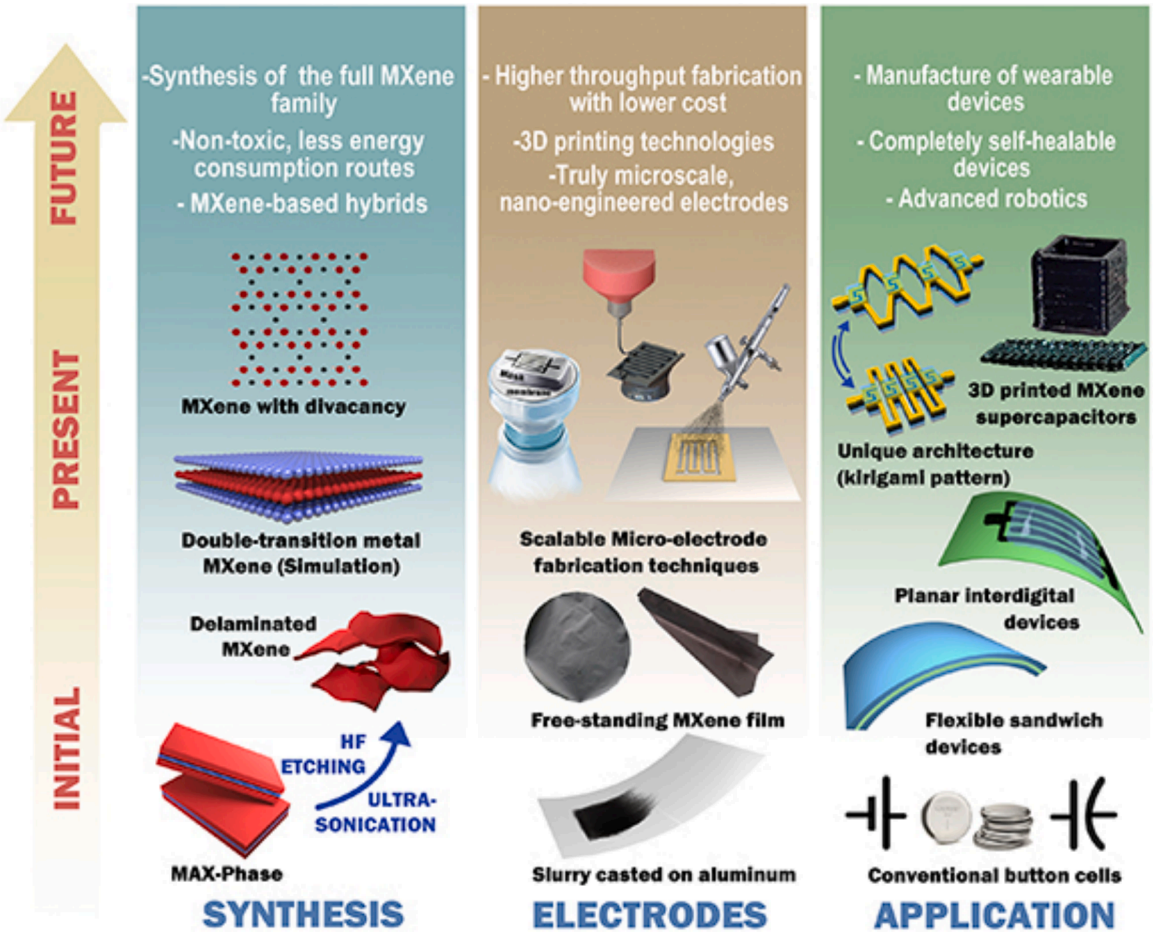

Fig. 7. (Left) The purposes behind the synthesis of MXene have evolved over time. These objectives have advanced from HF etching of the MAX phase to preparing MXene with ordered divacancy and modeling the double-TM MXene (Das and Wu, 2020). Vacuum-filtered free-standing MXene films were prepared in (Tao et al., 2017) (Middle) thanks to the development of methods for creating electrodes on aluminum using conventional slurry-casting. (Right) Button cells have been replaced in SCs and MXene-based batteries with more flexible alternatives. In addition to 3D-printed devices, they have also been used in unusual architectures such as kirigami patterns (Jiao et al., 2019; Ling et al., 2014).

Fig. 8. Essential strategies for the bottom-up and top-down synthesis of MXene, Dai P (Dai et al., 2023).

Among the notable characteristics of MXene are its enhanced electric and thermal conductivities, tunable bandwidth, and maximum range of Young's modulus, which are acknowledged as unique and advantageous. Shahzad et al., 2016, MXenes differ from other two-dimensional materials like graphene because they are hydrophilic and have better thermal conductivities (Shahzad et al., 2016). Low thickness, high conductivity, and suitable flexible materials that block electromagnetic interference (EMI) are highly desired; this is especially true if the materials can be readily made into films. MXenes are two-dimensional metal nitrides and carbides that have hydrophilic surfaces and metallic conductivity s combined. Numerous MXenes and their derived polymer composites have shown great potential in EMI shielding applications. The best EMI shielding efficacy of 92 dB was demonstrated by a 45-μm-thick $Ti_3C_2T_x$ film out of synthetic materials of comparable thickness produced to date (>50 dB for a 2.5-μm film). The numerous internal reflections from $Ti_3C_2T_x$ flakes in free-standing films and the high electrical conductivity (4600 Siemens per centimeter) of $Ti_3C_2T_x$ films are responsible for this performance. MXenes and their composites can efficiently shield surfaces from electromagnetic interference on any shape because they are easily coated and mechanically flexible characteristics of electricity.

Numerous computer studies have been conducted on the giant electronic anisotropy (Khazaei et al., 2015), massless Dirac dispersion close to the topological insulator function and Fermi level, and other electronic properties of MXenes (Liang et al., 2017). Even though most predicted properties have not yet been observed experimentally, these attributes make MXenes one of the most researched two-dimensional materials. This section of the review includes recommendations for potential experiments to validate the predictions and an overview of the theoretical research.

The d-electrons from the "M" TMs are responsible for the high electron densities observed in prime MXenes, which are close to the Fermi-level metallic conductivities. It is essential to highlight that in ordered double-M structures, the outer TM layers affect the electronic properties more than the metal inner layer.

Density functional theory (DFT) is employed by Liu, M. Z. et al. (Liu, M.-Z. et al., 2023) to investigate the quantum capacitance and electronic properties of N-doped and pristine Hf_2CO_2 (PH) systems. Every doped system exhibits metallic properties. The redshifts of the C-p, O-p, Hf-p and Hf-d states in the valence band progressively rise as the concentration of N-doping increases. N-doping is an effective way to modify the quantum capacitance and Hf_2CO_2 monolayer's electrode type. PH systems that are N-doped at concentrations of 11, 22, 33, 44, 56, and 67 % are viable candidates for anode materials. N-doped PH systems, on the other hand, are appropriate for symmetric electrode materials in an aqueous system at concentrations of 89 % and 100 %. PH systems with a 78 % N-doped concentration and phosphorus are examples of possible cathode materials. The PH system's electrode type is altered by the wide voltage at N-doped concentrations of 78, 89, and 100. Additional research is done on the N-doping MXene electrode type with mixed terminations (Liu et al., 2023; Yin et al., 2023).

When used as a supercapacitor electrode, MXenes exhibit superior electrochemical properties (Yin et al., 2023). The quantum capacitance and electronic properties of Zr_2CO_2 with atomic swapping through density functional theory, Yin et al., 2023. The atomic swap results in defects of the Schottky and Frenkel types appearing. The systems under study are stable, as confirmed by the negative binding energy. Because of the atomic exchange, the ZrO_1, ZrO_2 and ZrC_1, ZrC_2 systems continue to exhibit their indirect semiconductor features, whilst the CO_2 system displays a direct semiconductor property. The thermionic emission performance of Zr_2CO_2 MXene is significantly improved by atomic swapping. In an aqueous system, ZrO1 and ZrO2 systems make suitable anode materials. The electrode type is not significantly affected by the wide voltage in ideal ZrO_1, ZrO_2, Zr_2CO_2, CO_1, and CO_2 systems. On the other hand, it does change the aqueous cathode material in the ZrC1 and ZrC2 systems into an ionic/organic anode material. The work function and effective mass are still being investigated by Yin, S. H. et al. (Yin et al., 2023).

Evaluations are conducted on MXene's setup, characteristics, difficulties, and main discoveries. Because of their electronic and electrochemical characteristics, MXene offers a variety of options for adjusting their compositional stoichiometry. Emerging 2D materials are called MXenes, which are layered carbides, nitrides, or carbonitrides nanomaterials. The primary precursor of MXene is typically referred to as MAX phases, which are layered ceramics with a combination of ceramic and metal properties.

2.4. MXene-based microelectronic devices

The development of flexible and compact microbatteries (MBs) is imperative owing to the serious need for their integration with batteries of small sizes. Moreover, compatibility and miniaturization are needed for large-scale MB construction, so planar MBs with scalable shapes must be developed (Beidaghi and Gogotsi, 2014).

As the next-generation micro-power solutions with high safety, micro-SCs (MSCs) and MBs, based on non-flammable aqueous electrolytes, are seen as promising to serve the quickly expanding fields of wearable and implantable microelectronics (Beidaghi and Gogotsi, 2014). MSCs perform better electrochemically than rechargeable MBs in terms of rate capability, power density, and cycle life because of their quick electrode reactivity (Gao et al., 2011). However, the low energy density ($\leq$10 μWh cm^2) of MSCs is known to severely limit their application in industrial environments. Ion addition and extraction from the electrode material, however, is the basic process of charge storage in metal-based batteries. Li et al., 2019 found that although this bulk process may attain a high areal energy density, the insertion/extraction kinetics of ions with large ionic radii are slow, resulting in poor areal power density (Li et al., 2019). Therefore, it is a well-known issue that

neither MBs nor traditional MSCs can concurrently meet high power and energy density requirements. The field of hybrid micro-SCs (HMSCs), has gained attention lately.

HMSCs integrate the benefits of two separate energy storage technologies by joining the electrodes of an ion adsorption capacitor and ion intercalation battery. The quantity of ions that this hybrid device's capacitor-type electrode can effectively absorb or desorb determines the device's energy density (Sun et al., 2018).

In zinc-ion hybrid micro-SCs (ZHMSCs), two-dimensional TM carbide/nitride (MXenes) is a viable contender for novel capacitor-type electrode materials due to its structure being multi-layered and attainable metallic conductivity (Sun et al., 2018). MXenes' effective ions intercalation between layers allows them to store a significant amount of charge quickly. This is because MXenes operate on a recently identified method of intercalation pseudocapacitance, where charge transport proceeds without interference from diffusion into solid phases. The interlaminar gap between densely self-assembled MXene nanosheets is greatly reduced by strong vdW forces and hydrogen bond interaction between the few-layered MXenes, as has been observed in other two-dimensional materials. According to Cheng et al., 2021, multivalent ions typically have greater ionic radii and stronger coulomb interactions because to the many negative terminal groups on the MXene surface; this significantly hinders their ability to be inserted or deintercalated rapidly and reversibly (Fig. 9) (Cheng et al., 2021). This problem is a significant barrier to the development of prospective MXene-based ZHMSCs based on divalent zinc ions, even if it hasn't affected the energy capacity of conventional MXene-based MSCs based on monovalent hydrogen ions as much.

In addition to Cheng (Cheng et al., 2021), microSCs are not as advantageous as micro-batteries owing to their low energy densities. MXenes show promise as a more energy-dense substitute for zinc-ion hybrid micro-supercapacitors (ZHMSCs) in capacitor-type electrode materials. Nevertheless, large radius intercalation of multivalent zinc ions is inefficient due to their closely spaced layered structure. One approach to interlayer structural modification for capacitor-type electrodes based on MXene/BC@PPy toward ZHMSCs has been reported by Cheng et al (Cheng et al., 2021). This method inserts one dimensional core–shell conductive nanofibers based on BC@PPy between nanosheets of MXene. The method was found to significantly increase the areal capacitance of the MXene/BC@PPy film electrode, reaching 388 mF cm^{-2}, a 10 times increment over the pristine MXene film electrode. By effectively increasing electron and ion transport in the layered MXene structure, this was achieved. This involved utilizing the conductive BC@PPynanospacer to form conductive connections between the loose MXene layers in order to accomplish two goals at the same time: (i) expanding the interlayer space and (ii). The resultant ZHMSCs demonstrated an astounding 95.8 % capacity retention after 25,000 cycles when combined with CNTs/MnO_2 battery-type electrodes, with an aerial energy density of up to 145.4 μWh cm^{-2}. This MSC has the highest rating among the recently reported MXene-based MSCs when compared to micro-batteries. The inter-layer structural modification of the capacitor-type electrode based on MXene provided a feasible way to attain battery-level energy density in the ZHMSCs (Fig. 10).

As wearable electronics advance quickly, compatibility and small energy storage devices become increasingly important (Dai et al., 2023). MSCs, one of the most attractive alternatives, have garnered a lot of interest due to rapid charge/discharge rates, high power densities, and extended operating lifetimes. Deformable MSCs, which ensure the flawless operation of wearable electronics, are gaining popularity because they can withstand different deformations like twisting, bending, and stretching better than other materials. Compared to traditional, stiff MSCs, this is different. Dai et al, a unique class of two-dimensional TM nitrides/carbonitrides known as MXenes has a lot of potential for use as MSC electrode materials owing to their high metallic conductivity, high specific surface area, strong hydrophilicity, and surface chemical tunability. Based on MXene, stretchable MSCs with a planar, fiber-shaped configuration have been investigated (Dai et al., 2023). In order to ensure the continuous progress of MXene-based, stretchable MSCs, they have also highlighted the primary challenges and prospects for practical implementation.

2.5. MXene-based stretchable MSCs

According to Jiang et al., MSCs, a new breed of MESD, have several advantages over conventional SCs, including a longer operational lifetime (>100,000 cycles), a higher power density (>10 mW cm^{-2}), and a shorter ion transport pathway (Jiang et al., 2020). MSCs have many benefits, including a high-power density, fast charge/discharge rates, and an extraordinary lifetime (more than 100,000 cycles) that doesn't require maintenance (Jiang et al., 2020). Microscale electrochemical energy storage, or MSCs, is a potential replacement for conventional solid-state capacitors and (Tan et al., 2023).

Since fiber-shaped stretchable MSCs, also known as yarn-shaped stretchable MSCs or wire, have a unique one-dimensional structure and can be freely connected in series or parallel to form an integrated power module, Liu et al. (2016) have given them a lot of attention. Because of this, they are particularly well-suited to supply wearable electronics with steady power in a variety of demanding situations (Liu et al., 2016).

Micro-SCs, or MSCs, have garnered a lot of attention lately because of their potential uses as small device primary power sources. A planar interdigitated electrode on an insulating substrate that is physically separated to provide electrical isolation makes up the majority of MSCs (Wang et al., 2018). Micro batteries have a lower power density and

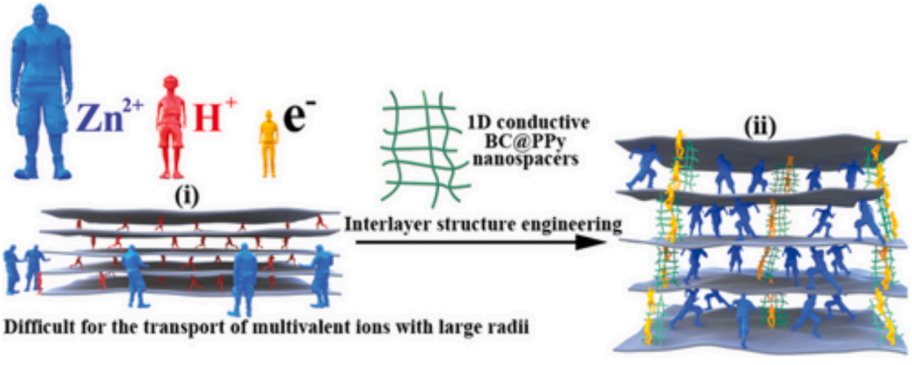

Fig. 9. An illustration of the MXene hybrid film's suggested interlayer structure engineering: (i) the well-known challenge of intercalating multivalent ions like Zn^{2+} that have a large ionic radius. Since the introduction of the smaller, more conventional hydrogen ions, this issue has not been as serious. (ii) Large ions can be inserted and deintercalated quickly and reversibly by inserting 1D nanospacers, which increase the gap between MXene nanosheets. Enhancement of electron flow between loose MXene nanosheets is also achieved by the nanospacers. Cheng et al. (Cheng et al., 2021).

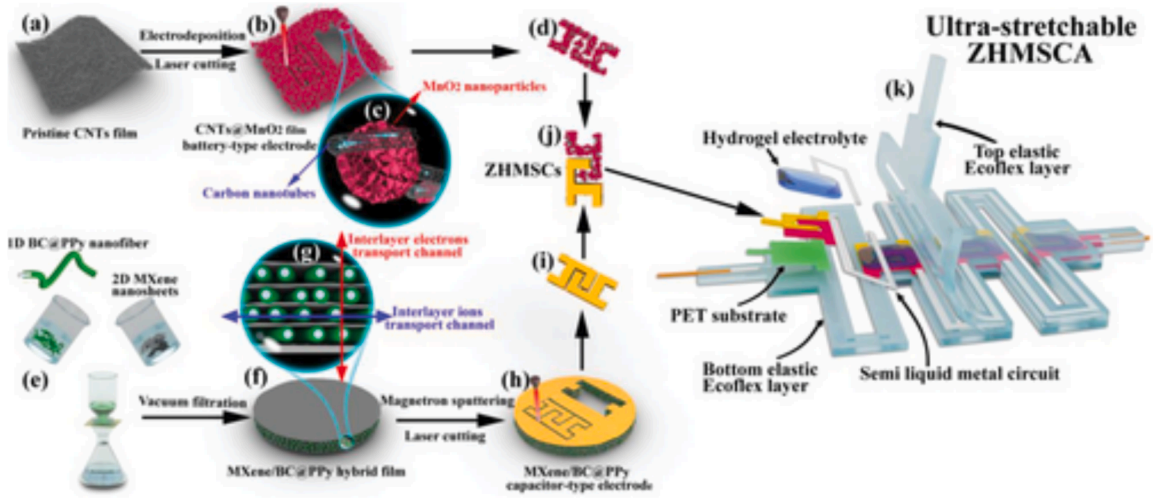

Fig. 10. An illustration of the ZHMSCA's ultra-stretchable production process (a) A pure carbon nanotube (CNT) film with randomly oriented carbon nanotubes; (b) MnO_2 nanoparticles electrodeposited on the CNTs film surface towards the CNTs@MnO_2 hybrid film, which was then laser-cut into an interdigital CNTs@MnO_2 battery-type electrode; (e) Following vacuum filtration, a blend of two-dimensional MXene nanosheets and one-dimensional BC@PPy nanofibers was generated; (f) MXene/BC@PPy hybrid film, which was then laser-cut into an electrode that resembled an interdigital capacitor; (j) ZHMSC was assembled; (k) The zoomed schematic diagrams of the microstructure; the ultra-stretchable ZHMSCA's decomposition diagram (c, g) (Cheng et al., 2021).

typically have a lifespan of 500–10,000 cycles. Additionally, as they get bigger, their volumetric performance characteristics get smaller. As the foundation for MSC device electrodes, two-dimensional materials with intrinsically large surface areas made electrochemically active and nm-thin layers aligned in the direction of electron/ion transport show promise (Khazaei et al., 2017; Tan et al., 2023). TM dichalcogenides, graphene, oxides, black phosphorus, and MXenes TM nitrides and carbides are examples of materials with high electrochemical activity that can support the rapid and reversible surface faradaic redox reaction that helps with charge storage in electrochemical devices. Their high electrical conductivity can also accelerate the rate at which the electrolyte ions diffuse, absorb, and release charges (Cai et al., 2018; Ma et al., 2017; Peng et al., 2016).

There are a number of benefits to using MXene as the MSC active electrode as opposed to other two-dimensional materials (Li et al., 2018). Because of the strong vdW interaction between neighboring nanosheets, two-dimensional materials frequently self-restack. It is believed that severe self-restacking affects intrinsic electrochemical properties like rate capability and reduces electrolyte ion access. A variety of materials have recently been introduced as spacers to hybridize with MXenes in an attempt to reduce restacking and improve the electrochemical performance; examples include black phosphorus (BP), carbon derivatives, carbon nanotubes (CNTs), graphene as EDLC materials (Tuzluca Yesilbag et al., 2023; Wang et al., 2016), hydroxides, polypyrrole, and MnO_2, as pseudocapacitive materials (Barsoum and Radovic, 2011; Huang et al., 2019).

The potential for using interdigitated MXene composite and MXene electrodes in the production of MXene MSCs has been limited due to their time-consuming nature, non-scalable nature and despite the development of numerous efficient methods to improve the devices' electrochemical performance. Scalable techniques for the necessary pattern transfer of current electrode materials onto substrates have recently been developed (Peng et al., 2016). Among these techniques are screen printing, inkjet printing, and spray coating. The printed architecture must be preserved using conductive additives, binders, or surfactants due to the rheological properties of printing materials (Peng et al., 2016). Moreover, this technology's highly interdigitated electrode footprint leads to low energy/power density and low capacitance, which are major barriers to its wider application. In order to realize the concept of "the Internet of everything," which is characterized by wearable, multifunctional, and integrative microelectronics, the development of MBs and MSCs has accelerated with the advent of "intelligent" electronics. Their application in implantable medical sensors, micro/nano-robots, self-powered supply systems, and patient tracking has garnered a lot of support. Creating "light, small and thin" portable electronics has become more and more popular in recent years. Micropower sources are desperately needed as a result of the push to reduce electronics from meter-scale devices like personal computers to millimeter-scale devices like portable devices and eventually micro/nano-scale devices (Peng et al., 2016).

In anticipation of future applications in portable, wearable, and tiny microelectronics, Kim, E. et al. (Kim et al., 2022) present a straightforward, reliable process for creating flexible, on-chip MSCs that can be scaled up and manufactured sustainably. MSCs are useful as integrated power supplies in electronic systems due to their extended lifespan and high-power density. Nevertheless, the lower energy density and volumetric capacitance of traditional double-layer carbon SCs restrict their usefulness. Using a photolithography-based solution process and microfabrication technique, interconnected three-dimensional nanoporous MXene electrodes and pristine MXene were micro-patterned in an interdigitated fashion. These were then put on flexible substrates after that. These 8-inch wafer-mounted, 107-chip flexible MSCs meet the requirements for scalable manufacturing. At the 8-inch level of integrated microelectronics, their exceptional 1,727F cm^{-3} volumetric capacitance—the best ever documented for MXenes—and their desired customization are all significant factors. They maintain an impressive energy density of 41.9 mWh cm^{-3} at a high-power density of 26.8 W cm^{-3}. Furthermore, only the two-dimensional MXene sheet planar interdigitated electrode micropatterns exposed to tensile stress on flexible polymer substrates showed a 140 % increase in volumetric capacitance after 10,000 bending cycles.

Because of their high metallic conductivity, adjustable interlayer spacing, and intercalation pseudocapacitance, MXenes have demonstrated great promise for micro-supercapacitors (MSCs). Specifically, MXenes' high hydrophilicity and negative surface charge make them appropriate for a range of solution processing techniques. However, we provide an overview of the MXene MSCs' integrated system and intelligent applications, as well as the difficulties and opportunities that still lie ahead for the creation of high-performance MXene MSCs.

2.6. Emerging materials based on MXenes for supercapacitor applications

SCs based on MXene exhibit exceptional cyclability, high power, and ultrahigh volumetric capacitance, which make them highly promising as electrochemical energy-storage devices (Pu et al., 2023; Yin et al., 2023). Table 2 illustrates the capacitive performance of MXenes and their composites-based symmetric and asymmetric supercapacitors. Although the underlying self-discharging mechanism is still unknown, they exhibit severe self-discharging behavior. Thus, a novel mitigation technique based on the surface electronic structure of MXenes is suggested by Pu et al.'s (Pu et al., 2023) analysis of the self-discharge properties of SCs based on MXene. By removing hydroxyl terminations, a superficial engineering technique based on bio-thermal treatment is created to successfully alter the surface electronic structure of $Ti_3C_2T_x$ MXenes. The elimination of hydroxyl groups from MXenes causes this decrease process by raising the work function and, eventually, the zero-charge potential. Electrolytes and MXene have higher surface free energy due to the increased surface dipole. MXenes have less robust self-discharge kinetics as a result of these two favorable effects. More accurately, there has been a notable decrease in the activation-controlled self-discharge process. It will be easier to develop high-performance energy storage if the relationship between self-discharge and electronic structure that coexists with surface engineering suppression techniques is made clear. Interestingly, flexible electronics like SCs require strong and high conductivity freestanding films (Tang et al., 2022).

Table 2
The electrochemical performance of MXene based supercapacitors.

MXene supercapacitor Electrode (Cathode// Anode) Electrolyte	Electrochemical performance (Capacitance, Energy density, and Power density)	References
V_2O_5//$Ti_3C_2T_x$ MXene ZIHMSC $ZnSO_4$ dissolved PAM hydrogel	Capacitance: 129 mF cm^{-2} at 0.34 mA cm^{-2} Energy density: 673 μW cm^{-2} Power density: 0.02 mWh cm^{-2} 10,000 cycles Capacitance retention: 77 %	(Zhang et al., 2016)
ONCFT//MNCFT PVA/H_2SO_4	Capacitance: 780 mFcm^{-2} Energy density: 277.3 μWh cm^{-2} Power density: 624 μW cm^{-2}	(Champagne and Charlier, 2021)
RGM-H_2SO_4 1 M H_2SO_4	Capacitance: 454.9F cm^{-3} at 10 mV s^{-1} Energy density: 39.4 Wh/L Power density: 180 W/L	(Zhang et al., 2015)
$Ti_3C_2T_x$/CNF/PC PVA/KOH.	Capacitance: 143 mF cm^{-2} at 0.1 Ma cm^{-2} Energy density: 2.4 μ Wh cm^{-2} Power density: 17.5 μW cm^{-2}	(Jing et al., 2021)
MGH//PGH 1 M KCl	Capacitance: 137.5F/g at 10 mV s^{-1} Energy density: 30.3 Wh kg^{-1} Power density: 1.13 kW kg^{-1}	(Jiang et al., 2020)
MAX (Ti_3AlC_2) phase diluted HF with HCl mixture of acidic solution	Capacitance: 105.75F/g Current density: 1 A/g. Over 10,000 cycles Capacitance retention: 97.72 %	(Thirumal et al., 2024b)
$Ti_3C_2T_x$ MXene/$NiCo_2O_4$ dimethyl sulfoxide (DMSO)	Energy density:36.67 Wh kg^{-1} Power density: 800 W kg^{-1} 5000 cycles Capacity retention: 88.2 %	(Wang, W. et al., 2024)
Sb-ball milled material, MXene, and Sb@MX composites (Ag/AgCl)	Specific capacitances of 184.72 F/g, 65.10 F/g, and 36.61 F/g, current density of 1 A/g within the voltage range of 0.00—1.44 V. Over 10,000 cycles Capacity retention: 53.10 %)	(Thirumal et al., 2024a)
CoAl-LDH/s-MXene electrode	Specific capacity of 1259.9 C/g at 1 A/g Energy density: 104 and 88 Wh kg^{-1} at 1500 and 6000 W kg^{-1}. Over 5000 laps at 10 A/g Capacitance retention: 86.6 % Coulomb efficiency: ~ 100 %	(Yan et al., 2024)
SnO_2/carbon dots@MXene	Specific capacitance: 1074F/g Energy density: 51.11 W h/kg Over 10,000 cycles Capacitance retention: 103 %	(Moniruzzaman et al., 2024)
WS_2/rGO/CNT Hybrid Electrodes Polymer-Based Ionic Liquid Electrolytes	Potential window: 3.5 V Capacitance of 5.04F cm^{-3} (67.60F/g) Current density:135.93 mA cm^{-3} Energy density: 115.01 Wh kg–1 (or 8.50 mWh cm^{-3}) Power density: 3.18 W kg^{-1} (235.30 mW cm^{-3})	(Sengupta and Kundu, 2024)

The cellulose filaments of micron/nano-size, MXene nanosheets, and Ag NWs were uniformly combined through the rapid and scalable vacuum-assisted filtration process to produce a hierarchical leaf-like structure of PM_xAg composite paper with high conductivity. In cellulose and MXene composites, Ag NWs can easily form multiple hydrogen bonds, making it easier for MXene nanosheets to wrap around the cellulose filament. This leads to the creation of a biomimetic nanostructure that resembles a leaf and has a conductive, interwoven 3D framework, just like a real leaf. Silver nanowires (Ag NWs), "vein-like" cellulose filaments, and "mesophylls-like" MXene (Ti_3C_2TX) nanosheets work together to create a freestanding paper through rapid vacuum filtration. The resulting nanocomposite paper has high conductivity (58 843 S/m^{-1}) and good mechanical properties (Young's modulus of 6 GPa and tensile strength of 34 MPa). It is composed of 25- wt% $Ti_3C_2T_X$ ($PMxAg_{25}$–8) and 8- wt% Ag NWs. The interactions between the three-dimensional interpenetrating frameworks and cellulose-MXene are responsible for these outcomes (Tang et al., 2022). The electrochemical performance of the nanocomposite papers can be further enhanced by this interpenetrating framework, Tang H et al. discussed that a foldable paper electrode (shown in Fig. 11) with only 25 wt% MXene can display a high capacitance of 505F g^{-1} (Tang et al., 2022). A common and robust structure is the leaf-like structure, as seen in (Fig. 11A). Inspired by the structure and function of natural leaves, biomimetic PM_xAg composite papers have been designed with faster ion channels and improved mechanical stability, as schematically shown in (Fig. 11B). Accordingly, the aqueous dispersion made up of MXene, cellulose filaments, and Ag NWs was filtered out using vacuum assistance to create the freestanding composite papers (PM_xAg) (Fig. 11C). With the use of this biomimetic approach, PM_xAg composite paper electrodes could be easily produced on a large scale without the need for costly equipment or additives. The resulting composite paper could be cut and folded into precise shapes without causing any obvious damage. It was strong and flexible (Fig. 11C). Scanning electron microscopy (SEM), as demonstrated in Fig. 11D, could be used to visually verify the formation of a leaf-like micro/nanostructure in composite paper. The successful coating of MXene nanosheets on the surface of cellulose filaments is indicated by the clearly visible MXene nanosheets coated on the fiber surface and their classic wrinkle layer structure of 2D-material nanosheets.

It is anticipated that the needs of sustainable development will be taken into consideration in the design of this new generation of highly integrated, adaptable, and portable SCs with excellent capacity and rate performance. In two-dimensional, TM nitride and carbide exhibit high prospects as energy-storage materials. However, two-dimensional nanosheets' propensity to reorganize and aggregate limits their electrochemical performance. Sun et. Al., (Sun et al., 2021), explains a novel heterostructure based on carbon fibers derived from hierarchical porous MXene/biomass (MXene/CF) that resembles "skin/skeleton" and effectively weakens MXene nanosheet stacking. The pyrolysis process was

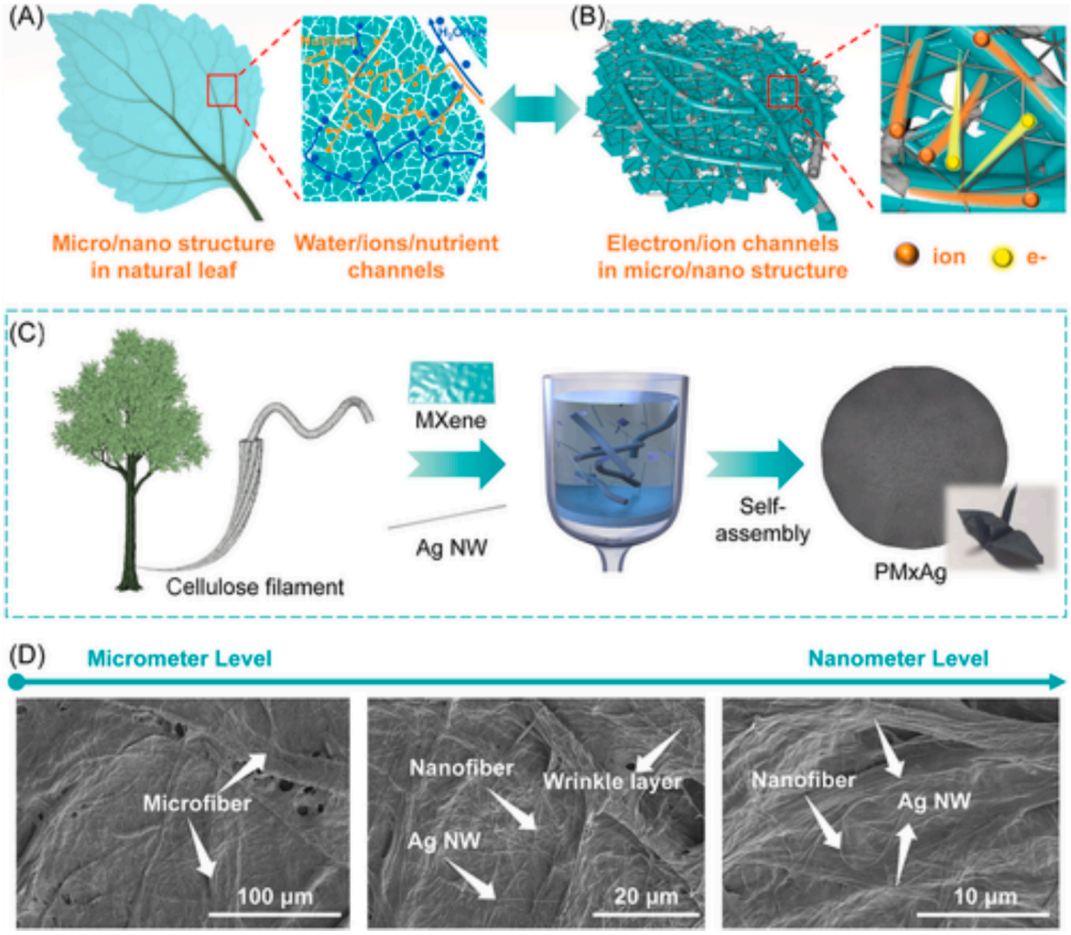

Fig. 11. Composite papers with a hierarchical structure and fast ion channels are fabricated using bioinspired techniques. (A) Schematic diagram showing the material transfer and micro network structure in a normal leaf. (B) Schematic diagram showing how paper materials with comparable structures and quick ion channels are designed. (C) The process of preparing composite papers by vacuum filtration and showcasing a paper bird folded using the flexible paper that is created (PM_xAg). (D) PM_xAg composite paper morphology from the microscale to the nanoscale (Tang et al., 2022).

done in one step. Functional MXene-based electrodes are also produced by the clearly defined porous hierarchical structure of MXene/CF, which permits electrolyte penetration and offers stable, effective channels for ions to diffuse quickly to the electrode (Sun et al., 2021). The MXene/CF heterostructure is a promising self-supporting electrode for SCs, with a high volumetric capacitance of 7.14F cm^{-3}, good rate characteristics (63.9 % from 0.5 to 100 A/g) and good cyclic stability (99.8 % after 5000 cycles). In addition, each assembled MXene/CF electrode-based solid-state symmetric supercapacitor exhibits high capacitance, rate performance, and long durability and remarkable flexibility. The device maintains its structural stability and steady capacitance at various bending angles even after 2500 cycles (Fig. 12) (Sun et al., 2021).

MXenes are typically used in applications related to energy storage. On the other hand, large nanosheets and restacking impede ion diffusion and lower its rate of diffusion. A technique for manufacturing porous and flexible electrodes based on MXene-M supercapacitor can be used to simultaneously create holes in the layers and increase the interlayer spacing. At a current density of 100 A/g, and after 100,000 cycles $Ti_3C_2T_x$–Mn shows an exceptionally long lifetime, holding 248F/g. In addition, the all-solid-state symmetric supercapacitor based on $Ti_3C_2T_x$–Mn demonstrates excellent volumetric energy up to 52.4 mWh cm^{-3} and maintains 38.4 mWh cm^{-3} at a very high volumetric power

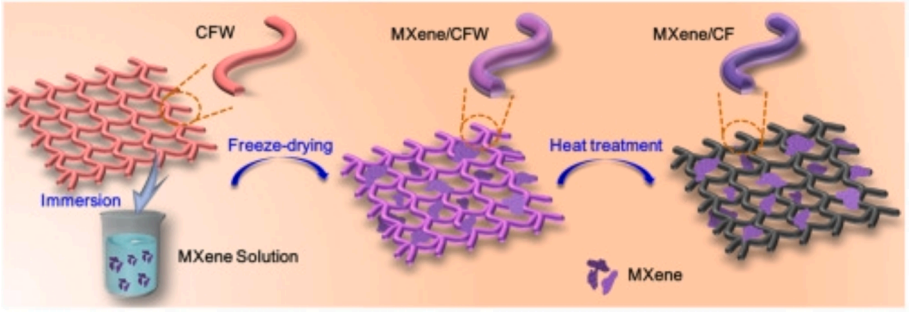

Fig. 12. Multilayered, porous carbon fibre heterostructure made of MXene and biomass-derived carbon fibres that resembles a "skin" or skeleton for flexible, self-sustaining solid-state SCs (Sun et al., 2021).

density of 55.3 W cm^{-3}. The next generation of realistic high-power density and energy density applications can greatly benefit according to Xu et al. (Xu et al., 2023). It also provides guidance for future MXene layer spacing regulation and porous structure design (Fig. 13).

Zhao et al. (Zhao et al., 2018) have reported the first-ever Ti_3C_2/Ni-Co-Al layered double hydroxide (LDH) heterostructures. The synthesis of these heterostructures involves the application of an electrostatic attraction hetero-assembly strategy and a simple liquid-phase co-feeding between positively charged Ni-Co-Al-LDH and negatively charged Ti_3C_2 nanosheets. The resulting structures are made of alternating stacks of molecular-level nanosheets (Fig. 14). Molecular-level Ti_3C_2/Ni-Co-Al-LDH heterostructures can show markedly improved dynamic behavior in the Faradaic reaction, leading to a high-power density, when both pseudocapacitive and conductive components are present. Although ions have the shortest diffusion pathway and the best charge transfer efficiency, they diffuse along two-dimensional galleries more quickly than electrons through Ti_3C_2 layers. The Ti_3C_2/Ni-Co-Al-LDH heterostructure, at a current density of 1 A g^{-1}, demonstrates a specific capacitance of 74–1. 8.2F g^{-1}, indicating an increased rate capacity. An all-solid-state flexible asymmetric supercapacitor with Ti_3C_2/Ni-Co-Al-LDH as the positive electrode can achieve an optimum energy density of 45.8 Wh kg. The findings suggest that molecular-level heterostructure may be a practical choice for high-energy SCs in the future.

Previously, only nontransparent, micrometer-thick films were studied; however, Zhang et al. (Zhang, C. et al., 2017) have reported the use of extremely conductive and transparent $Ti_3C_2T_x$ films as transparent solid-state SCs. If $Ti_3C_2T_x$ nanosheet colloidal solutions are spin-casted and then annealed at vacuum at ca. 200 °C, it yields transparent films. Films with transmittances of 29 % (≈88 nm) and 93 % (≈4 nm) exhibit DC conductivities of ≈5736 and ≈9880 S cm^{-1}, respectively. These conductive, highly transparent $Ti_3C_2T_x$ films exhibit a remarkable volumetric capacitance of 676F cm^{-3}, and they react rapidly. Moreover, transparent solid-state asymmetric SCs with a 72 % transmittance are made using films of single-walled carbon nanotubes (SWCNTs) and $Ti_3C_2T_x$. Compared to transparent devices based on SWCNT or graphene supercapacitors, the electrodes perform better. They also have a higher capacitance of 1.6 mF cm^{-2} and a longer lifespan (no capacitance decay over 20,000 cycles). Together, the $Ti_3C_2T_x$ films provide the most sophisticated transparent, conductive, and capacitive electrode technology currently accessible, and they have the potential to be a financially successful part of the upcoming generation of wearable and portable electronics.

MXenes are recently developed electrode materials designed to be used in capacitors with an electric double layer. The specific capacitance of these is greater than 300F/g. Though it is currently unknown how surface functional groups affect capacitive characteristics, recent advancements in synthesis techniques have made it possible to reduce surface functional groups and have chemical control over their design. Based on the terminated halogen elements of $Ti_3C_2T_2$ MXene electrodes, Shimada et al. were able to determine the atomic-scale double-layer structure of these electrodes (Shimada et al., 2022) and carried out a methodical investigation. Combining the reference interaction site model calculations, the effective screening medium, and the application of density functional theory. Fig. 15 shows the termination of the electric double-layer capacitance with a larger atomic number of halogen atoms (I > Br > Cl > F) (Shimada et al., 2022). Because of the lower electronegativity of the terminating atoms and lower valence electron numbers, electrons accumulate electrostatically at the electrode surface, increasing capacitance. When designing MXene surfaces with increased capacitance, this encouraging tendency offers a basis for new consideration.

The electrochemical characteristics of a single on-chip MSC are displayed in Fig. 16 (Xie et al., 2020). The CV curves of the on-chip MSCs show a good capacitive-like profile at various scan rates. Excellent capacitance retention occurs even at a high 200 mV s^{-1} scan rate, suggesting a feature for fast charge storage. Additionally, using the same MXene electrode thickness for comparison, symmetric on-chip MSCs based on MXene were created. Their CV curves exhibit a rather pronounced polarization at a scan rate of 10 mV s^{-1} when the voltage is close to 1.2 V. MXene performs nearly non-existent as the positive electrode because of its positive voltage and low specific capacitance, which removes any discernible redox peak. Remarkably, compared to symmetric on-chip MSCs, the areal capacitance of asymmetric on-chip MSCs is over five times greater (Fig. 16a). The Galvanostatic Charge Discharge (GCD) curves show the characteristic isosceles form at 100 A cm^2 (Fig. 16 b). Both the higher discharge duration and the bigger curve are indicative of asymmetric on-chip MSCs, these MSCs have an aerial capacitance that is significantly higher (7.8 mF cm^{-2}) than symmetric

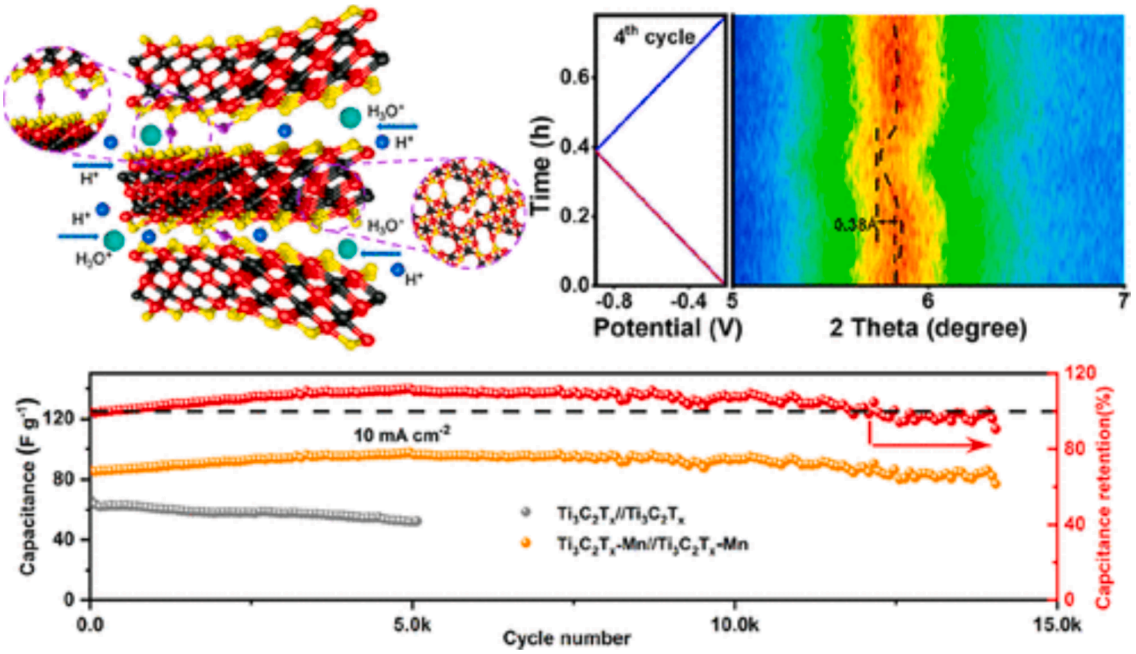

Fig. 13. Porous MXene with metal ion induction in all solid states for flexible SCs, Xu et al. (Xu et al., 2023).

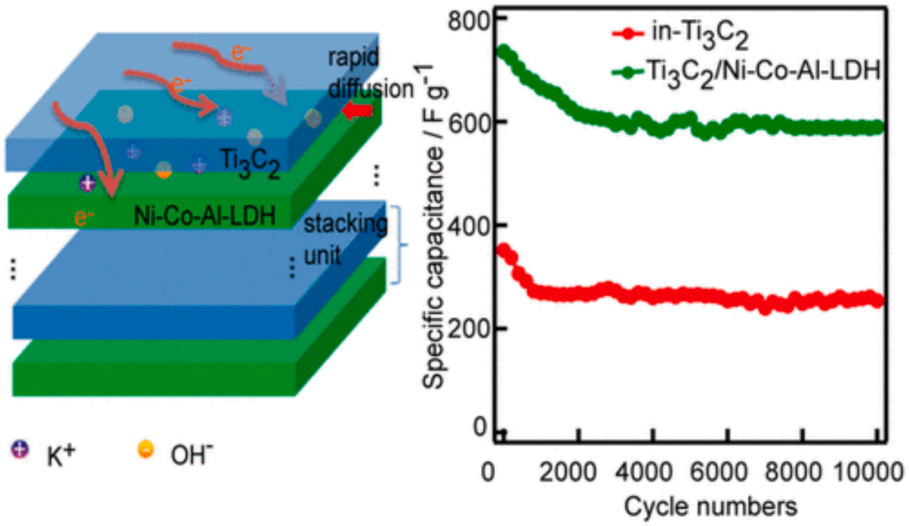

Fig. 14. Heterostructures at the molecular level built for all–flexible SCs from Ni–Co–Al layered double-hydroxide nanosheets and titanium carbide MXene (Zhao et al., 2018).

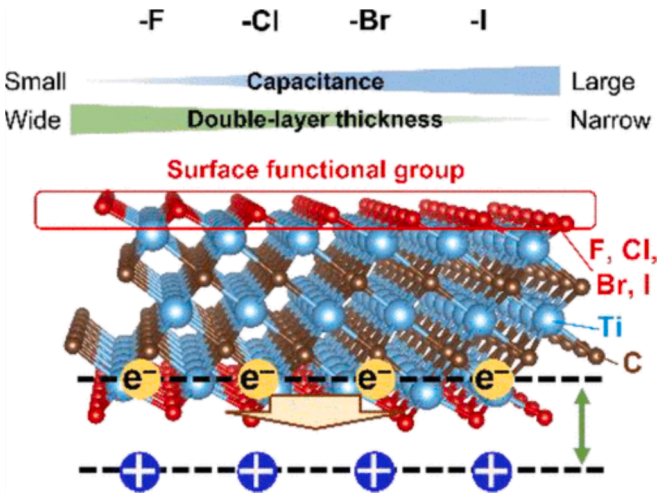

Fig. 15. Relationship between the surface functional groups and electric double-layer structure of the MXene electrode (Shimada et al., 2022).

MSCs (1.8 mF cm^{-2}).

The hydrophilicity of MXene electrodes is critical to their metallic conductivity, surface redox processes, and high-rate pseudocapacitive energy storage (Jiang et al., 2018). The voltage window of symmetric MXene SCs is restricted to about 0.6 V because of the risk of oxidation at high anodic potentials. An all-pseudocapacitive asymmetric device was developed in the study published by Jiang et al., (Jiang et al., 2018) by combining $Ti_3C_2T_x$, a titanium carbide MXene, serves as a positive electrode for ruthenium oxide (RuO_2). RuO_2 can function at negative potentials in an acidic electrolyte, which is how this was achieved. This asymmetric device operates at 1.5 V, and its voltage window is roughly twice as wide as that of symmetric MXene SCs. Out of all the SCs based on MXene that have been discovered so far, it has the largest voltage window. The device performance is significantly enhanced by RuO_2 and MXene's complementary working potential windows and proton-induced pseudocapacitance. Consequently, the asymmetric devices are able to produce a power density of 40 mW cm^{-2} and an energy density of 37 μW h cm^{-2}, and they are able to retain 86 % of their capacitance even after 20,000 cycles of charge and discharge. The results imply that pseudocapacitive negative MXene electrodes may be used in place of carbon-related components in asymmetric electrochemical capacitors to potentially boost energy density.

The formation of an electric double layer at the electro-electric interface (EEI) due to the piling of separated electric charges and the faradic redox reaction (surface-bound), which involves the transfer of charge between the electrolyte and the electrode material, are two significant phenomena that are governed by the charge storage mechanism of the supercapacitor (Wang, H. et al., 2018). Based on the aforementioned singularities, SCs have generally been classified as either pseudocapacitors or electric double capacitors. On the other hand, other carbonaceous materials are categorized as pseudocapacitive materials. Graphene, carbon nanotubes, activated carbon, MXenes, dichalcogenides (TMDCs), TM oxides (TMOs), and trichalcogenides (TMTCs), and among these substances are graphene (An et al.; Dall'Agnese et al., 2014; Ghosh et al., 2019; Lei et al., 2015). However, SCs are unable to achieve the required power density due to recurrent agglomeration and high internal resistance of these materials. Nevertheless, the ease of synthesis and high theoretical capacitance of materials for pseudocapacitive electrodes garnered a lot of interest. Nonetheless, the unstable design and lower conductivity of TMDCs and TMOs are still considered obstacles to high-performance SCs. The issues with both EDL and pseudocapacitive materials that were previously discussed can be avoided by choosing the appropriate nano-engineered material, including MXenes or vertically oriented graphene nanosheets (Dall'Agnese et al., 2014; Guirguis et al., 2020). While extremely porous vertically aligned self-supporting graphene nanosheets (VGN) address the difficulties of EDL-based materials, highly conductive MXene sheets circumvent the disadvantages of pseudocapacitive material (Thomas et al., 2022). These two materials indeed have capacitances; however, they are just a few $mF/cm^{2.}$ Therefore, it is possible to think of the combination of the EDL materials and pseudocapacitive as a traditional road map for achieving higher stability and better electrochemical performance. However, the performance of the SCs is mostly explained by the role of the current collector. The aforementioned issues can be resolved by combining sturdy Ti_3C_2 MXene with VGN (tangled bond through surface modification possessed VGN).

It is imperative to bear in mind that although MXenes' rich chemistry and surface functionalization enhance their electrochemical activity, they also considerably deteriorate their ability to self-discharge in SCs (Wang et al., 2020). Nasreen et al. (Nasrin et al., 2022) conducted extensive research on the improved surface functionalities of MXenes for SCs with intrinsically challenging flaws.

To achieve outstanding results, improving assembled two-dimensional/two-dimensional MXene heterostructures. Two-

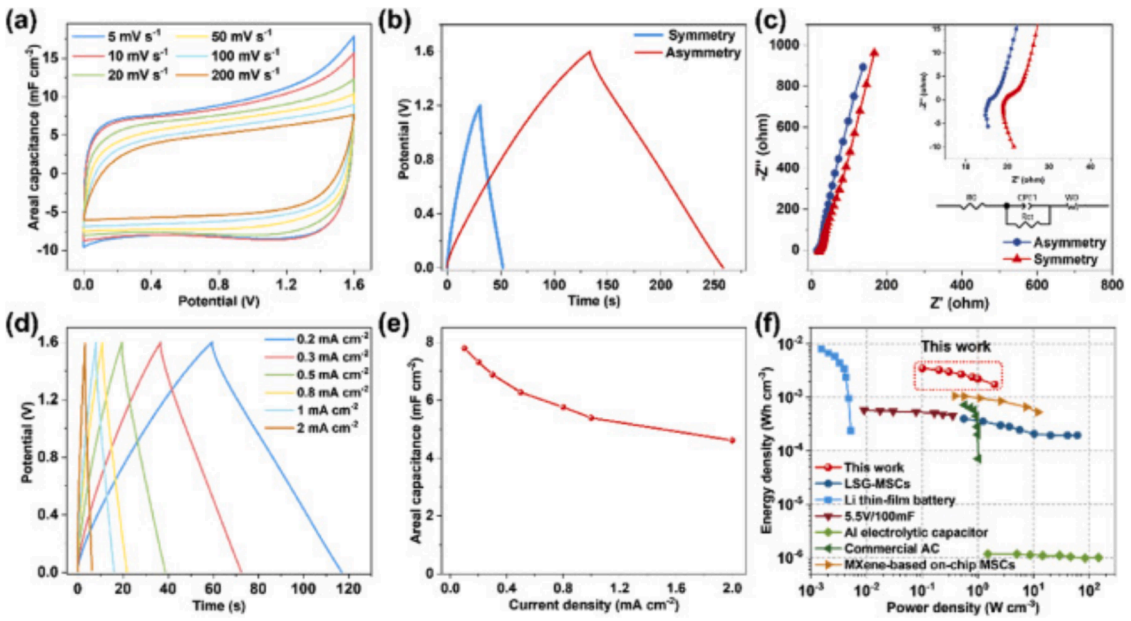

Fig. 16. The single-chip MSC based on MXene and its high-voltage electrochemical characteristics. The ones displayed are these ones: (a) CV curves at the scan rates varying from 5 to 200 mV s^{-1}; (b) GCD curves comparison of the asymmetric on-chip MSCs and the symmetric on-chip MSCs at 100 μA cm^{-2}; (c) The Nyquist plots and the fitted equivalent circuit; (d) GCD curves at different current densities; (e) The calculated areal capacitances; (f) The Ragone plots of the device.s (Xie et al., 2020).

dimensional MXene is a promising two-dimensional TM nitride, carbonitride, and carbide with hydrophilicity amazing potential, and excellent conductivity for charge storage. However, the self-discharge behavior and the underlying mechanism remain challenging issues. Wang et al. (Wang et al., 2020) have so far used a regulation strategy specific to the chemical interface to effectively address the self-discharge behavior of SCs based on $Ti_3C_2T_x$ MXene. In contrast to MXenes with higher F elements (~8.09 atom %), $Ti_3C_2T_x$ MXenes with lower F elements (~0.65 atom %) exhibit a positive decline in self-discharge rate of ~20 %. A substantial rise in tight-bonding ions brought on by a decrease in the *F* elements is associated with a process of individual self-discharge. The transition potential (*VT*) increases dramatically by 50 %. Because of this, the mixed self-discharge rate from ions with different numbers of F elements—loose-bonding and tight-bonding ions—decreases. The considerably altered local coordination data and average oxidation state on MXene acquired by chemically interface-tailored engineering impacted the interaction of counterpart ions. Delicate structures from X-ray absorption provided confirmation of this. Density functional theory theoretically explained the significantly improved self-discharge rate by pointing to more incredible adsorption energy at the electrode-electrolyte interface. This chemically interface-tailored technique may be used to create MXene-based SCs with high-performing and minimal self-discharge properties, supporting the broader commercial applications of this technology (Fig. 17).

One of the most promising integrated components is on-chip MSCs, which can supply sufficient energy support and peak power for electronic devices that are micro- and nanoscale in nature (Xie et al., 2020). However, their limited energy density and low operating voltage severely limit their large real applications, showing how to easily design and create high-voltage on-chip MSCs using a special cutting-spraying technique. The positive and negative electrodes are activated carbon and $Ti_3C_2T_x$ MXene, respectively. One asymmetric on-chip MSC can resolve the excessive polarization of MXene and provide a potential window of up to 1.6 V when using PVA/Na_2SO_4 as a neutral electrolyte. They outperform other competitors in on-chip energy storage at a power density of 100 mW cm^{-3} with an energy density of 3.5 mWh cm^{-3}. Additionally, they have a much higher stack-specific capacitance of 36.5F cm^{-3}, similar to an aerial capacitance of 7.8 mF cm^{-2}. Furthermore, MSCs exhibit exceptional capacity retention (91.4 % after 10,000 cycles), as depicted in Fig. 18. The high-voltage MXene-based on-chip MSCs depicted in Fig. 19 were built using a straightforward cutting-spraying technique, effectively resolving the issue where the positive and negative electrodes cannot be connected to the substrate without interfering with one another in order to balance the charge. In contrast

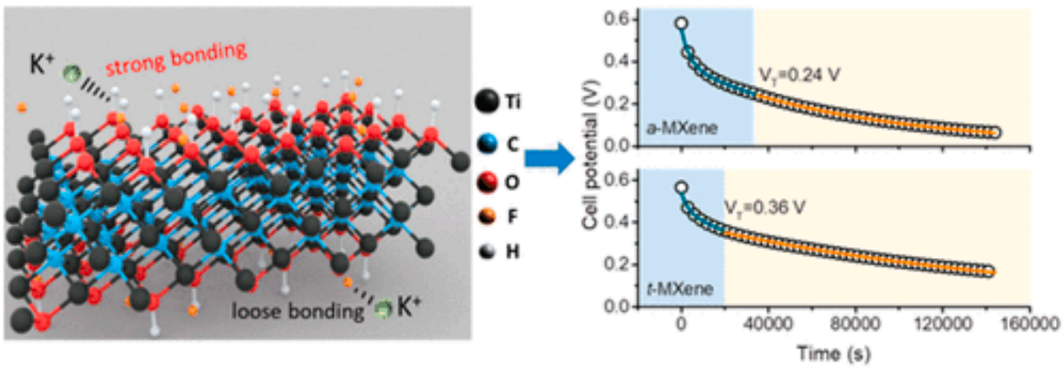

Fig. 17. Regulating and examining MXene-Based $Ti_3C_2T_x$ SCs' self-discharge behavior (Wang et al., 2020).

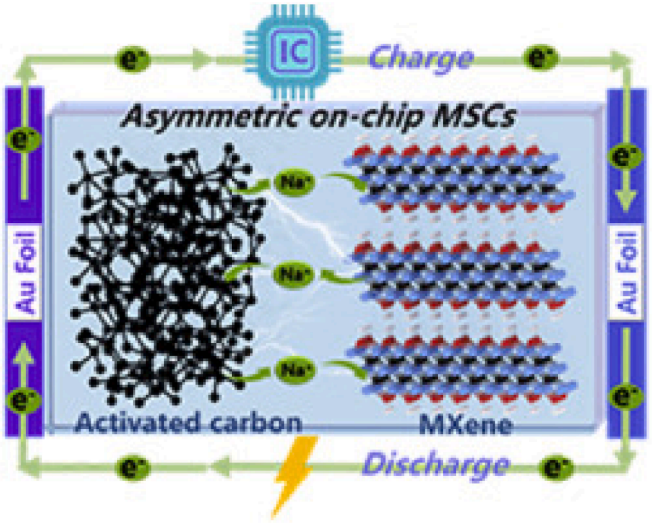

Fig. 18. MXene-based asymmetric on-chip micro-SCs with high voltage (Xie et al., 2020).

to traditional techniques for microfabrication, the "cutting-spraying" approach can prevent microelectrode burns and is well-suited for low-cost, large-scale production. Furthermore, establishing a buffer layer of Cr was used in place of the treating process in our previously described "treating-cutting-coating method." In the meantime, as shown in Fig. 19, the GCD curves show typical isosceles at 100 μA cm^{-2}. Furthermore, compared to symmetric MSCs (1.8 mF cm^{-2}), the larger curve and longer discharge time also point to significantly larger areal capacitance asymmetric on-chip MSCs (7.8 mF cm^{-2}). Additionally, the electrochemical capacitive behavior can be better understood by examining the electrochemical impedance spectroscopy (EIS) analysis (Fig. 19). It should be mentioned that inductance is the cause of the curve in the fourth quadrant. The corresponding GCD curves of asymmetric on-chip MSCs at different current densities ranging from 200 to 2000 μA cm^{-2} are displayed in (Fig. 19). The isosceles triangular shape displayed by all the curves indicates fast kinetics. Using GCD curves in (Fig. 19), the areal-specific capacitances of the high-voltage MXene-based on-chip MSCs at various current densities were computed. It is still possible to achieve an areal capacitance retention of 59 % when the current density increases from 100 to 2000 μA cm^{-2}.

The entire active area of the microelectrodes was defined with an interdigitated pattern using a low-cost, simple Kapton tape mask. The silicon wafer was then cut, and the pattern was etched using a cold ultraviolet (UV) laser with a wavelength of 355 nm (Step I). Next, magnetron sputtering was used to create a conductive layer of Au/Cr (Step II). Cr is included because of its ability to act as a buffer during the creation of the Au/Cr alloy, facilitating the effective adhesion of the Au layer to the silicon wafer (Liu, M.-Z. et al., 2023).

The electrode materials were sprayed selectively onto the gold microelectrodes after covering another electrode with a specially constructed PET mask (Steps III-IV). Otherwise, due to MXene's high potential, the Au layer would serve as a current collector and stop the accumulation of charge that would lead to MXene being noticeably polarized (Liu, M.-Z. et al., 2023).

The world's growing energy consumption and the depletion of fossil fuels are the two main forces driving the search for clean, renewable energy sources. In order to develop excellent energy storage devices that resemble SCs, the storage of these energy sources needs to be addressed right away (Patra et al., 2022). A variety of electrode materials have been investigated recently in an attempt to address the shortcomings of the two main types of SCs: electric double-layer (EDL) capacitors and pseudocapacitors. Among these drawbacks include low energy density, inconsistent performance, high internal resistance, etc. By utilizing $Ti_3C_2T_x$ MXene as a supercapacitive material and passivated VGN as a material for the current collector, the benefits of both material types were combined to construct a two-electrode symmetric device. The readily manufactured material was examined using a variety of characterization techniques, including field emission scanning electron microscopy, high-resolution transmission electron microscopy, X-ray diffraction, electrochemical techniques, surface area analysis, and contact angle measurements. Over 6000 repeated charge-discharge cycles and at 0.08 mA/cm^2, the device showed near-100 % columbic efficiency and exceptional stability with a high areal capacitance of 199 mF/cm^2. The energy density and matching power density, which peaked at 13.57 and 31.07 μW/cm^2, respectively, were noteworthy results. A large-scale Density Functional Theory (DFT) simulation conducted to quantitatively support our measurements and detailed the structural and electrical properties of pure VGN sheets and MXene@VGN. The interaction

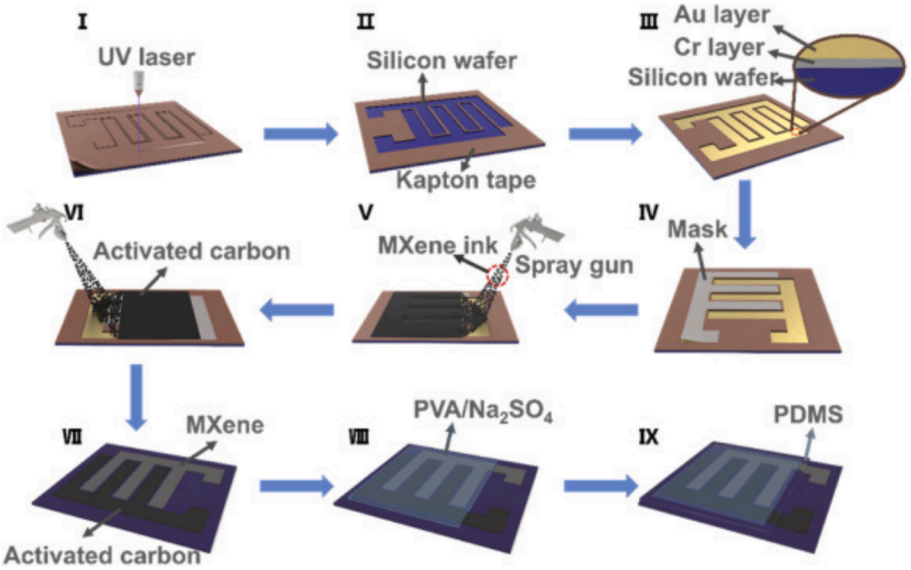

Fig. 19. For high-voltage on-chip MSCs, the cutting-spraying method is based on silicon wafers and MXene. A simple cold laser cutting and spraying procedure was utilized to create the asymmetric on-chip MSCs using the AC positive electrode and $Ti_3C_2T_x$ negative electrode. Additionally, a thin layer of polydimethylsiloxane (PDMS) was applied to the entire device using an enhanced mold-assisted forming technique (Xie et al., 2020).

between MXene and VGN is caused by a charge transfer from MXene's Ti 3d to VGN's C 2p orbital. The improved diffusion energy barrier for the ions in the electrolyte and increased quantum capacitance in MXene@VGN account for the modified structure's superior charge storage performance over that of MXene and pristine VGN. The order MXene@VGN > MXene > VGN indicates that the computed quantum capacitance is in good agreement with the specific capacitance trend seen in experiment Fig. 20 (Patra et al., 2022).

Si nanospheres get embedded into the interlayers of MXene by acting as spacers and enlarging channels for ion transport while reducing the transport resistance of ions. Due to the special qualities of Si and MXene, Mateen, A. et al. (Mateen et al., 2023) reported the V_2CTx@Si nanocomposite electrode material for SC. The greatest specific capacitance of the V_2CT_x@Si nanocomposite electrode is 557.7F/g at 1 A/g. DFT calculations show that the electrical characteristics of the V_2CT_x@Si electrode material account for its remarkable performance. It is advantageous for the rate performance of V_2CT_x@Si, according to these results, that V_2CT_x@Si has better conductivities than pristine MXene. The pristine material's energetically favorable E_{ads} value is 0.652 eV, whereas the V_2CT_x@Si has a value of − 0.845 eV. By connecting V_2CT_x@Si (sometimes referred to as V_2CT_x@Si//Zn) as the cathode and Zn foil as the anode, one can construct a zinc-ion supercapacitor (ZISC). The V_2CT_x@Si//Zn has a steady cyclic life (96.4 %) of up to 10,000 cycles and can operate over a broad potential range of 1.8 V. Moreover, at 1 A/g, a high capacitance of 318.25F/g is offered. Fig. 21 illustrates an overview of application-specific MXene properties for supercapacitors.

Their distinct characteristics and facile processing have established them as auspicious materials for an array of uses, encompassing energy storage, particularly in the context of supercapacitors. In this section, we hope to provide an overview of the most recent developments in MXene's supercapacitor research. We also review the latest developments in MXene-based supercapacitive energy storage and discuss different MXene-based supercapacitors' charge storage mechanisms.

2.7. Energy storage mechanism of the MXenes in supercapacitors

Because of their affordability, safety, and environmental friendliness, aqueous asymmetric supercapacitors (ASCs) offer promising prospects for electronic systems in the future that require high energy density, power density, and cycling life. The creation of complementary potential windows and coordinated charge storage kinetics in well-matched anodes and cathodes, however, continues to be a formidable obstacleA one-step gas-assisted foaming technique to create porous graphene and MXene-based films with nitrogenous and phosphorous terminals for high-performance aqueous ASCs is reported by (Xu, S., Li, Y., Mo, T., Wei, G., & Yang, Y.) in 2024. Surface engineering and porous structure are used in tandem to maximize the electrochemical characteristics of graphene and MXene electrodes. Black phosphorus (BP) nanosheets were exfoliated from bulk BP using ball-milling and ultrasonication, and few-layer $Ti_3C_2T_x$ MXene nanosheets were produced by selectively etching the MAX phase precursor Ti_3AlC_2. Then, via electrostatic interaction between the nanosheets and NH_4^+ ions, the MXene and BP nanosheets self-assembled in an ammonium bicarbonate (NH_4HCO_3) solution. Following vacuum filtration and an annealing process at 400 °C, the composite film was collected, yielding porous MXene films with nitrogenous and phosphorous terminals identified as N/P-PMF (Fig. 22a). The NH_3 and CO_2 gases that are released during the breakdown of NH_4HCO_3 create a three-dimensional network of porous structures in the film during the annealing process. In the meantime, −OP terminals formed as a result of surface reactions between BP and the functional groups of MXene. Porous graphene films (N/P-rGO) with nitrogenous and phosphorous terminals were also created using the same process (Fig. 22b). The matched N/P-PMF and N/P-rGO electrodes, when coupled as the anodes and cathodes in ASCs, were designed to optimize energy and power performance in a synergistic manner thanks to their porous structure and surface-modified active sites (Fig. 22c). Fast ion/electron transport was anticipated to be made possible by the porous framework, and surface redox reactions could be influenced by the −OP functional groups. Based on the porous MXene and graphene films, the assembled aqueous ASCs demonstrated exceptional energy density of 26.8 Wh kg^{-1} at 425 W kg^{-1}, high-rate performance, and remarkable cycling stability with 97.3 % retention after 20,000 cycles (Xu et al., 2024).

By using a straightforward hydrothermal reaction, Iyer et al. (2024) have created a ternary composite of a metal oxide-based electrode with graphitic nanofiber (GNF) and MXene (MX). The relationship between scan rate and peak current values demonstrated the electrode's battery-like behavior. When used as a battery-type electrode, a high specific capacitance of 819F/g and a 94 % capacitance retention after 5000 cycles are obtained at 1 A/g. After 20,000 charge/discharge cycles, an asymmetric supercapacitor device made of activated carbon as the positive and negative electrode and a bismuth antimonate ($BiSbO_4$) based nanocomposite produced a favorable specific capacitance of 147.8F/g. It also retained its capacity at 90.6 %. The presence of the conductive element GNF and the accordion-type MXene structure is responsible for the improved performance of the BSO–GF–MX electrode.

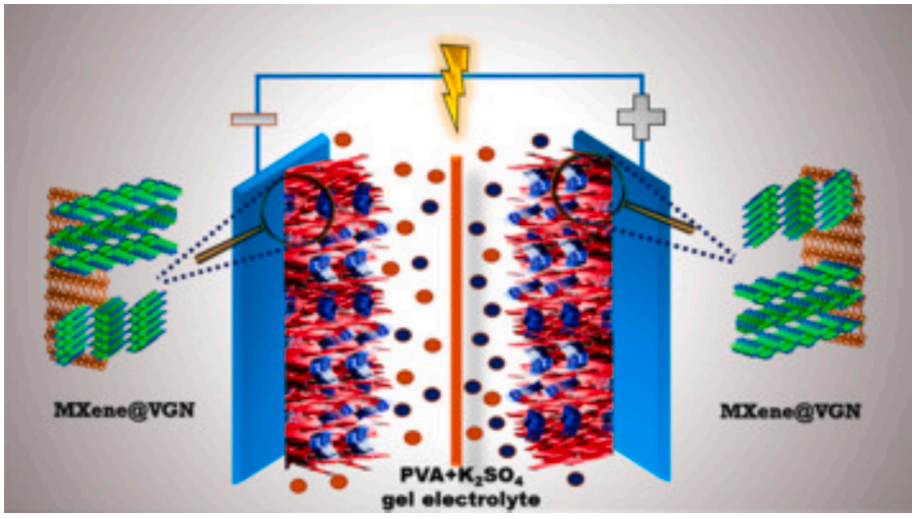

Fig. 20. Vertebral graphene arrays are used as the current collector in the MXene-based all-solid-state supercapacitor, allowing it to store more charge (Patra et al., 2022).

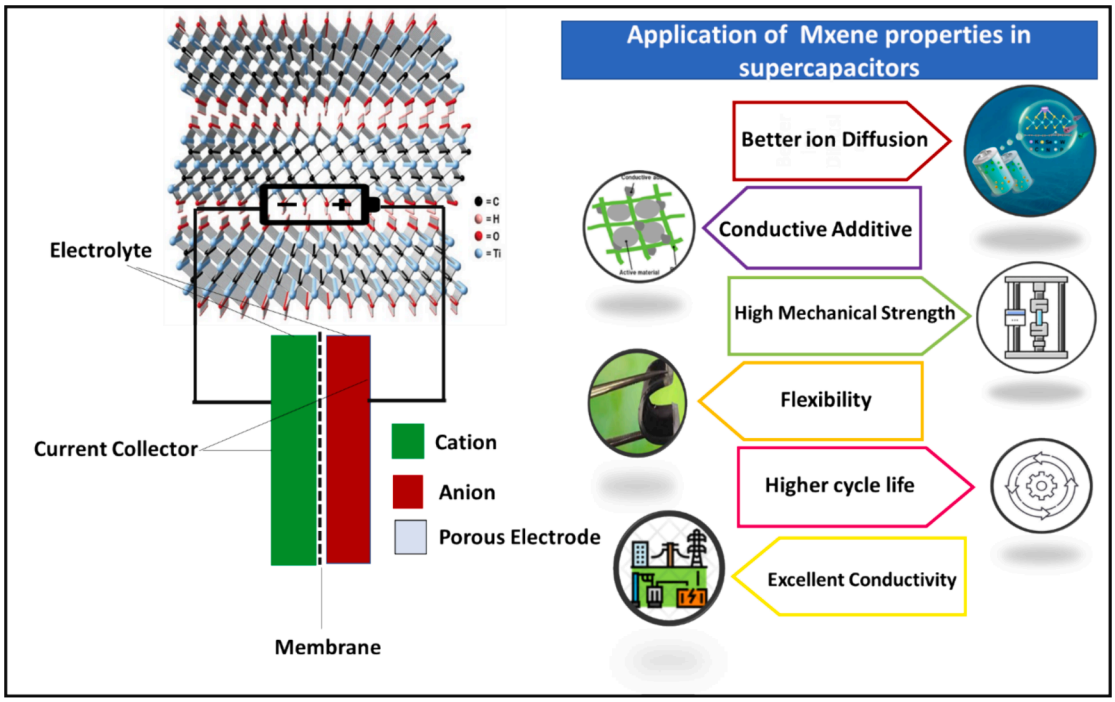

Fig. 21. An overview of application-specific MXene properties for supercapacitors.

By offering efficient channels for electron transport, the GNF raises the electrode's total conductivity. Additionally, the BSO–GF–MX||AC asymmetric supercapacitor device retains 90.6 % of its initial capacitance and delivers a superior energy density of 46 Wh kg^{-1} at a power density of 750 W kg^{-1}. This device is constructed with activated carbon as the negative electrode (Iyer et al., 2024). A synergistic in-situ intercalation and surface modification strategy for improving $Ti_3C_2T_x$ electrochemical performance is demonstrated (Li et al., 2024). Using an in-situ reduction technique, Ag nanoparticles were intercalated into the interplanar of $Ti_3C_2T_x$ to expose active sites and open ion diffusion channels. An annealing treatment was then applied to remove the deleterious termination. Thanks to the structural modification, the resulting a-Ag/$Ti_3C_2T_x$ film electrode has better rate performance and cyclic stability, as well as a higher specific capacitance of 471F/g at 1 A/g and a two-fold increase in intercalation pseudocapacitance compared to the pristine $Ti_3C_2T_x$. Moreover, the asymmetric supercapacitor produces a high energy density of 24.6 Wh kg^{-1} with a positive electrode of RuO_2@CC and a negative electrode of a-Ag/Ti_3C_2Tx (Li et al., 2024). $Ti_3C_2T_x$ MXene hydrogel was effectively prepared (Ji et al., 2024) by a quick and easy zinc-assisted electrodeposition technique using a low-concentration MXene solution. This self-assembled three-dimensional porous structure shortens the electrolyte ion transport/diffusion pathways, increases the number of electrochemically active sites exposed, and inhibits the stacking of MXene layers. Zn-$Ti_3C_2T_x$ shows good rate performance (73.3 % at 1 V s^{-1}) and good capacitance (352F/g at 2 mV s^{-1}) as a supercapacitor electrode. Under a power density of 104.85 W kg^{-1}, the assembled Zn-$Ti_3C_2T_x$/carbon cloth all-solid symmetric supercapacitor device shows excellent energy density (11.65 Wh kg^{-1}) (Ji et al., 2024). This study suggests a novel strategy of replacing –F with –N terminal groups by Hu et al. (2024) in light of the limited ion binding sites associated with –O terminal groups and the hindered electrolyte ion transport caused by –F terminal groups. With a large number of –N terminal groups, the modulated MXene-N electrode exhibits a very high gravimetric capacitance of 566F/g (at a scan rate of 2 mV s^{-1}) or 588F/g (at a discharge rate of 1 A/g) in 1 M H_2SO_4 electrolyte, and the potential window is greatly expanded. Furthermore, the mechanism related to –N terminal groups is examined through the use of density functional theory calculations and subsequent spectra analysis (Hu et al., 2024). A simple in-situ reaction successfully combines mxene with TMS. The MXene/CoS/NF heterostructure electrode exhibits an area capacitance of 0.91 mAh/cm^2, which is 9.78 times greater than that of pure MXene at a current density of 2 mA/cm^2, according to the electrochemical analysis. Remarkably, even after 10,000 cycles, the assembled asymmetric supercapacitor still holds a respectable 85.21 % of its initial capacity. The assembled supercapacitor has an energy density of 1.42 mWh cm^{-3} and a power density of 49.15 mW cm^{-3} (Liang et al., 2024). In order to determine the ideal conditions for the highest specific capacitance (sCap) enhancement of supercapacitor (SC) electrodes made using a multi-layer nanostructure of $Ti_3C_2T_x$ MXene, this study looked at direct-current hydrogen plasma (DCHP) parameters such as exposure time, power, and treatment temperature. Three-electrode C-V measurements yielded a high sCap of 642 mF cm^{-2}, more than twice as high as the primary value of the untreated MXene electrode. With the help of hydrogen plasma, multilayer (<20-layer) MXene flakes were mobilized on grafoil electrodes, and under ideal plasma conditions, a record-breaking sCap of 642 mF cm^{-2} could be reached (at a scan rate of 5 mV/s) (Pourjafarabadi et al., 2024).

Next, the species, stability, properties, and structure of layered MXenes are presented. The mechanisms of capacitive energy storage and the variables influencing the electrochemical behavior and performance of supercapacitors are then the main topics of discussion. In addition, a summary of the different kinds of MXene-based supercapacitors is provided to emphasize the importance of MXenes in the construction of energy storage devices. Lastly, opportunities and challenges in this rapidly expanding field are discussed in order to encourage the continued development of MXenes in supercapacitors.

2.7.1. The electrode material of the MXene in supercapacitors

It is essential to investigate new supercapacitor electrode materials to advance the development of supercapacitors and their uses in contemporary electronics (Ma et al., 2021). Because of its distinct physicochemical characteristics, $Ti_3C_2T_x$ MXene, a prominent member of the emerging 2D MXenes, has demonstrated enormous potential for supercapacitor electrodes.

(Jiang et al., 2018) combine two-dimensional $Ti_3C_2T_x$ MXene sheets with one-dimensional MnO_2 nanoneedles to create a novel structure

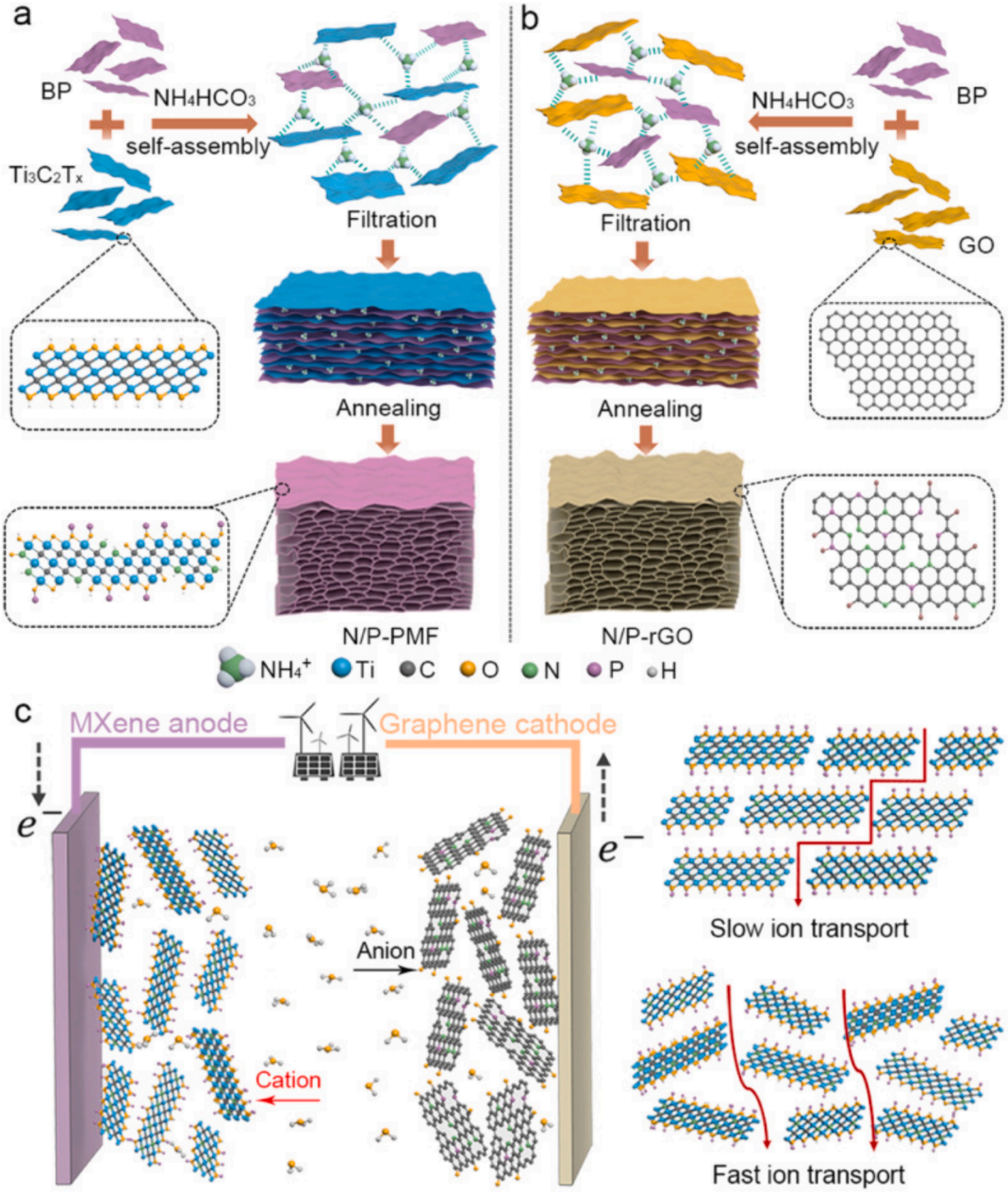

Fig. 22. Diagrammatic representation of the steps involved in preparing (a) N/P-PMF, (b) N/P-rGO, and (c) the asymmetric supercapacitors [(Xu, S., Li, Y., Mo, T., Wei, G., & Yang, Y. (2024)].

electrode material for flexible supercapacitors. Due to the strong synergistic effect between the MnO_2 nanoneedles and $Ti_3C_2T_x$ sheets, which not only ensures a robust structure for the nanocomposite but also greatly facilitates electron transfer and ion diffusion in the nanocomposite, the resulting $MnO_2/Ti_3C_2T_x$ nanocomposite exhibited a much improved electrochemical performance in terms of capacitance and stability than bare MnO_2. Based on $MnO_2/Ti_3C_2T_x$ nanocomposites, the flexible supercapacitor exhibits exceptional flexibility, strong electrochemical performance, and exceptional cycling stability. When compared to bare MnO_2 and $MnO_2/Ti_3C_2T_x$ electrodes, the $MnO_2/Ti_3C_2T_x$ electrode clearly has the lowest charge transfer resistance (Rct) of approximately 2.5 Ω and the lowest ion diffusion impedance (Wion) of approximately 0.026 Ω. This clearly indicates that the chemical interaction between MnO_2 and $Ti_3C_2T_x$ is able to clearly promote the electron transfer and ion diffusion in the nanocomposites, which in turn leads to the improved electrochemical performance of $MnO_2/Ti_3C_2T_x$. Additionally, the EIS spectra provide evidence at this point, where the Wion decreases by 56.3 % and the Rct (3.2 Ω) of $MnO_2/Ti_3C_2T_x$ decreases by 15.7 % in comparison to that of bare MnO_2 (3.8 Ω). The durability of the corresponding electrodes was tested using the GCD method at 4A/g in order to investigate the long-term stability of the prepared $MnO_2/Ti_3C_2T_x$ nanocomposites as electrode materials.

By (Wang et al., 2019), two-dimensional multi-layered V_4C_3 MXene is synthesized by etching Al from V_4AlC_3. It exhibits good rate performance, a stable long cyclic performance with a capacitance retention rate of 97.23 % after 10,000 cycles at 10 A g^{-1} in 1 M H_2SO_4, and a high capacitance of 209 F g^{-1} at 2 mV s^{-1}. It is noteworthy that approximately 37 % of the total capacity (~268.5 F g^{-1}) for the V_4C_3 MXene electrode is accounted for by the pseudocapacitance (~100.1 F g^{-1}). It exhibits good rate performance, high capacitance (approximately 209 Fg^{-1} at 2 mV s^{-1}), and stable long cyclic performance as a supercapacitor electrode in 1 M H_2SO_4 electrolyte (capacitance retention rate

is 97.23 % after 10,000 cycles at 10 A/g) Fig. 23.

For the first time, researchers looked into the electrochemical characteristics of supercapacitors (Syamsai, R., & Grace, A. N. (2019)). Tantalum carbide MXene is created by utilizing HF to etch "Al" out of its MAX phase. Additionally, the manufactured Swagelok cell supercapacitor yielded a maximum specific capacitance of 120F/g.

The order of stability of functionalized $Nb_{n+1}C_n$ MXenes is $Nb_{n+1}C_nO_2 > Nb_{n+1}C_n(OH)_2 > Nb_{n+1}C_nF_2 > Nb_{n+1}C_n(OCH_3)_2$ (Xin, Y., & Yu, Y. X. (2017)). At the anode, the $Nb_{n+1}C_n$ MXenes' quantum capacitance is reduced by F-, O-, OH–, and OCH_3 functionalization. That OCH_3-functionalized $Nb_{n+1}C_n$ MXene sheets are appropriate for the field emitters with an ultralow work function of 1.0 eV, and that bare Nb_2C MXene sheet is a promising material for electrodes of supercapacitors with theoretical quantum capacitances of 1828.4 and 1091.1F/g at positive and negative electrodes, respectively.

Zheu et al. (2020) used two distinct techniques to prevent the restacking of $Ti_3C_2T_x$-MXene layers: a simple hard templating method and a pore-forming technique. Based on crumpled layers, the expanded MXene produced by employing MgO nanoparticles as hard templates showed an open morphology (Fig. 24 A). Over 5,000 charge-discharge cycles, the corresponding electrode material retained 99 % of its initial capacitance at 5 A/g while delivering 180F/g at 1 A/g. The binder-free electrode made from the resulting MXene foam demonstrated a high capacitance of 203F/g at 5 A/g current density, with 99 % of that capacitance remaining after 5,000 cycles, owing to its foamy porous structure. In contrast, under the same operating conditions, the pristine MXene-based electrode only produced 82F/g Fig. 24 (B). An asymmetric device with a positive MnO_2 electrode and a negative MXene foam electrode demonstrated an appealing energy density of 16.5 Wh kg^{-1} (or 10 Wh/L) and a power density of 160 W kg^{-1} (or 8.5 kW/L).

(Ma et al. 2022) For $T_3C_2T_x$ MXene-based supercapacitor electrodes, highly enhanced capacitance, rate capability, cyclic stability, and good mechanical flexibility are obtained simultaneously by engineering the electrode structure, modifying the surface chemistry, and optimizing the fabrication process through an optimized integration approach. In this approach, three methods—carbonizing in situ grown polymer, or "Cpolymer"—on the MXene, alkali treatment, or "A" and template sacrificing, or "P"—are combined and, more importantly, optimized. The optimized processes result in a higher number of active sites, faster ion accessibility, better chemical stability, and good mechanical flexibility. The resulting P-MXene/Cpolymer-A electrodes exhibit superior rate performance and much larger capacitances than the pristine MXene electrode. They are also binder-free and self-supporting, with good mechanical flexibility. In particular, when compared to the pristine MXene (79.6 % retention) and P-MXene-A (77.3 % retention) electrodes, the P-MXene/CPAQ-A electrode (PAQ: quinone-amine polymer) achieves a high capacitance of 532.9F/g at 5 mV s^{-1}, along with superior rate performance and improved cyclic stability (97.1 % capacitance retention after 40,000 cycles at 20 A/g).

Carbonization and vacuum filtration were used to create the N-doped MXene film (Shi et al 2022). At 2000 mV s^{-1}, N-MXene-300 film displays an impressive capacitance of 193F/g. At 90 kW k g^{-1}, the asymmetric capacitor shows a high energy density of 16.04 W h k g^{-1} Fig. 25.

MXene was used as an electrode material to study the size refinement effect of flexible supercapacitors (Sun,et al., 2021). The MXene electrodes' strength and toughness were enhanced through size refinement, leading to a rise in flexibility. A theoretical understanding of size refinement-induced increased flexibility was obtained through finite elemental analysis. Furthermore, the MXene supercapacitors' specific surface area, electric conductance, ion transport, and water wetting qualities were all enhanced by the size refinement, which also resulted in significantly higher energy and power densities. This section provides a thorough review of the most recent developments in $Ti_3C_2T_x$-based supercapacitor electrodes, with a focus on the critical role that $Ti_3C_2T_x$ MXene plays in the remarkable electrochemical performance and related mechanisms.

Supercapacitors' MXene-based electrode material demonstrates remarkable electrochemical performance, including high capacitance, low internal resistance, high power density, exceptional electrode conductivity, and long-term cycling stability.

2.7.2. *Superior properties of MXenes for use in SSS*

Moon et al., (2023) used the ionophilic MXene $Ti_3C_2T_x$ as a nanofiller to increase the ionic conductivity of organo-hydrogel electrolytes. The abundance of hydroxyl groups on the surface of the ionophilic MXene resulted in a strong affinity for Li^+ ions and good dispersibility in water/glycerol. An anti-freezing supercapacitor based on the MXene/poly (vinyl alcohol) organo-hydrogel electrolyte (MXPVA-OHE) demonstrated a gravimetric capacitance as high as 19.84F/g at room temperature and 3.49F/g at −20 °C because of the enhanced Li-ion hopping through the abundant hydroxyl groups. MXPVA-OHE-based supercapacitors are thus superior energy-storage devices because of their high ionic conductivity, wide potential window, and favorable post-freezing recyclability (Moon et al., 2023). As shown in Fig. 26, two kinds of functional groups could be affixed to the ionophilic MXene surface: (1) functional groups with electronegative oxygen to create a path for Li ions to hop on, and (2) functional groups that caused PVA and MXene to form hydrogen bonds, increasing the mechanical strength of the MXPVA-HM. One popular method for polymer gelation is the freeze-thaw method. According to Lai et al. (2024), altering the Si–O bond of organo-silane headgroups in $Ti_3C_2T_x$ can result in an extremely high level of piezoelectricity. The Si–O bond of surface functionalized $Ti_3C_2T_x$–FOTS produces localized lattice distortion and strengthens the

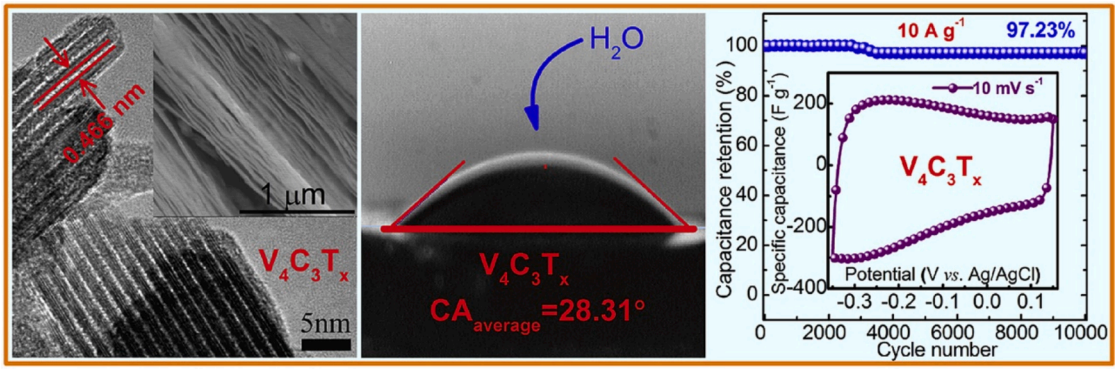

Fig. 23. the creation of multilayered, two-dimensional V_4C_3 MXene and its electrochemical properties as an electrode for supercapacitors. As-prepared V_4C_3 MXene provides large interlayer spacing, specific surface area, and exceptional hydrophilicity, making it a high-performance electrode material for supercapacitors (Wang et al. 2019a,b).

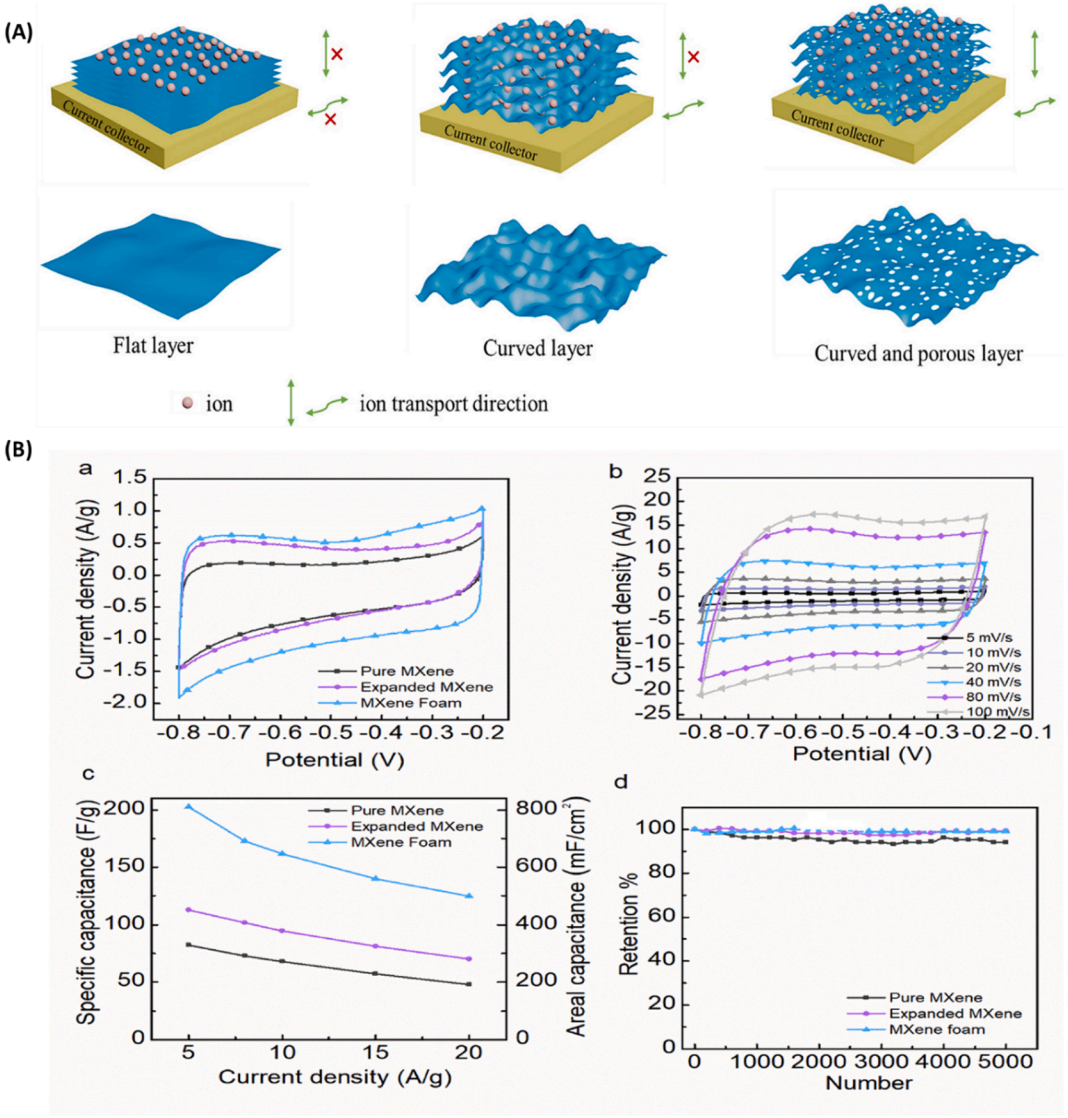

Fig. 24. (A) MXene layer modifications for supercapacitors. (B) Binder-free electrodes' electrochemical properties in three electrode configurations with an electrolyte of 1 M KOH. (a) Examining the prepared materials' CV curves at a scan rate of 5 mV s^{-1}. (b) MXene foam electrode CV curves at different scan rates. (c) A comparison of the prepared material's specific capacitances in relation to applied current densities. (d) A comparison of the capacity retention over 5000 charge-discharge cycles between pristine, expanded, and MXene foam at 5 A/g. The MXene Foam dashed curve represents data that was removed due to equipment malfunction. (Zhu et al. 2020).

noncentrosymmetric structure on the $Ti_3C_2T_x$ surface, according to a theoretical calculation. Butterfly loops are substantially more prevalent in $Ti_3C_2T_x$-FOTS than in pure $Ti_3C_2T_x$. For dye degradation, $Ti_3C_2T_x$-FOTS had a computed rate constant of 0.9 min^{-1}, which was 15 times greater than $Ti_3C_2T_x$-CPTMS and 111 times greater than pristine $Ti_3C_2T_x$. Three times faster than $Ti_3C_2T_x$, $Ti_3C_2T_x$-FOTS has a hydrogen evolution rate of 900.46 μmo1 $g^{-1}h^{-1}$. The hydrogen evolution reaction (HER) and wastewater breakdown can be catalyzed simultaneously by the bifunctional surface functionalized $Ti_3C_2T_x$-FOTS, proving that $Ti_3C_2T_x$-FOTS, which is created by surface engineering $Ti_3C_2T_x$, is an excellent piezocatalyst (Lai et al., 2024). The FeCo-Ti_3C_2 MXene composite was created by (He et al., 2019) utilizing an in-situ hydrothermal process. The formation of magnetic FeCo nanoparticles on the laminated Ti_3C_2 MXene is demonstrated by the results of XRD, VSM, SEM, and EDS. Notably, the FeCo-Ti_3C_2 MXene composite, as prepared, exhibits comparatively low complex permittivity and additional magnetic loss, which simultaneously contribute to improved microwave attenuation ability and improved impedance matching. The microwave absorption property of Ti_3C_2 MXene can be improved by adding magnetic FeCo nanoparticles. In particular, the FeCo-Ti_3C_2 MXene composite showed only 1.6 mm and a wide effective bandwidth (RL < − 10 dB) of 8.8 GHz. A method for creating $Ti_3C_2T_x$ MXene/V_2O_5 (MV) films as flexible electrode materials for supercapacitors is described in (Luo et al., 2023) and involves vacuum-assisted filtration of a mixture of MXene nanosheets and V_2O_5 nanofibers. By adjusting the quantity of V_2O_5 nanofibers, the introduction of V_2O_5 nanofibers simultaneously controls the thickness of the MV films and effectively suppresses the self-stacking phenomenon of MXene nanosheets. Thanks to the effective intercalation of V_2O_5 nanofibers, the $Ti_3C_2T_x$ MXene/V_2O_5 (20 mg) (MV_2) film, used as the electrode, exhibits good cycling stability (70.4 %, 5000 cycles, 3 A g^{-1}) and capacitive performance (319.1F g^{-1}, 0.5 A g^{-1}). Moreover, the MV_2//MV_2 symmetric supercapacitor (SSC) and the MV_2//MnO_2 asymmetric supercapacitor (ASC), which individually have capacitance retention of 72.1 % and 83.9 % after 8000 cycles of charge and discharge at 2 A g^{-1}, are assembled. Both the SSC and the ASC demonstrate a good energy storage capacity with energy densities of 18.43 Wh kg^{-1} at 603.2 W kg^{-1} and 20.83 Wh kg^{-1} at 374.94 W kg^{-1} power density, respectively (Luo et al., 2023).

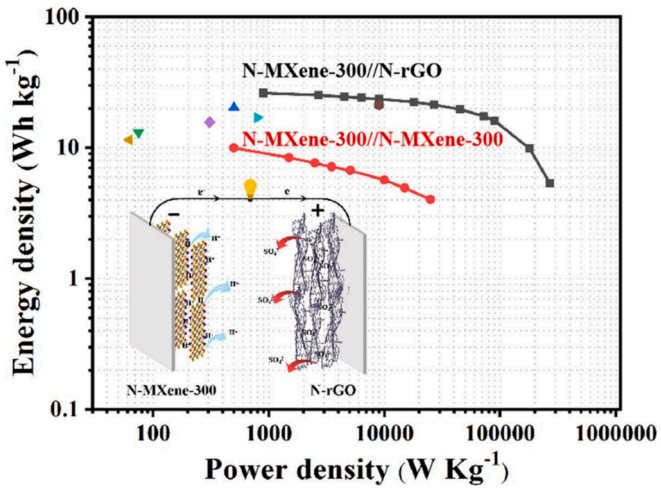

Fig. 25. Hexamethylenetetramine regulates the MXene film's layer spacing and functional surface group for high-performance supercapacitors (Shi et al 2022)).

2.8. *Eco-friendly green MXenes*

One of the major topics of discussion that the world is currently facing is environmental pollution, which is growing daily and posing a serious threat to the planet. Because human beings are dependent so heavily on a variety of portable devices, electrical energy storage, or EES, is essential to daily life. One use for green technology is environmental remediation (Venkateshalu and Grace, 2020). MXene is a brand-new substance with enormous potential for environmental cleanup. Using straightforward, affordable, secure, and environmentally friendly methods that work well is imperative for the synthesis and surface functionalization of MXenes-based nanostructures based on green chemistry principles (Iravani, 2022). To produce MXenes, a few methods like ultrasonication or microwave-assisted synthesis can be used. These methods have the advantages of being simple to use, having a high production rate and yield, being easy to operate, being environmentally friendly, and being cost-effective. It has been determined that the special qualities of MXenes are highly interesting for a number of new applications. Nevertheless, a significant disadvantage of MXenes is that they are generally fabricated in large quantities using hazardous and environmentally damaging materials, utilizing a high-temperature solid-state reaction followed by selective etching. In the meantime, determining MXenes' final applications requires understanding how they are made. Thus, in order to commercialize at a competitive price, it is essential to take strategic approaches to synthesize greener, safer, more sustainable, and environmentally friendly MXenes. It is essential to gather, condense, and synthesize the most recent advancements in MXenes' green technology due to the growing number of reports of green synthesis that support cutting-edge technologies and non-toxic agents (Amrillah et al., 2022). The EES materials and devices will assist in meeting the challenge of providing a steady distribution of energy. Furthermore, there are significant challenges in producing small but potent EES devices due to the ongoing demands for the miniaturization of electronic devices, the integration of portable technology into our daily lives, and the much-anticipated "Internet of Things." Obtaining a secure and sustainable energy source is one of the most complex and frequent challenges of our time. As the dependency on a variety of mobile electric devices has increased, the EES is essential to our way of life. In a similar vein, grid and transport use require large and inexpensive EES devices (Khan et al., 2020). Notably, synthesis blockages have made it difficult to fabricate MXenes and their derivatives with upscalable and industrial capacities—only a small number have been produced in large quantities. However, in bottom-up methods, where production is dependent on substrate size and precursor availability for chemical preparation and/or exfoliation, these difficulties are more apparent. When compared to these methods, the selective wet etching approach for producing MXenes did not exhibit the same synthesis constraints because the reaction occurred throughout the entire volume, allowing the process to be quickly scaled with reactor volume (Khan et al., 2020). Flexible MXene triboelectric nanogenerators can harvest electrical power from simple muscle movements (e.g., texting) even when the device is bent by approximately 30° angle. They can generate high open-circuit voltages ranging from ~ 500 to ~ 650 V and increase the instantaneous peak power to ~ 0.5–0.65 mW, resulting in a power higher than that of 60 light-emitting diodes or the quick charge a 1 μF capacitor up to 50 V. Currently, less toxic etching agents like NaOH, NaCl, ZnCl, $NaBF_4$, LiF + HCl, etc. are used to replace the HF etching agent in the green synthesis of MXenes-based materials (Li et al., 2018), or with a chemical-free etching agent, including thermal electrochemical etching (Pang et al., 2019). These green synthesis methods have a number of benefits, including reduced toxicity—using non-toxic etching agents, like $NaBF_4^{+}$HCl, and avoiding strong acid HF greatly reduces the chemical's toxicity. Additionally, the use of non-toxic etching agents makes the synthesis facile and environmentally friendly, and the experimental procedure is simpler than when using a toxic etching agent. Toxic etching agents should be used with extreme

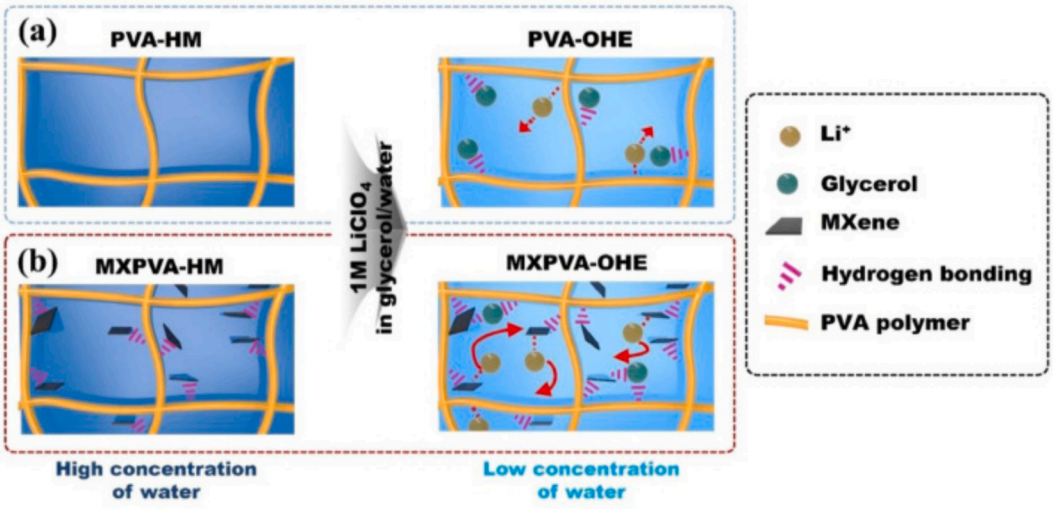

Fig. 26. Diagrammatic representation of the steps involved in the synthesis of (a) PVA-OHE and (b) MXPVA-OHE (Moon et al., 2023).

caution during practical application to avoid explosions. Commercialization is an important factor, i.e., using a non-toxic etching agent, which is less toxic, easy to handle, and has a low cost, realizing the green synthesis of MXenes-based materials potential for commercialization. The use of non-toxic agents is low cost; that is, using a non-toxic etching agent makes it more cost-effective by eliminating pieces of equipment. Gels of reduced graphene oxide/titanium carbide (Ti_3C_2Tz/rGO) were made using a single hydrothermal step. With an average pore diameter of 3.6 nm and a surface area of approximately 224 m^2/g, the gels exhibit a highly porous structure (Saha et al., 2021). To produce distinct microstructures, the reaction precursor's GO and Ti_3C_2Tz nanosheet content was adjusted. Ti_3C_2Tz/rGO gels' supercapacitor performance varied greatly depending on their composition. At first, specific capacitance rose as Ti_3C_2Tz content increased, but gels cannot form at high Ti_3C_2Tz content. Additionally, as the Ti3C2Tz content increased, the capacitance's retention dropped. Compared to pure rGO and Ti_3C_2Tz, Ti_3C_2Tz/rGO gel electrodes show improved supercapacitor characteristics, including a large specific capacitance (920 F/g) and a high potential window (1.5 V). The improved supercapacitor performance was caused by the joint action of redox capacitance from Ti_3C_2Tz and EDLC from rGO. Asymmetric two-electrode supercapacitor cell was built using Ti_3C_2Tz/rGO, exhibiting a large energy density (~31.5 μW h cm^{-2}, corresponding to a power density of ~370 μW cm^{-2}), long stability (~93 % retention) after 10,000 cycles, and an extremely high areal capacitance (158 mF cm^{-2}) (Saha et al., 2021).

Huang et al. in 2023, took advantage of MXenes' unique property to produce MXenes at a never-before-seen reaction rate and yield in a packed-bed electrochemical reactor with very little chemical waste. As the green electrolyte, a straightforward NH_4F solution was utilized, which could be utilized again and again without losing its effectiveness. Remarkably, it was discovered that ammonium and fluoride were equally important for the electrochemical etching, functionalization, and expansion of the layered parent materials (MAXs), which allowed ammonia gas to be released. When used as supercapacitor electrodes, the electrochemically produced MXenes with exceptional conductivity could provide a volumetric energy density of 75.8 Wh/L and an ultrahigh volumetric capacity of 1408 F cm^{-3}. Along with opening the door for MXenes to be produced on an industrial scale, this innovative green, energy-efficient, and scalable electrochemical method will also allow for a wide range of adaptable electrochemical modifications for better functional MXenes (Huang et al., 2023). Zhang et al. (2019) described the rapid freezing of liquid nitrogen to create 3D macroporous MXenes film (3d-$Ti_3C_2T_x$-film) and aerogel. Comparing the specific area with the $Ti_3C_2T_x$-film (which was vacuum-filtered and air-dried), the increase was between 5 and 22 times greater. More surface-active sites are provided by the large specific surface area, which also improves double-layer capacitance. In a 3 M H_2SO_4 electrolyte, the specific capacitance of 3d-$Ti_3C_2T_x$-film is 372F/g (1355F cm^{-3}), while aerogel has 404F/g (1293F cm^{-3}) at a current density of 1 A/g. Furthermore, at a power density of 946 W/L, the supercapacitor made of 3d-$Ti_3C_2T_x$-film exhibits an exceptional volumetric energy density of 32.2 Wh/L. Compared to the template method, the fabrication method using liquid nitrogen rapid freezing is simpler, less expensive, and more environmentally friendly (Zhang et al., 2019). For the first time, Garg et al. (2020) described the creation of the best-optimized MXene film on a flexible polypropylene (PP) substrate using the optimal parameters for supercapacitor applications. The results are compared with those obtained on glass and polyethylene terephthalate (PET) substrates. Lower contact resistance of 141 O, areal capacitance of 82.6 mF/cm^2 at 5 mV/s, and capacitive retention of 73.3 % are all displayed by the PP-supported MXene device. This creates new avenues for the development of high-performance devices using various MXene morphologies, flake sizes, and combinations of these (Garg et al., 2020). $Ti_3C_2T_x$ (T = –OH, −O) MXenes are obtained from Ti_3AlC_2 by a hydrothermal reaction aided by NaOH, as reported by Khan et al. (2024). In particular, the $Ti_3C_2T_x$@Al-NaOH (30 M) MXene terminated with –OH and −O functional groups show optimized electrochemical performance as supercapacitor electrodes after being treated in Alkali for 15 h at 280 °C. The specific capacity value of these electrodes is 565C/g at 2 mVs^{-1} (Khan et al., 2024).

Furthermore, possible directions for moving MXenes in the direction of next-generation technologies are indicated.

2.8.1. The disadvantages of 2D materials

The preparation of 2D materials has received a lot of attention over the last 20 years, and several preparation methods have been created (Tang and Xu, 2024). Graphene and hexagonal boron nitride (hBN) are two commonly grown membranes within the class of two-dimensional materials (Rout, 2024). These two materials have been the subject of much research because of their similar characteristics, which provide useful performance comparisons. Chemical vapour deposition (CVD) is a widely used process for growing all of these materials, and it can be scaled up to allow for the fabrication of large-area monolayer membranes in the future. An alternative is to mechanically exfoliate these and a variety of other crystals, which results in immaculate 2D material but is severely limited in area. Although nanosheet membranes can be produced very quickly and in relatively large quantities, they are not suitable for use as sensing platforms and instead require a costly pressure-fed system (Alsaman et al., 2024). Conversely, lateral channels form a narrow Angstrom scale channel that can be used for ionic selectivity and sensing even though they are thicker overall. Although it is more difficult to fabricate them, the utilization of various materials yields ready functionalisability. Despite the great results obtained from employing MXene hybrids in energy storage devices, there are several obstacles that prevent the integration of MXenes into various types of batteries and supercapacitors. For example, it can be challenging to strike a balance between the electrochemical properties of flexible SCs and the mechanical properties of MXenes, such as their innate propensity for face-to-face restacking and random aggregation, strength, plasticity, and durability. Fig. 27 provides a summary of a few drawbacks of 2D materials (Caglar and Keyser, 2021). Various methods have been employed thus far to address the restacking challenge, chief among them being the incorporation of extra nanomaterials. Additionally, at high current density values, stacking the MXenes layers eliminates the MXenes material's rate capacity due to a significant vertical ionic diffusion resistance.

MXenes have multiple applications in batteries and supercapacitors, such as ion redistribution, steric hindrance, ion transfer regulation, redox-type ion storage, double-layered ion storage, electrocatalysts, electrodeposition substrates, etc. Ion storage and redox-type ion storage, ion transfer regulation, steric hindrance, ion redistribution, electrocatalysts, electrodeposition substrates, and other roles are all carried out by these materials in batteries and supercapacitors (Yin et al., 2024). MXene does present certain difficulties, though. MXene's deficient delamination and compact multilayer structure may prevent it from being used in supercapacitors, resulting in low-rate capabilities and a reduction in storage capacity. Moreover, MXene's performance may be diminished by the layers' attraction to one another due to the van der Waals force between them. MXene exhibits promise overall for energy storage applications, but more study is required to resolve these issues and maximize its functionality in various cell configurations (Lian et al., 2022).

Another issue that needs to be considered is the oxidation of MXenes (Panda et al., 2022). There are defects on the surface of the MXenes or at the edges of the flakes as a result of the severe chemical etching process, which is assumed to be an active component of the oxidation reaction of MXenes. Because of this, when the highly crystalline MXenes are exposed to oxygen or water, they can break down into TMOs like TiO_2 and amorphous carbon. Since the substance must be stored before use, the first action that might be taken to prevent this is to suppress the dissolved oxygen. The solution could be kept in argon-sealed containers to achieve this. Throughout the synthesis process, purging dry nitrogen is a useful method to remove dissolved oxygen and prevent MXene

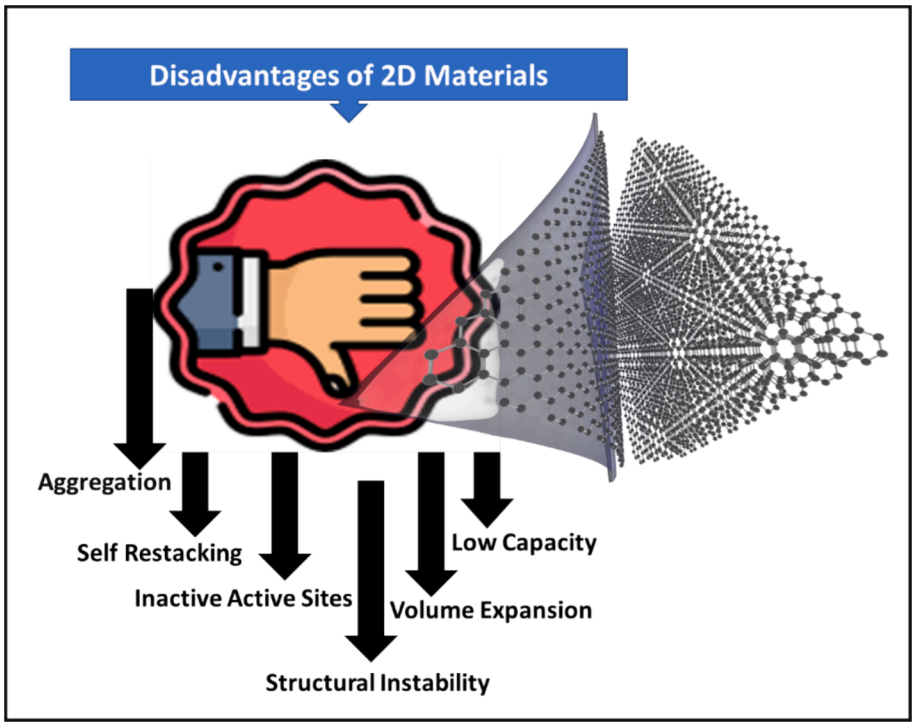

Fig. 27. An overview of some disadvantages of 2D materials.

oxidation. A few of the variables that need to be managed to create a favorable environment for the storage of MXenes include the temperature, content, and pH of the aqueous dispersions, all of which must be kept at a lower temperature to slow the rate of oxidation. Consequently, the problems pertaining to the accumulation of the generated MXenes and their sub-zero storage must be resolved. Using polymers to create MXene–polymer-based composites is very advantageous to improve the stability of the MXenes since MXene oxidation tends to start at the edge active sites. To increase the interlayer gap, polar polymers with charged nitrogen ends exhibited a strong propensity to interact with the $Ti_3C_2T_x$ layers. Among other strategies to address the oxidation problem, physical vapour deposition, and atomic layer deposition have been proposed as appropriate ways to lessen the oxidation of MXenes, improving their chemical stability in aqueous electrolytes. More consideration should be given to methods that control how exfoliated MXene nanosheets interact with different solvents and lower production costs without sacrificing MXene quality. There is also a need to address the environmental hazards of MXenes since exposure to them can have negative effects on the skin, digestive tract, and respiratory system.

3. Challenges and Future Perspectives

For synthetic organic chemists working on graphene substitutes, the scalable synthesis of basic 2D materials remains a challenge (Sahoo et al., 2023). Producing borophene can be difficult because 2D and 3D boron bonding topologies differ significantly in energy. Furthermore, the synthesis of borophene frequently requires the use of sophisticated instruments and very low pressures. Then, boron compounds could be synthesized by a variety of methods, including top-down and bottom-up approaches, exfoliation techniques such as sonochemical, liquid phase, and micromechanical exfoliation, and deposition techniques such as CVD, PVD, ion-intercalation, and solvothermal/hydrothermal process.

MXenes for solid-state energy storage devices (SSESDs) have made encouraging progress recently because of special parameters. The present developments in cathode/anode optimization, interface medication, electrolyte fillers, and other areas of supercapacitors involving MXenes and their derivatives; first, the fundamentals of MXenes are demonstrated, including precursors, etching/delamination techniques and better qualities for energy storage devices. and design approach of MXenes to enhance the electrochemical behaviors of SSESDs are thoroughly examined and talked about. Finally, viewpoints and difficulties regarding the upcoming MXenes construction strategies for SSESDs are suggested (Man et al., 2023). When it comes to rate performances, the latest MXene-based SSSs are not as good as aqueous devices. The performance of MXene-based SSS by using a methanesulfonic acid/polyvinyl acetate (MSA/PVA) hydrogel as the electrolyte. This hydrogel is green, highly ionic conductive, and resistant to low temperatures. With its extended cycle life (92 %, 80,000 cycles), low-temperature resistance (−30 °C), flexibility, and high areal capacitance (1719 mF cm^{-2}), the assembled SSS (FT-SSS) performs better than the one made using the conventional liquid electrolyte casting method. More significantly, FT-SSS outperforms the equivalent aqueous supercapacitor (AQS) in terms of capacitance and rate performance. When compared to AQS, the areal capacitance rises by 127 % at 1000 mV s^{-3}. The results of X-ray diffraction, energy dispersive spectroscopy maps, and X-ray photoelectron spectroscopy analysis show that MSA pre-intercalate into $Ti_3C_2T_x$ to form electrodes with a wrinkled and porous structure that improves electrolyte accessibility and lessens the MXene stacking effect. The content of –OH and H_2O (physisorbed to –OH) in $Ti_3C_2T_x$ increases as well, further enhancing the pseudocapacitive performance of MXene (Liu et al., 2023; Man et al., 2023). However, when compared to aqueous devices, the state-of-the-art MXene-based SSSs exhibit lower rate performances. All things considered, MXene's exceptional conductive properties with a plethora of possible uses are primarily attributable to its distinct structure, which includes transition metal elements and a large number of chemical functional groups. Because of the MXene's superior conductivity, high-power density supercapacitors can be achieved quickly through electron transfer. The energy density of the entire device is increased because conductive agents and current collectors are not even required during the electrode manufacturing process (Liu et al; 2023), Methanesulfonic acid/polyvinyl acetate (MSA/PVA) hydrogel is a green, low-temperature resistant, and highly ionic conductive electrolyte that can be used to maximize the performance of MXene-based SSS. With its long cycle life (92 %, 80,000 cycles), low-temperature

resistance (−30 °C), flexibility, and high areal capacitance (1719 mF cm^{-2}), the assembled SSS (FT-SSS) performs better than the one made using the standard liquid electrolyte casting method. More significantly, FT-SSS outperforms the equivalent aqueous supercapacitor (AQS) in terms of capacitance and rate performance. When compared to AQS, the areal capacitance rises by 127 % at 1000 mV s^{-1}. Energy dispersive spectroscopy maps, X-ray diffraction and X-ray photoelectron spectroscopy analysis reveal that MSA pre-intercalate into $Ti_3C_2T_x$, forming electrodes with a wrinkled and porous structure, which reduces MXene stacking effect and enhances electrolyte accessibility. –OH and H_2O (physisorbed to –OH) content in $Ti_3C_2T_x$ rise, too, further improving MXene pseudocapacitive performance (Liu, C. et al., 2023). The integration of "clean-solar-to-electric energy" and "sensing platforms" in photofuel cells can facilitate the development of next-generation biosensors for a range of environmental and medical applications. Unfortunately, photoelectrodes' poor performance frequently leads to insufficient solar-to-power conversion, which is necessary for accurate molecular detection. In order to solve this issue, Sun et al. in 2022, developed a dual-photoelectrode genosensor that can detect traces of miRNA-21 without the need for membranes, precious metals, or ubiquitous bio-enzymes. This platform's excellent performance is a result of the nanomaterials for both photoelectrodes being properly chosen and interfaced. The 3D $Ti_3C_2T_x$|CdS photoanode functioned as a Schottky junction, which efficiently enabled the separation of photogenerated carriers and encouraged visible light absorption. More importantly, the synergistic effect between the two photoelectrodes greatly improved the photoelectric conversion efficiency to endow the sensing platform with large output (Sun et al., 2022). The electrochemical performance of alkaline Zn-based batteries and supercapacitors can be greatly improved by rational design and the fabrication of efficient electrode materials, particularly at high current densities. The crystalline/amorphous nickel–cobalt phosphide@nickel–cobalt boride core-shell nanospheres (NiCoP@NiCo–B) are synthesized successfully (Shi et al., 2024) by combining the amorphous NiCo–B (shell) with the nanosheet-assembled NiCoP hollow nanospheres (core). In the meantime, the amorphous NiCo-B shell promotes electrolyte ion diffusion, while the crystalline NiCoP core can offer steady mechanical support. The well-engineered NiCoP@NiCo–B heterostructure exhibits rapid charge transfer/transport kinetics, a large number of redox-active sites, and strong interface interactions. The ideal electrode, NiCoP@NiCo–B-70, provides ultrahigh rate capability (87.4 % of the initial specific capacity at 20 A/g) and a specific capacity as high as 193.1 mAh g^{-1} at 1 A/g. At 400.0 W kg^{-1}, the assembled NiCoP@NiCo–B-70//AC asymmetric supercapacitor achieves a power density and an energy density of 40.8 Wh kg^{-1}. In addition, the NiCoP@NiCo–B-70//Zn battery exhibits exceptional rate capability, a high output voltage platform, and a discharge capacity of 194.5 mAh g^{-1} at a current density of 1 A/g. There is a lot of promise for the synthetic crystalline/amorphous core–shell heterostructure in terms of useful applications in the next generation of aqueous energy storage devices (Shi et al., 2024). A novel metal-coordination-driven self-assembly strategy is proposed to fabricate organic-inorganic composite co-assemblies by combining iron-containing polymer self-assemblies as a soft templates and resorcinol–formaldehyde resin as carbon precursor. Following high-temperature pyrolysis, co-assemblies are converted into porous iron/carbon (Fe/C) composites with spherical Fe nanoparticles and micro-mesopores that form in graphited carbon matrix. Fe/C-800 composite in paraffin matrix with 10 % filler loading can have a minimum reflection loss of −57.8 dB, and its effective absorption bandwidth of 5.3 GHz can span the entire X band. For high-efficiency electromagnetic wave absorption, it is thought that the microstructure derived from co-assemblies and the magneto-dielectric composition play a role in multiple reflection, polarization loss, conductive loss, ferromagnetic resonance, and eddy current loss. Overall, this work provides new opportunities for the design and preparation of high-performance magneto-dielectric absorbers through the use of a novel self-assembly strategy driven by metal coordination (Li et al., 2022).

MXenes have properties like aggregation, oxidation, stability over time, and mechanical and thermal properties that might make it impossible to use them indefinitely (Greaves et al., 2020).

A crucial factor in creating these products is choosing cutting-edge functional nanomaterials. The development of electrochemical devices for energy storage applications has received significant attention due to the introduction of advanced functional materials. The comparison of the structural and morphological characteristics of various nanocomposites based on MXene is useful in helping select the ones that best suit the intended uses. Both MXene-based nanocomposites exhibit high levels of efficiency for energy conversion and storage due to their excellent charge-discharge capacity, long lifetime, and high power density in electrochemical performance. MXene has the potential to significantly alter polymers' mechanical, electrical, and thermal properties. Because it was etched with a strong acid during the fabrication process, MXene has significant hydrophilic properties that make it perfect for the solution-blending method of nanocomposite creation. However, due to the polymer's macromolecular structure, the mixing impact of MXene in the polymer matrix still needs to be increased (Abdah et al., 2023). Therefore, the use of MXenes in material development has shown great promise in resolving these constraints. The difficulties and advancements in MXenes material development toward core-shell structures and their applications are discussed in this review (Hong et al., 2019). The techniques and procedures required for MXenes to properly attach as a core or shell are specifically examined and evaluated, and the obstacles and remedies related to using MXenes are also covered. Furthermore, a review and analysis of significant discoveries, assessments, and applications of the MXene core-shell in energy storage and conversion are carried out (Dall'Agnese et al., 2015; Zhao et al., 2017).

MXene stands out among the other cutting-edge nanomaterials in the two-dimensional family due to its exceptional qualities. Over the past 10 years, a lot of research has been done to examine the characteristics of MXene however not all of these studies are perfect. To overcome these obstacles and make them broadly applicable, further work has to be done. If MXene is developed to the same level as graphene, it's energy density and specific capacitance in SCs may rise because of its reduced specific surface area. To overcome the stiff nanosheets of MXene, new techniques such as concentrated acid + base treatment (Lamiel et al., 2022) can be used to create holes in the electrodes. Further increasing the energy density would be the possibility of freeing up additional space for various kinds of appropriate ions and pseudocapacitive nanoparticles from high-voltage electrolytes (Zhao et al., 2017). In order to attain higher voltage (Dall'Agnese et al., 2015) or rate capability, Na, Li, Zn, and K ion capacitors, among other metal ion-based capacitors, must maintain the recent surge (Hong et al., 2019).

Two-dimensional materials called MXenes have a lot of potential for electrochemical energy storage. Although MXene electrodes perform well in aqueous electrolytes in terms of specific capacitance and power rate, these systems' practical utility is constrained by their small potential window. New synthesis techniques, like the molten salt approach, have been developed to prepare MXenes, expanding the range of precursors that can be employed. Furthermore, these techniques enable tuning of the surface functional groups' composition and nature at the MXene surface. MXene electrodes performed well in nonaqueous electrolytes, according to recent studies, with high capacity, high voltage, and quick charge-discharge rates. These results, which are attributed to control over the MXene/electrolyte interface, present new possibilities for developing high-rate materials for use in energy storage applications in the next generation of materials. MXenes, or two-dimensional transition-metal carbides/nitrides, are becoming more and more popular in a variety of scientific domains, including electrochemical energy storage. This brief review highlights some recent developments in the electrochemical performance of MXene as high-rate electrodes, particularly in nonaqueous electrolytes. Finally, the limitations of the present and the outlook for the future are emphasized (Lin

et al., 2020).

On the other hand, MXene provides versatility and can be used for a wide range of applications. However, there are important issues that need to be carefully considered regarding the stability of MXene in colloidal solutions. It is a difficult task to choose the correct MXene variant for a given application from a large group. Both emerging stars in the electronics industry, MXene and graphene exhibit substantial potential as functional materials across advanced applications. However, in order to successfully develop these materials for use on an industrial scale, ongoing research is necessary. To sum up, MXene outperforms graphene even after solution processing because of its inherent hydrophilicity and increased electrical conductivity. Furthermore, MXene's exceptional electrochemical qualities offer great potential for planar devices and flexible electronics. MXenes are typically made from strong MAX materials using dangerous fluoride-containing reagents, which regrettably leave many inactive fluoride functional groups on the surface that significantly reduce their functionality. All things considered, efforts to create novel nanosystems and nanoparticles are growing by employing techniques based on green chemistry principles. An extensive list of the most recent advancements in environmentally friendly methods for manufacturing MXene is presented, and viable alternatives to traditional techniques are suggested. MXenes have become a promising species among 2D materials due to factors such as the availability of environmentally friendly synthesis and post-processing methods. Let's now investigate the potential of these green-MXenes to address practical issues in the energy and energy-mediated fields. MXenes and MXene composites are useful in a variety of industrial sectors due to their attributes such as flexible terminations, high selectivity, mass manufacturability, low cost, and surface functionality. The commercial impact of one-dimensional ensembles should be observed through green synthesis of structures containing nanoribbons or nanotubes. The primary motivation for investigating green MXenes is to consciously move closer to the objective of a sustainable future (Saxena et al., 2023).

In conclusion, MXene has proven to be a dependable electrode in electrochemical energy storage systems by overcoming several obstacles, and this trend is expected to continue. It is highly anticipated that MXene's full potential will be achieved and two-dimensional materials will be able to be used in industrial settings. The use of materials based on MXene in supercapacitors shows enhanced performance and retention of capacitance. MXenes are of interest to scientists and technologists in many domains, including energy-storage devices such as supercapacitors. Due to its distinct optical, mechanical, electrical, electrochemical, and physicochemical qualities, pure MXene and its hybrids can be used in a range of energy storage systems. Several MXene and MXene hybrid materials have shown promising values for energy parameters recently, such as power density, specific capacity, energy density, gravimetric capacity, and volumetric capacity. This review focuses on the synthesis techniques, characteristics, and features of MXene and MXene hybrid materials while summarizing current advancements in storage applications. The complex design of MXenes' Nano-microstructures is given special attention because of how many uses they have, including as protective layers for metal anodes, electrodes, and multifunctional components. Potential avenues for future investigation into the synthesis, structure, characteristics, examination, and manufacturing of MXene materials are discussed in the paper's conclusion.

CRediT authorship contribution statement

Nujud Badawi: Conceptualization, Writing – original draft. **Mrutunjaya Bhuyan:** . **Mohammad Luqman:** . **Rayed S. Alshareef:** . **Mohammad Rafe Hatshan:** . **Abdulrahman Al-Warthan:** . **Syed Farooq Adil:** Writing – original draft, Writing – review & editing.

Declaration of competing interest

The authors declare that they have no known competing financial interests or personal relationships that could have appeared to influence the work reported in this paper.

References

Abdah, M.A.A.M., Awan, H.T.A., Mehar, M., Mustafa, M.N., Walvekar, R., Alam, M.W., Khalid, M., Umapathi, R., Chaudhary, V., 2023. Advancements in MXene-polymer composites for high-performance supercapacitor applications. J. Energy Storage 63, 106942.

Alhabeb, M., Maleski, K., Anasori, B., Lelyukh, P., Clark, L., Sin, S., Gogotsi, Y., 2017. Guidelines for synthesis and processing of two-dimensional titanium carbide ($Ti_3C_2T_x$ MXene). Chem. Mater. 29, 7633–7644.

Alsaman, A.S., Maher, H., Ghazy, M., Ali, E.S., Askalany, A.A., Baran Saha, B., 2024. 2D materials for adsorption desalination applications: a state of the art. Therm. Sci. Eng. Prog. 49, 102455.

Amrillah, T., Abdullah, C.A., Hermawan, A., Sari, F.N., Alviani, V.N. Towards Greener and More Sustainable Synthesis of MXenes: A Review *Nanomater.* [Online], 2022.

An, H., Habib, T., Shah, S., Gao, H., Radovic, M., Green, M.J., Lutkenhaus, J.L., Surface-agnostic highly stretchable and bendable conductive MXene multilayers. Sci. Adv. 4, eaaq0118.

Barsoum, M.W., Radovic, M., 2011. Elastic and Mechanical Properties of the MAX Phases. Annu. Rev. Mater. Res. 41, 195–227.

Beidaghi, M., Gogotsi, Y., 2014. Capacitive energy storage in micro-scale devices: recent advances in design and fabrication of micro-supercapacitors. Energy Environ. Sci. 7, 867–884.

Bhimanapati, G.R., Lin, Z., Meunier, V., Jung, Y., Cha, J., Das, S., Xiao, D., Son, Y., Strano, M.S., Cooper, V.R., Liang, L., Louie, S.G., Ringe, E., Zhou, W., Kim, S.S., Naik, R.R., Sumpter, B.G., Terrones, H., Xia, F., Wang, Y., Zhu, J., Akinwande, D., Alem, N., Schuller, J.A., Schaak, R.E., Terrones, M., Robinson, J.A., 2015. Recent advances in two-dimensional materials beyond graphene. ACS Nano 9, 11509–11539.

Caglar, M., Keyser, U.F., 2021. Ionic and molecular transport in aqueous solution through 2D and layered nanoporous membranes. J. Phys. d: Appl. Phys. 54, 183002.

Cai, Y., Shen, J., Ge, G., Zhang, Y., Jin, W., Huang, W., Shao, J., Yang, J., Dong, X., 2018. Stretchable $Ti_3C_2T_x$ MXene/carbon nanotube composite based strain sensor with ultrahigh sensitivity and tunable sensing range. ACS Nano 12, 56–62.

Cai, M., Wei, X., Huang, H., Yuan, F., Li, C., Xu, S., Liang, X., Zhou, W., Guo, J., 2023. Nitrogen-doped $Ti_3C_2T_x$ MXene prepared by thermal decomposition of ammonium salts and its application in flexible quasi-solid-state supercapacitor. Chem. Eng. J. 458, 141338.

Champagne, A., Charlier, J.-C., 2021. Physical properties of 2D MXenes: from a theoretical perspective. J. Phys. Mater. 3, 032006.

Chen, R., Xue, J., Gong, Y., Yu, C., Hui, Z., Xu, H., Sun, Y., Zhao, X., An, J., Zhou, J., Chen, Q., Sun, G., Huang, W., 2021. Mesh-like vertical structures enable both high areal capacity and excellent rate capability. J. Energ. Chem. 53, 226–233.

Cheng, W., Fu, J., Hu, H., Ho, D., 2021. Interlayer structure engineering of MXene-based capacitor-type electrode for hybrid micro-supercapacitor toward battery-level energy density. Adv. Sci. 8, 2100775.

Dai, P., Zhang, W., Jiang, T., Xiong, Y., Mingzai, W., 2023. Recent progress of stretchable MXene based micro-supercapacitors. APL Mater. 11.

Dall'Agnese, Y., Taberna, P.-L., Gogotsi, Y., Simon, P., 2015. Two-Dimensional Vanadium Carbide (MXene) as Positive Electrode for Sodium-Ion Capacitors. J. Phys. Chem. Lett. 6, 2305-2309.

Dall'Agnese, Y., Lukatskaya, M.R., Cook, K.M., Taberna, P.-L., Gogotsi, Y., Simon, P., 2014. High capacitance of surface-modified 2D titanium carbide in acidic electrolyte. Electrochem. Commun. 48, 118–122.

Das, P., Wu, Z.-S., 2020. MXene for energy storage: present status and future perspectives. J. Phys. Energy 2, 032004.

Deka, B.K., Hazarika, A., Kang, G.-H., Hwang, Y.J., Jaiswal, A.P., Chan Kim, D., Park, Y.-B., Park, H.W., 2023. 3D-Printed structural supercapacitor with MXene-N@Zn-Co selenide nanowire based woven carbon fiber electrodes. ACS Energy Lett. 8, 963–971.

Enyashin, A.N., Ivanovskii, A.L., 2013. Two-dimensional titanium carbonitrides and their hydroxylated derivatives: Structural, electronic properties and stability of *MX*enes $Ti_3C_{2-x}N_x(OH)_2$ from DFTB calculations. J. Solid State Chem. 207, 42–48.

Fatima, S., Sajid, I.H., Khan, M.F., Rizwan, S., 2024. Synthesis and characterization of erbium decorated V_2CT_x for water splitting properties. Int. J. Hydrogen Energy 55, 110–117.

Gao, W., Singh, N., Song, L., Liu, Z., Reddy, A.L.M., Ci, L., Vajtai, R., Zhang, Q., Wei, B., Ajayan, P.M., 2011. Direct laser writing of micro-supercapacitors on hydrated graphite oxide films. Nat. Nanotechnol. 6, 496–500.

Garg, R., Agarwal, A., Agarwal, M., 2020. Synthesis and optimisation of MXene for supercapacitor application. J. Mater. Sci.-Mater. El. 31, 18614–18626.

Ghosh, S., Polaki, S.R., Sahoo, G., Jin, E.-M., Kamruddin, M., Cho, J.S., Jeong, S.M., 2019. Designing metal oxide-vertical graphene nanosheets structures for 2.6V aqueous asymmetric electrochemical capacitor. J. Ind. Eng. Chem. 72, 107–116.

Greaves, M., Barg, S., Bissett, M.A., 2020. MXene-Based anodes for metal-ion batteries. Batter. Supercaps 3, 214–235.

Guirguis, A., Polaki, S.R., Sahoo, G., Ghosh, S., Kamruddin, M., Merenda, A., Chen, X., Maina, J.W., Szekely, G., Dumee, L., 2020. Engineering high-defect densities across

vertically-aligned graphene nanosheets to induce photocatalytic reactivity. Carbon 168, 32–41.
Guo, Y., Zhou, X., Wang, D., Xu, X., Xu, Q., 2019. Nanomechanical properties of Ti_3C_2 Mxene. Langmuir 35, 14481–14485.
Hart, J.L., Hantanasirisakul, K., Lang, A.C., Anasori, B., Pinto, D., Pivak, Y., van Omme, J. T., May, S.J., Gogotsi, Y., Taheri, M.L., 2019. Control of MXenes' electronic properties through termination and intercalation. Nat. Commun. 10, 522.
Hong, X., Mei, J., Wen, L., Tong, Y., Vasileff, A.J., Wang, L., Liang, J., Sun, Z., Dou, S.X., 2019. Nonlithium Metal-Sulfur Batteries: Steps Toward a Leap. Adv. Mater. 31, 1802822.
Hu, X., Gong, N., Zhang, Q., Chen, Q., Xie, T., Liu, H., Li, Y., Li, Y., Peng, W., Zhang, F., Fan, X., 2024. N-Terminalized $Ti_3C_2T_x$ MXene for supercapacitor with extraordinary pseudocapacitance performance. Small 20, 2306997.
Hu, M., Li, Z., Li, G., Hu, T., Zhang, C., Wang, X., 2017. All-Solid-State flexible fiber-based MXene supercapacitors. Adv. Mater. Technol. 2, 1700143.
Huang, H., Chu, X., Su, H., Zhang, H., Xie, Y., Deng, W., Chen, N., Liu, F., Zhang, H., Gu, B., Deng, W., Yang, W., 2019. Massively manufactured paper-based all-solid-state flexible micro-supercapacitors with sprayable MXene conductive inks. J. Power Sources 415, 1–7.
Huang, Z., Qin, J., Zhu, Y., He, K., Chen, H., Hoh, H.Y., Batmunkh, M., Benedetti, T.M., Zhang, Q., Su, C., Zhang, S., Zhong, Y.L., 2023. Green and scalable electrochemical routes for cost-effective mass production of MXenes for supercapacitor electrodes. Carbon Energy 5, e295.
Ingason, A.S., Dahlqvist, M., Rosen, J., 2016. Magnetic MAX phases from theory and experiments; a review. J. Phys.: Condens. Matter 28, 433003.
Iravani, S., 2022. MXenes and MXene-based (nano)structures: A perspective on greener synthesis and biomedical prospects. Ceram. Int. 48, 24144–24156.
Iyer, M., Rajkumar, P., Sanghavi, B., Parvathy, G., Aravinth, K., Kim, J., 2024. Elevating energy storage performance of bismuth antimonate coupled with MXene and graphitic nanofibers in advanced supercapacitors. J. Power Sources 602, 234379.
Ji, P., Chen, W., Luo, Y., Wang, Y., Gu, N., Meng, G., Wu, J., Li, B., Wu, K., Liu, Z., 2024. 3D porous MXene induced by zinc-assisted electrodeposition for flexible all-solid-state supercapacitors. J. Alloys Compd. 997, 174426.
Jiang, X., Kuklin, A.V., Baev, A., Ge, Y., Ågren, H., Zhang, H., Prasad, P.N., 2020b. Two-dimensional MXenes: From morphological to optical, electric, and magnetic properties and applications. Phys. Rep. 848, 1–58.
Jiang, Q., Kurra, N., Alhabeb, M., Gogotsi, Y., Alshareef, H.N., 2018. All pseudocapacitive MXene-RuO_2 asymmetric supercapacitors. Adv. Energy Mater. 8, 1703043.
Jiang, Q., Lei, Y., Liang, H., Xi, K., Xia, C., Alshareef, H.N., 2020a. Review of MXene electrochemical microsupercapacitors. Energy Storage Mater. 27, 78–95.
Jiao, S., Zhou, A., Wu, M., Hu, H., 2019. Kirigami patterning of MXene/bacterial cellulose composite paper for all-solid-state stretchable micro-supercapacitor arrays. Adv. Sci. 6, 1900529.
Jing, H., Yeo, H., Lyu, B., Ryou, J., Choi, S., Park, J.-H., Lee, B.H., Kim, Y.-H., Lee, S., 2021. Modulation of the electronic properties of MXene ($Ti_3C_2T_x$) via surface-covalent functionalization with diazonium. ACS Nano 15, 1388–1396.
Kajiyama, S., Szabova, L., Iinuma, H., Sugahara, A., Gotoh, K., Sodeyama, K., Tateyama, Y., Okubo, M., Yamada, A., 2017. Enhanced Li-Ion accessibility in MXene titanium carbide by steric chloride termination. Adv. Energy Mater. 7, 1601873.
Karmur, R.S., Gogoi, D., Sharma, S., Das, M.R., Dalvi, A., Ghosh, N.N., 2024. High-performance flexible solid-state asymmetric supercapacitor with $NiCo_2S_4$ as a cathode and a MXene-reduced graphene oxide sponge as an anode. J. Mater. Chem.: A 12, 12762–12776.
Kewate, O.J., Punniyakoti, S., 2023. Ti_3AlC_2 MAX phase and $Ti_3C_2T_X$ MXene-based composites towards supercapacitor applications: a comprehensive review of synthesis, recent progress, and challenges. J. Energy Storage 72, 108501.
Khan, K., Tareen, A.K., Aslam, M., Mahmood, A., khan, Q., Zhang, Y., Ouyang, Z., Guo, Z., Zhang, H., 2020. Going green with batteries and supercapacitor: Two dimensional materials and their nanocomposites based energy storage applications. Prog. Solid State Chem. 58, 100254.
Khan, U., Gao, B., Kong, L.B., Chen, Z., Que, W., 2024. Green synthesis of fluorine-free MXene via hydrothermal process: a sustainable approach for proton supercapacitor electrodes. Electrochim. Acta 475, 143651.
Khazaei, M., Arai, M., Sasaki, T., Chung, C.-Y., Venkataramanan, N.S., Estili, M., Sakka, Y., Kawazoe, Y., 2013. Novel Electronic and magnetic properties of two-dimensional transition metal carbides and nitrides. Adv. Funct. Mater. 23, 2185–2192.
Khazaei, M., Arai, M., Sasaki, T., Ranjbar, A., Liang, Y., Yunoki, S., 2015. OH-terminated two-dimensional transition metal carbides and nitrides as ultralow work function materials. Phys. Rev. B 92, 075411.
Khazaei, M., Ranjbar, A., Arai, M., Sasaki, T., Yunoki, S., 2017. Electronic properties and applications of MXenes: a theoretical review. J. Mater. Chem. C 5, 2488–2503.
Kim, E., Song, J., Song, T.-E., Kim, H., Kim, Y.-J., Oh, Y.-W., Jung, S., Kang, I.-S., Gogotsi, Y., Han, H., Ahn, C.W., Lee, Y., 2022. Scalable fabrication of MXene-based flexible micro-supercapacitor with outstanding volumetric capacitance. Chem. Eng. J. 450, 138456.
Kumar, J.A., Prakash, P., Krithiga, T., Amarnath, D.J., Premkumar, J., Rajamohan, N., Vasseghian, Y., Saravanan, P., Rajasimman, M., 2022. Methods of synthesis, characteristics, and environmental applications of MXene: a comprehensive review. Chemosphere 286, 131607.
Kumar, Y.A., Raorane, C.J., Hegazy, H.H., Ramachandran, T., Kim, S.C., Moniruzzaman, M., 2023. 2D MXene-based supercapacitors: a promising path towards high-performance energy storage. J. Energy Storage 72, 108433.
Lai, S.-N., Chen, W.Y., Yen, C.-C., Liao, Y.-S., Chen, P.-H., Stanciu, L., Wu, J.M., 2024. An ultraefficient surface functionalized $Ti_3C_2T_x$ MXene piezocatalyst: synchronous hydrogen evolution and wastewater treatment. J. Mater. Chem.: A 12, 3340–3351.
Lamiel, C., Hussain, I., Ogunsakin, O.R., Zhang, K., 2022. MXene in core–shell structures: research progress and future prospects. J. Mater. Chem.: A 10, 14247–14272.
Lei, J.-C., Zhang, X., Zhou, Z., 2015. Recent advances in MXene: preparation, properties, and applications. Front. Phys. 10, 276–286.
Li, Z., Huang, Y., Zhang, Z., Wang, J., Han, X., Zhang, G., Li, Y., 2021. Hollow C-LDH/Co_9S_8 nanocages derived from ZIF-67-C for high- performance asymmetric supercapacitors. J. Colloid Interface Sci. 604, 340–349.
Li, Z., Jiang, M., Wu, F., Wu, L., Zhang, X., Li, L., 2024. Synergistic *in-situ* intercalation and surface modification strategy for $Ti_3C_2T_x$ MXene-based supercapacitors with enhanced electrochemical energy storage. J. Energy Storage 84, 110772.
Li, X., Li, M., Yang, Q., Liang, G., Huang, Z., Ma, L., Wang, D., Mo, F., Dong, B., Huang, Q., Zhi, C., 2020. In situ electrochemical synthesis of MXenes without acid/alkali usage in/for an aqueous zinc ion battery. Adv. Energy Mater. 10, 2001791.
Li, M., Lu, J., Luo, K., Li, Y., Chang, K., Chen, K., Zhou, J., Rosen, J., Hultman, L., Eklund, P., Persson, P.O.Å., Du, S., Chai, Z., Huang, Z., Huang, Q., 2019b. Element replacement approach by reaction with lewis acidic molten salts to synthesize nanolaminated MAX phases and MXenes. J. Am. Chem. Soc. 141, 4730–4737.
Li, H., Ma, L., Han, C., Wang, Z., Liu, Z., Tang, Z., Zhi, C., 2019a. Advanced rechargeable zinc-based batteries: recent progress and future perspectives. Nano Energy 62, 550–587.
Li, Y., Qin, Y., Wu, G., Zheng, Y., Ban, Q., 2022. Metal-coordination-driven self-assembly synthesis of porous iron/carbon composite for high-efficiency electromagnetic wave absorption. J. Colloid Interface Sci. 623, 1002–1014.
Li, T., Yao, L., Liu, Q., Gu, J., Luo, R., Li, J., Yan, X., Wang, W., Liu, P., Chen, B., Zhang, W., Abbas, W., Naz, R., Zhang, D., 2018. Fluorine-free synthesis of high-purity $Ti_3C_2T_x$ (T=OH, O) via alkali treatment. Angew. Chem. Int. Ed. 57, 6115–6119.
Lian, X., Shi, Y., Li, S., Ding, B., Hua, C., Wang, L., 2022. Applications of MXene-based memristors in neuromorphic intelligence applications. Contemp. Phys. 63, 87–105.
Liang, X., Chen, Y., Jiao, Z., Demir, M., Du, M., Han, J., 2024. MXene-transition metal sulfide composite electrodes for supercapacitors: Synthesis and electrochemical characterization. J. Energy Storage 88, 111634.
Liang, Y., Khazaei, M., Ranjbar, A., Arai, M., Yunoki, S., Kawazoe, Y., Weng, H., Fang, Z., 2017. Theoretical prediction of two-dimensional functionalized MXene nitrides as topological insulators. Phys. Rev. B 96, 195414.
Lim, K.R.G., Shekhirev, M., Wyatt, B.C., Anasori, B., Gogotsi, Y., Seh, Z.W., 2022. Fundamentals of MXene Synthesis. Nat. Synth. 1, 601–614.
Lin, Y., Shang, J., Liu, Y., Wang, Z., Bai, Z., Ou, X., Tang, Y., 2024. Chlorination Design for Highly Stable Electrolyte toward High Mass Loading and Long Cycle Life Sodium-Based Dual-Ion Battery. Adv. Mater. n/a, 2402702.
Lin, Z., Shao, H., Xu, K., Taberna, P.-L., Simon, P., 2020. MXenes as high-rate electrodes for energy storage. Trends Chem. 2, 654–664.
Ling, Z., Ren, C.E., Zhao, M.-Q., Yang, J., Giammarco, J.M., Qiu, J., Barsoum, M.W., Gogotsi, Y., 2014. Flexible and conductive MXene films and nanocomposites with high capacitance. Proc. Natl. Acad. Sci. 111, 16676–16681.
Liu, L., Li, Y., Zhang, Y., Shang, X., Song, C., Meng, F., 2023b. Ni_3S_2 thin-layer nanosheets coupled with Co_9S_8 nanoparticles anchored on 3D cross-linking composite structure CNT@MXene for high-performance asymmetric supercapacitor. Electrochim. Acta 439, 141694.
Liu, M.-Z., Li, X.-H., Yan, H.-T., Zhang, R.-Z., Cui, H.-L., 2023c. Influence of N-doped concentration on the electronic properties and quantum capacitance of Hf_2CO_2 MXene. Vacuum 210, 111826.
Liu, C., Wu, H., Wang, X., Fan, J., Su, H., Yang, D., Wei, Y., Du, F., Dall'Agnese, Y., Gao, Y., 2023a. Flexible solid-state supercapacitor integrated by methanesulfonic acid/polyvinyl acetate hydrogel and Ti3C2Tx. Energy Storage Mater. 54, 164–171.
Liu, F., Zhou, A., Chen, J., Zhang, H., Cao, J., Wang, L., Hu, Q., 2016. Preparation and methane adsorption of two-dimensional carbide Ti_2C. Adsorption 22, 915–922.
Luo, W., Sun, Y., Lin, Z., Li, X., Han, Y., Ding, J., Li, T., Hou, C., Ma, Y., 2023. Flexible $Ti_3C_2T_x$ MXene/V_2O_5 composite films for high-performance all-solid supercapacitors. J. Energy Storage 62, 106807.
Ma, Y., Liu, N., Li, L., Hu, X., Zou, Z., Wang, J., Luo, S., Gao, Y., 2017. A highly flexible and sensitive piezoresistive sensor based on MXene with greatly changed interlayer distances. Nat. Commun. 8, 1207.
Maleski, K., Mochalin, V.N., Gogotsi, Y., 2017. Dispersions of two-dimensional titanium carbide MXene in organic solvents. Chem. Mater. 29, 1632–1640.
Man, Q., An, Y., Shen, H., Wei, C., Zhang, X., Wang, Z., Xiong, S., Feng, J., 2023. MXenes and their derivatives for advanced solid-state energy storage devices. Adv. Funct. Mater. 33, 2303668.
Maqsood, M.F., Latif, U., Sheikh, Z.A., Abubakr, M., Rehman, S., Khan, K., Khan, M.A., Kim, H., Ouladsmane, M., Rehman, M.A., Kim, D.-K., Khan, M.F., 2023. A comprehensive study of $Bi_2Sr_2Co_2O_y$ misfit layered oxide as a supercapacitor electrode material. Inorg. Chem. Commun. 158, 111487.
Mateen, A., Ahmad, Z., Ali, S., Hassan, N.U., Ahmed, F., Alshgari, R.A., Mushab, M., Eldin, S.M., Ansari, M.Z., Javed, M.S., Peng, K.-Q., 2023. Silicon intercalation on MXene nanosheets towards new insights into a superior electrode material for high-performance Zn-ion supercapacitor. J. Energy Storage 71, 108151.
Moniruzzaman, M., Maity, C.K., De, S., Kim, M.J., Kim, J., 2024. SnO_2 Nanosphere/carbon dot-embedded $Ti_3C_2T_x$ MXene nanocomposites for high-performance binder-free asymmetric supercapacitor electrodes. ACS Appl. Nano Mater. 7, 6636–6649.
Moon, J., Lee, J., Kang, Y.C., Kim, J.H., Park, J.T., Kim, S.J., 2023. Designing ionophilic MXene-based organohydrogel electrolytes for high performance supercapacitor with wide-potential-window and anti-freezing properties. Electrochim. Acta 466, 143007.

Naguib, M., Halim, J., Lu, J., Cook, K.M., Hultman, L., Gogotsi, Y., Barsoum, M.W., 2013. New two-dimensional niobium and vanadium carbides as promising materials for Li-Ion batteries. J. Am. Chem. Soc. 135, 15966–15969.

Naguib, M., Barsoum, M.W., Gogotsi, Y., 2021. Ten years of progress in the synthesis and development of MXenes. Adv. Mater. 33, 2103393.

Nan, J., Guo, X., Xiao, J., Li, X., Chen, W., Wu, W., Liu, H., Wang, Y., Wu, M., Wang, G., 2021. Nanoengineering of 2D MXene-based materials for energy storage applications. Small 17, 1902085.

Nasrin, K., Sudharshan, V., Subramani, K., Sathish, M., 2022. Insights into 2D/2D MXene Heterostructures for improved synergy in structure toward next-generation supercapacitors: a review. Adv. Funct. Mater. 32, 2110267.

Okubo, M., Sugahara, A., Kajiyama, S., Yamada, A., 2018. MXene as a charge storage host. Acc. Chem. Res. 51, 591–599.

Orangi, J., Hamade, F., Davis, V.A., Beidaghi, M., 2020. 3D printing of additive-free 2D $Ti_3C_2T_x$ (MXene) Ink for fabrication of micro-supercapacitors with ultra-high energy densities. ACS Nano 14, 640–650.

Panda, S., Deshmukh, K., Khadheer Pasha, S.K., Theerthagiri, J., Manickam, S., Choi, M. Y., 2022. MXene based emerging materials for supercapacitor applications: recent advances, challenges, and future perspectives. Coord. Chem. Rev. 462, 214518.

Pang, S.-Y., Wong, Y.-T., Yuan, S., Liu, Y., Tsang, M.-K., Yang, Z., Huang, H., Wong, W.-T., Hao, J., 2019. Universal strategy for HF-Free facile and rapid synthesis of two-dimensional MXenes as multifunctional energy materials. J. Am. Chem. Soc. 141, 9610–9616.

Patra, A., Mane, P., Polaki, S.R., Chakraborty, B., Rout, C.S., 2022. Enhanced charge storage performance of MXene based all-solid-state supercapacitor with vertical graphene arrays as the current collector. J. Energy Storage 54, 105355.

Peng, Y.-Y., Akuzum, B., Kurra, N., Zhao, M.-Q., Alhabeb, M., Anasori, B., Kumbur, E.C., Alshareef, H.N., Ger, M.-D., Gogotsi, Y., 2016. All-MXene (2D titanium carbide) solid-state microsupercapacitors for on-chip energy storage. Energy Environ. Sci. 9, 2847–2854.

Peng, C., Wei, P., Chen, X., Zhang, Y., Zhu, F., Cao, Y., Wang, H., Yu, H., Peng, F., 2018. A hydrothermal etching route to synthesis of 2D MXene (Ti_3C_2, Nb_2C): enhanced exfoliation and improved adsorption performance. Ceram. Int. 44, 18886–18893.

Pourjafarabadi, M., Rahighi, R., Jamehbozorg, R., Imanpour, A., Eskandary, A., Ansari, M.Z., Abdi, Y., 2024. Mechanism of hydrogen plasma chemo-mechanical effect on properties of a MXene-based energy storage system. J. Energy Storage 77, 109811.

Pu, S., Wang, Z., Xie, Y., Fan, J., Xu, Z., Wang, Y., He, H., Zhang, X., Yang, W., Zhang, H., 2023. Origin and Regulation of self-discharge in MXene supercapacitors. Adv. Funct. Mater. 33, 2208715.

Radovic, M., Barsoum, M.W., 2013. MAX phases: bridging the gap between metals and ceramics. Am. Ceram. Soc. Bull. 92, 20–27.

Raghavendra, K.V.G., Vinoth, R., Zeb, K., Muralee Gopi, C.V.V., Sambasivam, S., Kummara, M.R., Obaidat, I.M., Kim, H.J., 2020. An intuitive review of supercapacitors with recent progress and novel device applications. J. Energy Storage 31, 101652.

Ronchi, R.M., Arantes, J.T., Santos, S.F., 2019. Synthesis, structure, properties and applications of MXenes: Current status and perspectives. Ceram. Int. 45, 18167–18188.

Rout, C.S., 2024. Engineered 2D Materials for Electrocatalysis Applications. IOP Publishing:.

Saha, S., Arole, K., Radovic, M., Lutkenhaus, J.L., Green, M.J., 2021. One-step hydrothermal synthesis of porous $Ti_3C_2T_z$ MXene/rGO gels for supercapacitor applications. Nanoscale 13, 16543–16553.

Sahoo, B.B., Pandey, V.S., Dogonchi, A.S., Thatoi, D.N., Nayak, N., Nayak, M.K., 2023. Exploring the potential of borophene-based materials for improving energy storage in supercapacitors. Inorg. Chem. Commun. 154, 110919.

Sarycheva, A., Gogotsi, Y., 2020. Raman spectroscopy analysis of the structure and surface chemistry of $Ti_3C_2T_x$ MXene. Chem. Mater. 32, 3480–3488.

Saxena, S., Johnson, M., Dixit, F., Zimmermann, K., Chaudhuri, S., Kaka, F., Kandasubramanian, B., 2023. Thinking green with 2-D and 3-D MXenes: Environment friendly synthesis and industrial scale applications and global impact. Renew. Sust. Energ. Rev. 178, 113238.

Sengupta, S., Kundu, M., 2024. All-solid-state flexible asymmetric supercapacitors based on WS_2/rGO/CNT hybrid electrodes and polymer-based ionic liquid electrolytes. ACS Appl. Energy Mater. 7, 4243–4251.

Shahzad, F., Alhabeb, M., Hatter, C.B., Anasori, B., Man Hong, S., Koo, C.M., Gogotsi, Y., 2016. Electromagnetic interference shielding with 2D transition metal carbides (MXenes). Science 353, 1137–1140.

Shao, Y., Wang, J., Wu, H., Liu, J., Aksay, I.A., Lin, Y., 2010. Graphene based electrochemical sensors and biosensors: a review. Electroanalysis 22, 1027–1036.

Sheikh, Z.A., Katkar, P.K., Kim, H., Rehman, S., Khan, K., Chavan, V.D., Jose, R., Khan, M.F., Kim, D.-K., 2023. Transition metal chalcogenides, MXene, and their hybrids: an emerging electrochemical capacitor electrodes. J. Energy Storage 71, 107997.

Shi, M., Zhao, M., Zheng, Q., Li, F., Jiao, L., Su, Z., Li, M., Song, X., 2024. Constructing crystalline NiCoP@Amorphous nickel-cobalt boride core-shell nanospheres with enhanced rate capability for aqueous supercapacitors and rechargeable Zn-based batteries. Energy Fuel 38, 1525–1537.

Shimada, T., Takenaka, N., Ando, Y., Otani, M., Okubo, M., Yamada, A., 2022. Relationship between Electric Double-Layer Structure of MXene Electrode and Its Surface Functional Groups. Chem. Mater. 34, 2069–2075.

Sokol, M., Natu, V., Kota, S., Barsoum, M.W., 2019. On the Chemical Diversity of the MAX Phases. Trends Chem. 1, 210–223.

Sun, L., Fu, Q., Pan, C., 2021. Hierarchical porous "skin/skeleton"-like MXene/biomass derived carbon fibers heterostructure for self-supporting, flexible all solid-state supercapacitors. J. Hazard. Mater. 410, 124565.

Sun, Y., Li, F., Liu, X., Qin, T., Li, T., Zheng, H., Alwarappan, S., Ostrikov, K., 2022. Inter-lamellar nanostructures-by-design for high-performance dual-photoelectrode photofuel cell based genosensor. Sens. Actuator B-Chem. 350, 130838.

Sun, G., Yang, H., Zhang, G., Gao, J., Jin, X., Zhao, Y., Jiang, L., Qu, L., 2018. A capacity recoverable zinc-ion micro-supercapacitor. Energy Environ. Sci. 11, 3367–3374.

Tan, R., Sivanantham, A., Jansi Rani, B., Jeong, Y.J., Cho, I.S., 2023. Recent advances in surface regulation and engineering strategies of photoelectrodes toward enhanced photoelectrochemical water splitting. Coord. Chem. Rev. 494, 215362.

Tang, Y., Xu, H., 2024. Preparation of 2D Materials, in: Two-Dimensional Materials for Nonlinear Optics. 1-20.

Tang, H., Chen, R., Huang, Q., Ge, W., Zhang, X., Yang, Y., Wang, X., 2022. Scalable manufacturing of leaf-like MXene/Ag NWs/cellulose composite paper electrode for all-solid-state supercapacitor. EcoMat 4, e12247.

Tao, Q., Dahlqvist, M., Lu, J., Kota, S., Meshkian, R., Halim, J., Palisaitis, J., Hultman, L., Barsoum, M.W., Persson, P.O.Å., Rosen, J., 2017. Two-dimensional $Mo_{1.33}C$ MXene with divacancy ordering prepared from parent 3D laminate with in-plane chemical ordering. Nat. Commun. 8, 14949.

Thanigai Vetrikarasan, B., Nair, A.R., Karthick, T., Shinde, S.K., Kim, D.-Y., Sawant, S.N., Jagadale, A.D., 2023. Co-precipitation synthesis of pseudocapacitive λ-MnO_2 for 2D MXene ($Ti_3C_2T_x$) based asymmetric flexible supercapacitor. J. Energy Storage 72, 108403.

Thirumal, V., Rajkumar, P., Kim, J.-H., Babu, B., Yoo, K. Binder-Free Two-Dimensional Few-Layer Titanium Carbide MXene Ink for High-Performance Symmetric Supercapacitor Device Applications *Crystals* [Online], 2024b.

Thirumal, V., Rajkumar, P., Babu, B., Kim, J.-H., Yoo, K., 2024a. Performance of asymmetric hybrid supercapacitor device based on antimony-titanium carbide MXene composite. J. Alloys Compd. 982, 173598.

Thomas, S.A., Patra, A., Al-Shehri, B.M., Selvaraj, M., Aravind, A., Rout, C.S., 2022. MXene based hybrid materials for supercapacitors: Recent developments and future perspectives. J. Energy Storage 55, 105765.

Tuzluca Yesilbag, F.N., Yesilbag, Y.O., Huseyin, A., Salih, A.J.S., Ertugrul, M., 2023. Rational design of MXene/Boron Carbon Nitride nanotube composite electrode for supercapacitors with improved electrochemical properties. J. Energy Storage 72, 108446.

Venkateshalu, S., Grace, A.N., 2020. MXenes—a new class of 2D layered materials: synthesis, properties, applications as supercapacitor electrode and beyond. Appl. Mater. Today 18, 100509.

Wang, W., Chen, G., Kong, W., Chen, J., Pu, L., Gong, J., Zhang, H., Dai, Y., 2024b. Sandwich-like high-performance $Ti_3C_2T_x$ MXene/$NiCo_2O_4$ nanosphere composites for asymmetric supercapacitor application. J. Energy Storage 86, 111097.

Wang, M., Jiang, C., Zhang, S., Song, X., Tang, Y., Cheng, H.-M., 2018b. Reversible calcium alloying enables a practical room-temperature rechargeable calcium-ion battery with a high discharge voltage. Nat. Chem. 10, 667–672.

Wang, S., Liu, Y., He, L., Sun, Y., Huang, Q., Xu, S., Qiu, X., Wei, T., 2024a. A gel polymer electrolyte based on IL@NH2-MIL-53 (Al) for high-performance all-solid-state lithium metal batteries. Chin. J. Chem. Eng. 69, 47–55.

Wang, Y., Wang, X., Li, X., Bai, Y., Xiao, H., Liu, Y., Liu, R., Yuan, G., 2019b. Engineering 3D ion transport channels for flexible MXene films with superior capacitive performance. Adv. Funct. Mater. 29, 1900326.

Wang, Y., Wang, X., Li, X., Li, X., Liu, Y., Bai, Y., Xiao, H., Yuan, G., 2021. A high-performance, tailorable, wearable, and foldable solid-state supercapacitor enabled by arranging pseudocapacitive groups and MXene flakes on textile electrode surface. Adv. Funct. Mater. 31, 2008185.

Wang, Z., Xu, Z., Huang, H., Chu, X., Xie, Y., Xiong, D., Yan, C., Zhao, H., Zhang, H., Yang, W., 2020. Unraveling and regulating self-discharge behavior of $Ti_3C_2T_x$ MXene-based supercapacitors. ACS Nano 14, 4916–4924.

Wang, Z., Wei, C., Jiang, H., Zhang, Y., Tian, K., Li, Y., Zhang, X., Xiong, S., Zhang, C., Feng, J., 2024c. MXene-based current collectors for advanced rechargeable batteries. Adv. Mater. 36, 2306015.

Wang, H., Wu, Y., Yuan, X., Zeng, G., Zhou, J., Wang, X., Chew, J.W., 2018a. Clay-inspired MXene-based electrochemical devices and photo-electrocatalyst: state-of-the-art progresses and challenges. Adv. Mater. 30, 1704561.

Wang, L., Zhang, H., Wang, B., Shen, C., Zhang, C., Hu, Q., Zhou, A., Liu, B., 2016. Synthesis and electrochemical performance of $Ti_3C_2T_x$ with hydrothermal process. Electron. Mater. Lett. 12, 702–710.

Wang, K., Zheng, B., Mackinder, M., Baule, N., Qiao, H., Jin, H., Schuelke, T., Fan, Q.H., 2019a. Graphene wrapped MXene via plasma exfoliation for all-solid-state flexible supercapacitors. Energy Storage Mater. 20, 299–306.

Wei, X., Cai, M., Yuan, F., Lu, D., Li, C., Huang, H., Xu, S., Liang, X., Zhou, W., Guo, J., 2022. The surface functional modification of $Ti_3C_2T_x$ MXene by phosphorus doping and its application in quasi-solid state flexible supercapacitor. Appl. Surf. Sci. 606, 154817.

Wei, T., Zhang, Z.-H., Wang, Z.-M., Zhang, Q., Ye, Y.-s., Lu, J.-H., Rahman, Z.u., Zhang, Z.-W., 2020. Ultrathin solid composite electrolyte based on $Li_{6.4}La_3Zr_1.4Ta0.6O_{12}$/PVDF-HFP/LiTFSI/succinonitrile for high-performance solid-state lithium metal batteries. ACS Appl. Energy Mater. 3, 9428–9435.

Xie, Y., Zhang, H., Huang, H., Wang, Z., Xu, Z., Zhao, H., Wang, Y., Chen, N., Yang, W., 2020. High-voltage asymmetric MXene-based on-chip micro-supercapacitors. Nano Energy 74, 104928.

Xu, H., Fan, J., Su, H., Liu, C., Chen, G., Dall'Agnese, Y., Gao, Y., 2023. Metal ion-induced porous MXene for all-solid-state flexible supercapacitors. Nano Lett. 23, 283-290.

Xu, S., Li, Y., Mo, T., Wei, G., Yang, Y., 2024. Highly matched porous MXene anodes and graphene cathodes for high-performance aqueous asymmetric supercapacitors. Energy Storage Mater. 69, 103379.
Yan, Y., Wu, W., Tian, X., Wei, C., Xu, T., Li, X., 2024. Facial design and synthesis of CoAl-LDH-doped MXene with nanosheet structure for high-performance asymmetric supercapacitors. J. Solid State Electrochem.
Yin, S.-H., Cui, X.-H., Li, X.-H., Wang, S.-J., Zhang, R.-Z., Cui, H.-L., Yan, H.-T., 2023a. Theoretical study on the electronic properties and quantum capacitance of Zr_2CO_2 MXene with atomic swap. Int. J. Quantum Chem 123, e27135.
Yin, X., Zheng, W., Tang, H., Zhang, P., Sun, Z., 2023b. Novel 2D/2D 1T-MoS_2/$Ti_3C_2T_z$ heterostructures for high-voltage symmetric supercapacitors. Nanoscale 15, 10437–10446.
Yin, X., Zheng, W., Tang, H., Yang, L., Zhang, P., Sun, Z., 2024. Enhancing ion storage and transport in $Ti_3C_2T_z$ MXene via a "sacrificial cations" strategy. J. Mater. Chem.: A 12, 8952–8962.
Yu, L., Lu, L., Zhou, X., Xu, L., Alhalili, Z., Wang, F., 2021. Strategies for fabricating high-performance electrochemical energy-storage devices by MXenes. ChemElectroChem 8, 1948–1987.
Zhan, C., Naguib, M., Lukatskaya, M., Kent, P.R.C., Gogotsi, Y., Jiang, D.-E., 2018. Understanding the MXene pseudocapacitance. J. Phys. Chem. Lett. 9, 1223–1228.
Zhan, X., Si, C., Zhou, J., Sun, Z., 2020. MXene and MXene-based composites: synthesis, properties and environment-related applications. Nanoscale Horiz. 5, 235–258.
Zhang, C., Anasori, B., Seral-Ascaso, A., Park, S.-H., McEvoy, N., Shmeliov, A., Duesberg, G.S., Coleman, J.N., Gogotsi, Y., Nicolosi, V., 2017a. Transparent, flexible, and conductive 2D titanium carbide (MXene) films with high volumetric capacitance. Adv. Mater. 29, 1702678.
Zhang, X., Liu, X., Dong, S., Yang, J., Liu, Y., 2019. Template-free synthesized 3D macroporous MXene with superior performance for supercapacitors. Appl. Mater. Today 16, 315–321.
Zhang, H., Wang, L., Chen, Q., Li, P., Zhou, A., Cao, X., Hu, Q., 2016. Preparation, mechanical and anti-friction performance of MXene/polymer composites. Mater. Des. 92, 682–689.
Zhang, F., Zhang, Z., Wang, H., Chan, C.H., Chan, N.Y., Chen, X.X., Dai, J.-Y., 2017b. Plasma-enhanced pulsed-laser deposition of single-crystalline Mo_2C ultrathin superconducting films. Phys. Rev. Mater. 1, 034002.
Zhang, X., Zhao, X., Wu, D., Jing, Y., Zhou, Z., 2015. High and anisotropic carrier mobility in experimentally possible Ti_2CO_2 (MXene) monolayers and nanoribbons. Nanoscale 7, 16020–16025.
Zhao, L., Dong, B., Li, S., Zhou, L., Lai, L., Wang, Z., Zhao, S., Han, M., Gao, K., Lu, M., Xie, X., Chen, B., Liu, Z., Wang, X., Zhang, H., Li, H., Liu, J., Zhang, H., Huang, X., Huang, W., 2017. Interdiffusion reaction-assisted hybridization of two-dimensional metal-organic frameworks and Ti3C2Tx nanosheets for electrocatalytic oxygen evolution. ACS Nano 11, 5800–5807.
Zhao, R., Wang, M., Zhao, D., Li, H., Wang, C., Yin, L., 2018. Molecular-level heterostructures assembled from titanium carbide MXene and Ni–Co–Al layered double-hydroxide nanosheets for all-solid-state flexible asymmetric high-energy supercapacitors. ACS Energy Lett. 3, 132–140.